UC Riverside
UC Riverside Electronic Theses and Dissertations

Title

Examining the Role of Astrocyte Swelling and Swelling-Induced Glutamate Release in Two Models of Neuronal Hyperexcitability

Permalink

https://escholarship.org/uc/item/9qr9z06n

Author

Murphy, Thomas R.

Publication Date

2016

Peer reviewed|Thesis/dissertation

UNIVERSITY OF CALIFORNIA
RIVERSIDE

Examining the Role of Astrocyte Swelling and Swelling-Induced Glutamate
Release in Two Models of Neuronal Hyperexcitability

A Dissertation submitted in partial satisfaction
of the requirements for the degree of

Doctor of Philosophy

in

Neuroscience

by

Thomas Robert Murphy

June 2016

Dissertation Committee:
     Dr. Todd A. Fiacco, Chairperson
     Dr. Devin K. Binder
     Dr. Peter W. Hickmott

The Dissertation of Thomas Robert Murphy is approved:

_____

_____

_____
Committee Chairperson

University of California, Riverside

ACKNOWLEDGEMENTS

Special thanks to my mother and father, Donna and Robert Murphy, for their love and support; most especially to my mother, for fostering my love of science from an early age. Thanks to my siblings Brennan and Alissa for their interest in my work, even if they didn't always understand it. Thanks as well to the Siemens family for their support and encouragement throughout. Finally, the most immense of thanks to my wife, Sarah B. Siemens, for the years of love and support which helped me get to this point. Her constant patience and encouragement, especially these past several months, defies understanding and there are truly no words to adequately convey my gratitude.

ABSTRACT OF THE DISSERTATION

Examining the Role of Astrocyte Swelling and Swelling-Induced Glutamate
Release in Two Models of Neuronal Hyperexcitability

by

Thomas Robert Murphy

Doctor of Philosophy, Graduate Program in Neuroscience
University of California, Riverside, June 2016
Dr. Todd A. Fiacco, Chairperson

Epilepsy, a spectrum of over 40 different disorders, is estimated to affect 1

in 26 people worldwide. It is generally characterized by the appearance of

spontaneous, recurrent and unpredictable seizures. Approximately one-third of

epileptic patients cannot control their seizures with current medications, while the

remaining two-thirds of patients often experience negative cognitive side effects,

highlighting the need to better understand epilepsy mechanisms. A common

theme in multiple seizure models is that cellular swelling is necessary for seizure

initiation and recurrence. In experiments described in this dissertation, I set out to

determine: 1) The extent to which neurons and astrocytes swell in two

experimental conditions that lead to neuronal bursting and epileptiform activity; 2)

The mechanisms governing neuronal vs. astrocyte swelling; and 3) The

contribution of astrocytes, specifically, to increases in neuronal excitability. These

experiments were carried out in acute hippocampal slices from wild type and

transgenic mice using a combination of electrophysiology and imaging

approaches. The main findings from these studies were as follows: 1) Both reduced extracellular osmolarity and elevations of extracellular potassium ions ($[K^+]_o$) elevated neuronal excitability within minutes in an NMDA receptor-dependent manner; 2) Contrary to published reports, neurons are not osmoresistant and swell just as readily as astrocytes in hypoosmolar conditions, while astrocytes swell selectively in elevated $[K^+]_o$ conditions; 3) Neuronal swelling is not an artifact of our experimental approaches, nor is it a result of NMDA receptor-driven excitotoxicity; and 4) Astrocytic volume-regulated anion channels (VRAC) may contribute to increased excitability of neurons through release of glutamate. Taken together, these findings have important implications for seizure disorders and for understanding the scope of neuron-glial interactions in the brain.

Table of Contents

List of Figures

Chapter 1: Introduction

1.1. Epilepsy, seizures and seizure disorders

Epilepsy is one of the most common neurological disorders in the world (Hirtz et al., 2007), with an estimated 65 million cases worldwide (Ngugi et al., 2010). Epileptic seizures are currently defined by the International League Against Epilepsy (ILAE) as transient events manifesting from excessive or synchronous neuronal activity in the brain. Accordingly, epilepsy is a disorder characterized by a recurrence of, and abnormal predisposition to, epileptic seizures (Fisher et al., 2005).

1.1.1. Classifying epileptic seizures and epilepsy syndromes

Although the name "epilepsy" suggests a single disease, it is in fact a spectrum of many seizure disorders with widely-varying etiologies. Many of these seizure types are symptomatic of other neurological disorders or afflict only certain age groups (Behr et al., 2016). Classifying epileptic seizures and syndromes has been an ongoing challenge for decades. Most of the commonly-used terminology in epileptic seizure and epilepsy research is based on over 20-year-old definitions published by the International League Against Epilepsy, or ILAE (Commission on Classification and Terminology of the International League Against Epilepsy, 1981, 1989). These definitions were recently updated in 2010, although their usage is not yet universal. In the interest of clarity, the next two sections will address both sets of definitions.

In the 1981 ILAE report, seizures are divided into 2 main groups based upon the extent of their spread across the brain, recorded on an electroencephalogram (EEG). *Partial* seizures are those which initiate and spread within only one hemisphere of the brain. Partial seizures were, in the past, further subdivided as "complex" if consciousness was impaired or clouded, and "simple" if not. In some cases, partial seizures can also become "secondarily generalized" if they subsequently spread to the other hemisphere (Commission on Classification and Terminology of the International League Against Epilepsy, 1981). Partial seizures have since been re-named to "focal" seizures, and the aforementioned subdivisions are no longer used due to difficulties in implementation. However, the authors note that impaired consciousness remains an important aspect when evaluating a patient (Berg et al., 2010). By contrast, *generalized* seizures are those initiating bilaterally. Generalized seizures can also impair consciousness, but are instead subdivided by the type of muscle contractions evoked (tonic, clonic, or tonic-clonic rhythms) or conversely by a sudden arrest of behavior ("absence" seizures). These definitions have not changed appreciably in the new report (Commission on Classification and Terminology of the International League Against Epilepsy, 1981; Berg et al., 2010). The third group, *unclassified*, includes epileptic seizures which cannot be classified using the existing definitions (Commission on Classification and Terminology of the International League Against Epilepsy, 1981). "Epileptic spasms", a unique and variable type of motor seizure which often begin in

infancy, were added to the unclassified group in 2010 (Goldstein and Slomski, 2008; Berg et al., 2010).

In general, an individual is diagnosed with epilepsy if they have at least two unprovoked seizures occurring at least 24h apart (Fisher et al., 2014a). The term "unprovoked" can be somewhat ambiguous, but in general refers to a seizure not caused by systemic or brain insult such as alcohol withdrawal (Beghi et al., 2010). Over 40 different epilepsies and epileptic syndromes are currently recognized by ILAE (Berg et al., 2010). In contrast to epileptic seizures themselves (which are categorized by their effect on brain activity and behavior), epilepsies themselves are categorized by their underlying cause. Earlier ILAE definitions (1989) grouped epilepsy syndromes into 3 broad categories: Idiopathic, Symptomatic, and Cryptogenic. Idiopathic epilepsies are those with no apparent cause nor symptoms apart from the seizures themselves, and are presumed to be genetic in nature. Symptomatic epilepsies are those resulting from an underlying CNS disorder; Cryptogenic epilepsies are presumed to be symptomatic, but the cause is unknown (Commission on Classification and Terminology of the International League Against Epilepsy, 1989). These groups were renamed and restructured when ILAE definitions were revised in 2010, into 3 new categories: Genetic, Structural/Metabolic, and Unknown. Genetic epilepsies are those caused by a known underlying genetic defect. Structural/Metabolic epilepsies include any in which seizures result from a known structural or metabolic condition or damage in the brain, including acquired

conditions such as stroke. Finally, Unknown encompasses all remaining epilepsies with an as-yet unknown cause, making it functionally identical to the older "idiopathic" designation. (Berg et al., 2010).

1.1.2. Ineffective treatments and risks of living with epilepsy

While current antiepileptic drugs (AEDs) are sufficient to control seizures in the majority of patients, such treatments come at the cost of side effects. Most AEDs are designed to broadly reduce neuronal firing in the brain, either through direct action at ion channels or potentiation of inhibitory neurotransmission (Kwan et al., 2001). Such mechanisms inevitably lead to cognitive deficits, and nearly every AED is associated with at least mild cognitive impairment (Aldenkamp, 2001; Aldenkamp et al., 2003; Lagae, 2006). In many cases more than one AED is required to fully control seizures, amplifying these effects (Kwan and Brodie, 2000).

For at least 30% of epileptic patients, seizures persist regardless of AED treatment (Kwan and Brodie, 2000). This number is not static across all types of epilepsy; surprisingly, "symptomatic" (structural) epilepsies (such as Mesial Temporal Lobe Epilepsy (MTLE), which generally results from damage to temporal lobe structures) tend to be more drug-resistant (Kwan and Brodie, 2001b; Stephen et al., 2001). Both cognitive and social impairments are rampant among those with uncontrolled seizures, and it is little surprise that depression is common as well (Kwan and Brodie, 2001a; Boylan et al., 2004). Uncontrolled seizures may also increase mortality risk, especially from sudden unexplained

4

death in epilepsy patients (SUDEP) which may result from inappropriate activation of autonomic functions during a seizure (Devinsky, 2004; Laxer et al., 2014).

1.2. Classifying seizure activity in vivo and in vitro

Abnormal ("epileptiform") brain activity is commonly measured externally as an electroencephalogram (EEG), using electrodes attached to the surface of the scalp, or using the more invasive (but far more accurate) intracranial electrodes (Fisher et al., 2014b). Regardless of the underlying epileptic disorder, epileptiform activity is broadly grouped either as "ictal" or "interictal" activity. Ictal events correspond to the seizure itself - they last several tens of seconds, and generally consist of a "tonic" phase of high-frequency activity (HFA) which gradually synchronize into large, low-frequency bursts ("clonic" phase). Interictal events, which occur between seizures, consist of low-frequency bursts and generally do not manifest as an overt change in behavior (Fisher et al., 2014b). The precise relationship between interictal and ictal activity is unclear; in some animal models, interictal events appear to gradually increase in intensity before the eruption of an ictal discharge, suggesting that ictal activity is simply an interictal event which has passed a certain threshold (Jensen and Yaari, 1988; Traynelis and Dingledine, 1988). However, interictal events are not necessarily required for ictal discharge (Jensen and Yaari, 1988). It is possible that interictal spikes, which appear in damaged tissue long before seizures do, may influence

synaptic plasticity and cultivate the conditions necessary for spontaneous seizures (Staley et al., 2005).

1.3. Experimental models of epilepsy

Epilepsy in humans encompasses a wide range of disorders, which complicates the development of a generally-applicable experimental model. Experimental models of epilepsy *in vivo* are therefore tailored to be general models of spontaneous, recurrent seizures (SRS). SRS have traditionally been attained by one of two methods. In the so-called "kindling" method, electrical stimulations to a selected area of the brain are used to evoke seizures repeatedly over time, the stimulation inducing synaptic plasticity which eventually renders the tissue hyperexcitable enough to spontaneously generate seizures. In the "status epilepticus" methods, a continuous seizure or cluster of seizures (deemed status epilepticus or SE, for its continuous nature) is evoked generally by focal application of chemical convulsants such as penicillin, pentylenetetrazol (PTZ), or pilocarpine, although electrical stimulation may also be used (Morimoto et al., 2004). It is important to note that status epilepticus, a medical emergency in humans, is an effective model because of the brain damage it causes (Morimoto et al., 2004). Following a latent period of sometimes several weeks (during which interictal bursts can be detected), animals begin to display SRS (Curia et al., 2008; Levesque and Avoli, 2013). Of course, these are far from the only models capable of evoking a seizure *in vivo* (Broberg et al., 2008). As in humans, seizures in animal models are gauged by behavioral markers and by the

presence of ictal activity on an EEG or deep electrode (Matsumoto and Marsan, 1964a). Interictal, or "paroxysmal" spikes are technically classified only by their electrophysiological footprint, but due to their frequency (and other factors, to be discussed below) have historically received more in-depth study. In the penicillin model of focal seizures, intracellular and extracellular recordings of single neurons revealed that interictal spikes arose from a large, "paroxysmal depolarization shift" (PDS) occurring simultaneously in many neurons in the seizure focus (Matsumoto and Marsan, 1964b; Dichter and Spencer, 1969). As a result, the PDS is generally accepted as the intracellular correlate of the interictal spike. PDSs, like the interictal spikes they represent, may be of interest for their role in precipitating the ictal seizure.

Epilepsy models have also been developed *in vitro* using slices of brain tissue, often from the hippocampus which is generally accepted to be particularly seizure-prone (Morimoto et al., 2004). Interpretations of data from slice models generally must be made much more cautiously than for *in vivo* models. Clinical diagnoses of epilepsy, and epileptic seizures, are based upon both behavioral and electrophysiological signs (Fisher et al., 2014b; Stafstrom and Carmant, 2015). In the absence of the former, electrophysiological activity in a brain slice must be designated as "ictal" or "interictal" purely by comparison to *in vivo* models. Fortunately, epileptiform activity observed in slices is similar to that observed *in vivo* (Cohen et al., 2002). What the brain slice model loses in behavioral measures and applications to real-world epilepsy, it gains in flexibility

– individual cells can be recorded or patch-clamped, extracellular and intracellular contents may be manipulated as necessary, and drugs may be applied without regard to the blood-brain barrier. Various studies have demonstrated that seizures, or seizure-like activity, in brain slices can be directly evoked (or strongly potentiated) by low magnesium (Mody et al., 1987; Tancredi et al., 1990), low calcium (Jefferys and Haas, 1982; Yaari et al., 1986), low chloride (Yamamoto, 1972; Avoli et al., 1990), blockers of potassium channels (Rutecki et al., 1987, 1990), or modest elevations in potasssium (Rutecki et al., 1985; Traynelis and Dingledine, 1988). High-$[K^+]_o$ has been particularly well-characterized due to its relevance for *in vivo* seizure models, as seizure foci *in vivo* exhibit localized $[K^+]_o$ elevations in response to interictal and ictal discharges (Moody et al., 1974; Fisher et al., 1976). Like *in vivo* models, high-$[K^+]_o$ in slices (particularly from the hippocampus) reliably induces PDS activity which gradually builds in intensity before the eruption of a seizure-like event (SLE) (Rutecki et al., 1985; Traynelis and Dingledine, 1988; Jensen and Yaari, 1997). Additionally, the intensity and frequency of epileptiform bursting correlates directly to $[K^+]_o$ in multiple models (Rutecki et al., 1985; Yaari et al., 1986; Tancredi and Avoli, 1987). These aspects make the high-$[K^+]_o$ model in hippocampal slices an attractive model for the study of epilepsy.

1.4. Tissue swelling and seizures

Space within the brain is both limited and tightly regulated, and neuronal function depends upon the careful balancing of water, ions and neurotransmitter

concentrations in the extracellular space (ECS). Accordingly, losing this balance can be devastating. Acute reductions in plasma osmolality (termed "hyponatremia", or "water intoxication" more generally) have been known for nearly a century to cause direct swelling of the brain, muscle spasms, generalized seizures and even death (Rowntree, 1926). Multiple disorders which can acutely reduce plasma osmolality are also associated with seizures, including syndrome of inappropriate ADH secretion (SIADH), dialysis disequilibrium syndrome, transurethral resection of the prostate (TURP) syndrome and diabetes mellitus, as well as simple accidental cases of overhydration as might occur in psychgenic polydipsia (compulsive water drinking, a symptom of schizophrenia) or rapid water intake following dehydration (Andrew, 1991). Excess water in the brain causes "cellular" edema (sometimes referred to by the sub-classification "osmotic" edema), as water flows into neural cells causing them to swell (Kimelberg, 1995; Thrane et al., 2014), which in turn reduces the ECS (Andrew and MacVicar, 1994; Chebabo et al., 1995b). In addition to increasing effective concentrations of ions and neurotransmitters, ECS reductions bring neurons closer together and increase nonsynaptic, neuron-neuron electrical field (ephaptic) interactions, resulting in more synchronous firing and bursting activity (Dudek et al., 1986). Unsurprisingly, neuronal excitability is highly sensitive to extracellular osmolality (Chebabo et al., 1995a; Azouz et al., 1997; Huang et al., 1997; Lauderdale et al., 2015); moreover, these nonsynaptic interactions enhance seizure susceptibility, as neurons in hypoosmolar

9

conditions are both more likely to fire and more likely to synchronize. Multiple studies have demonstrated that seizures and other epileptiform activity can be either induced by lowering extracellular osmolarity, or blocked by increasing extracellular osmolarity (Traynelis and Dingledine, 1989; Dudek et al., 1990; Rosen and Andrew, 1990; Roper et al., 1992; Saly and Andrew, 1993; Kilb et al., 2006). Similarly, seizures produced by other means are also preceded by constriction of the extracellular space (Traynelis and Dingledine, 1989; Binder et al., 2004b; Broberg et al., 2008).

1.4.1. AQP4 and potassium homeostasis

In general, brain water content is thought to be controlled by astrocytes, which are the most prone to osmotic swelling (Andrew et al., 2007; Hirrlinger et al., 2008; Risher et al., 2009). Astrocytic water permeability is generally attributed to the water channel aquaporin-4 (AQP4), which is expressed almost exclusively by astrocytes in the CNS. AQP4 expression is particularly enriched at astrocytic endfeet adjoining cerebral vasculature, providing tight control of water fluxes into and out of the brain (Nagelhus et al., 2004); as such, AQP4 expression is essential for recovery from vasogenic edemas (involving fluid accumulation in the ECS), but can exacerbate cellular/cytotoxic (intracellular) edema (Papadopoulos and Verkman, 2007).

Water influx through AQP4 channels also forms an essential component of astrocyte potassium and glutamate uptake. Increases in extracellular potassium, whether activity-induced or bath-applied, correlate with a reduction in

size of the extracellular space and cause astrocyte swelling (Dietzel et al., 1980; Walz and Hinks, 1985; Andrew and MacVicar, 1994; Holthoff and Witte, 1996; Risher et al., 2009). This activity-dependent cell swelling is lost in AQP4 null mice (Kitaura et al., 2009). At least two general mechanisms for potassium uptake have been described in astrocytes, although their individual contributions to potassium regulation and activity-dependent astrocyte swelling remain somewhat unclear (Walz, 2000; Larsen et al., 2014). The astrocytic Na^+/K^+-ATPase is generally considered responsible for the rapid clearance of extracellular K^+ which enters the extracellular space following neuronal firing (D'Ambrosio et al., 2002). The other main pathway, the inwardly-rectifying potassium channel K_{ir} 4.1 (the predominant K^+ channel in glial cells), is essential for the high "resting" potassium conductance of astrocytes (Tang et al., 2009) and is associated with the spatial redistribution of K^+ throughout the astrocyte network (otherwise known as "potassium buffering") rather than direct removal of $[K^+]_o$ at the synapse (D'Ambrosio et al., 2002; Meeks and Mennerick, 2007). It should be noted, however, that the loss of effective potassium buffering in K_{ir} 4.1-null animals also has deleterious effects on stimulus-induced potassium currents normally associated with the Na^+/K^+-ATPase, and impairs glutamate uptake (Djukic et al., 2007; Chever et al., 2010). Both K_{ir} 4.1 and the Na^+/K^+-ATPase have been shown to physically and functionally interact with AQP4 (Nagelhus et al., 2004; Illarionova et al., 2010). K_{ir} 4.1 has been particularly well-studied in this context. Initial reports of K_{ir} 4.1 colocalizing with AQP4 in astrocytic endfeet provided the

first hints of a functional interaction (Connors et al., 2004; Nagelhus et al., 2004). These data have since received support from a number of studies using either AQP4$^{-/-}$ or α-syntrophin$^{-/-}$ mice (a scaffolding protein to which AQP4 and K$_{ir}$ 4.1 both bind), which mislocalizes AQP4. In both cases, K$^+$ clearance from the extracellular space is impaired (Amiry-Moghaddam et al., 2003; Binder et al., 2006; Strohschein et al., 2011). Interestingly, K$_{ir}$ 4.1 channels may directly influence astrocyte water permeability through phosphorylation of AQP4 channels (Song and Gunnarson, 2012).

In contrast to astrocytes, most neurons do not express any known water channels (Papadopoulos and Verkman, 2013) and are considered resistant to osmotically-driven volume changes (Andrew et al., 2007; Caspi et al., 2009), perhaps due to their functional roles in synaptic transmission as opposed to clearance of neurotransmitters and ions. This does not imply, however, that neuronal volume is static. For example, neurons are particularly susceptible to excitotoxic swelling, as might occur in stroke or traumatic brain injury (Choi, 1992). Excessive entry of Na$^+$ (often a result of overactive ionotropic glutamate receptors) depolarizes neurons and opens a voltage-gated Cl$^-$ channel. Both ions increase intracellular osmolarity, drawing water into and swelling the neuron (Choi, 1992; Lee et al., 1999; Rungta et al., 2015). Although this would seem to suggest that neuronal swelling is pathological, a possible physiological role has also been found for the minute amounts of swelling which occur in neuronal axons during action potential firing (Iwasa et al., 1980). Such swelling is sufficient

to open volume-regulated anion channels (VRAC; discussed further in section 1.5), enabling nonsynaptic communication through ATP efflux (Fields and Ni, 2010). The precise route of water influx in neurons is ill-defined, but may involve the contribution of water-permeable ion cotransporters. Such a mechanism has already been suggested as one of several possible non-AQP4-mediated mechanisms of astrocyte swelling (Kimelberg, 2005; Macaulay and Zeuthen, 2012).

1.4.2. AQP4, K_{ir} 4.1 and astrocyte swelling in epilepsy

In the last several years, astrocytes have received increasing attention for their potential role in various CNS diseases and disorders, including epilepsy (Wetherington et al., 2008). Astrocytes are a particularly attractive target for epilepsy given their control over neuronal excitability. Key changes contributing to hyperexcitability in epileptic tissue can be directly linked to changes in astrocyte function. For example, extracellular glutamate levels are excessively high in epileptic tissue (During and Spencer, 1993; Cavus et al., 2005), resulting at least in part from impaired astrocytic glutamate metabolism (Eid et al., 2004) and possibly glutamate transport (Proper et al., 2002). Potassium clearance and buffering in epileptic tissue is also impaired (Bordey and Sontheimer, 1998; Kivi et al., 2000), which can be attributed to the combined effects of reduced K_{ir} 4.1 channel expression, AQP4 mislocalization away from astrocytic endfeet, and decoupling of astrocyte gap junctions (Amiry-Moghaddam et al., 2003; Eid et al., 2005; Heuser et al., 2012; Bedner et al., 2015).

More specific evidence for the role of astrocytes in seizures and epilepsy has been observed through specific targeting of AQP4 or K_{ir} 4.1 in various seizure models. In a series of informative studies, Binder and colleagues (Binder et al., 2004a; 2004b; 2006) used pentylenetetrazol (PTZ) injections to evoke recurrent seizures in wild-type and AQP4$^{-/-}$ mice, and recorded the differences in evoked seizures for those mice lacking the AQP4 channel. Consistent with previous findings (Traynelis and Dingledine, 1989; Olsson et al., 2006), extracellular space in wild-type was observed to shrink just prior to a seizure. However, in AQP4$^{-/-}$ animals, no such ECS shrinkage was observed (Binder et al., 2004b). AQP4$^{-/-}$ animals also required a higher dose of PTZ to reach seizure threshold, but once this threshold was reached mice experienced seizures nearly 3 times the duration of wild-type animals (Binder et al., 2004a; 2006). Impaired K^+ uptake was hypothesized as the cause for prolonged seizure durations, as AQP4$^{-/-}$ mice have noticeably slower K^+ decay kinetics (Binder et al., 2006; Strohschein et al., 2011). It is interesting to note that, despite this impaired K^+ uptake (or perhaps as a result of it), AQP4$^{-/-}$ astrocytes are coupled to a greater degree through gap junctions than their wild-type counterparts (Strohschein et al., 2011). Loss of gap junctional coupling is associated with seizures and neuronal death (Bedner et al., 2015); conversely, the enhanced potassium buffering ability for AQP4$^{-/-}$ astrocytes resulting from their increased gap junctional coupling may contribute to the higher threshold observed in AQP4$^{-/-}$ animals.

1.5.   VRAC and volume regulation

Most cell types exhibit some form of volume regulation, including neural cells (Hoffmann et al., 2009). Even cells that swell readily in hypoosmolar conditions will, over time, gradually decrease in size back to baseline volume – despite the continued presence of the osmotic stressor. Similarly, shrunken cells will increase their volume to regain normal size. These two processes are termed regulatory volume decrease (RVD) and regulatory volume increase (RVI), respectively (Hoffmann et al., 2009). For purposes which shall become clear, this discussion will focus specifically on RVD. As in many cell types, RVD has been readily observed in swollen cultured astrocytes (Eriksson et al., 1992; Vitarella et al., 1994; Olson et al., 1995). Disagreement exists as to whether astrocytic RVD occurs *in vivo*, as some groups have observed osmotic swelling of glia or brain slices without a subsequent volume decrease (Andrew et al., 1997; Hirrlinger et al., 2008; Risher et al., 2009). The reason for this discrepancy is not clear, but may reflect the ability of intact tissue to maintain a relatively constant volume with more gradual changes in osmolarity, referred to as "isovolumetric" volume regulation or IVR (Franco et al., 2000). The mechanisms involved IVR are likely similar to those in RVD (Pasantes-Morales and Cruz-Rangel, 2010). An alternative (and perhaps complementary) explanation is that RVD is simply rendered impossible in brain slices due to a depletion of osmotically-active substances ("osmolytes") within the slice (Kreisman and Olson, 2003). It must

also be noted that RVD may depend on the method used to reduce extracellular osmolarity (Andrew et al., 1997; see Chapter 2 for further discussion).

In general terms, RVD involves the release of K^+, Cl^-, organic osmolytes and water from the cell through either active transport or the opening of stretch-activated channels (Chamberlin and Strange, 1989; Pasantes-Morales et al., 2006). While the exact transporters and channels involved have been somewhat difficult to identify clearly, it is generally agreed that the particular class of stretch-activated channel known as the "volume-regulated anion channel" (VRAC) is an essential component of astrocytic RVD (Benfenati and Ferroni, 2010). Until recently, VRAC were identifiable primarily by imperfect pharmacology, and secondarily (but more accurately) by their swelling-activated currents (Akita and Okada, 2014). In 2014, the subunits comprising VRAC were finally identified as belonging to the leucine-rich repeat containing protein 8 (LRRC8) family (Hyzinski-Garcia et al., 2014; Qiu et al., 2014). For clarity and consistency with prior literature however, the term "VRAC" will be used for the remainder of this section. VRAC are particularly interesting for their permeability to not only small inorganic anions such as F^- and Cl^-, but also to large anionic excitatory amino acids such as glutamate and aspartate (Akita and Okada, 2014). VRAC appear to be the primary pathway through which astrocytes release amino acid osmolytes following swelling in high-K^+ or hypoosmolar conditions (Kimelberg et al., 1990; Rutledge et al., 1998; Abdullaev et al., 2006). Moreover, VRAC play a pivotal role in the excitotoxic damage caused by ischemia (also known

experimentally as "oxygen-glucose deprivation", or OGD), a disorder which also induces rapid astrocytic swelling (Zhang et al., 2008; Risher et al., 2009). Importantly, VRAC in the CNS are likely not limited to astrocytes; neurons appear to also express VRAC, with similar activation by hypoosmolar solutions or OGD, but differing from astrocytic VRAC in specific pharmacology (Zhang et al., 2011). These data must be interpreted with some caution, however, as some of the most commonly-used VRAC antagonists have rather broad nonspecific effects (Evanko et al., 2004; see Chapter 3 for further discussion). At a bare minimum, it is clear that glutamate release through astrocytic VRAC is likely to be a key part of any disorder characterized by astrocytic swelling.

1.6. Astrocytes and NMDA receptor activation

There is little doubt that astrocytic glutamate can influence neuronal activity. In quiescent conditions, astrocytes are thought to maintain the so-called "ambient glutamate" concentration in the extracellular space (visible electrophysiologically as a tonic NMDA receptor-mediated current in neurons), possibly through release by VRAC or a related channel (Cavelier and Attwell, 2005; Le Meur et al., 2007). In hypoosmolar (pathological) conditions, spontaneous NMDA receptor-dependent slow inward currents (SICs) have also been observed in hippocampal CA1 neurons even when neuronal firing was blocked (Fiacco et al., 2007; Lauderdale et al., 2015), suggesting volume-dependent glutamate release from a nonsynaptic (presumably astrocytic) source. Previous groups had also found a similar effect of astrocytic glutamate, but under

isoosmotic conditions. In these studies, stimuli which evoked Ca^{2+} elevations in astrocytes including direct mechanical stimulation, group 1 metabotropic glutamate receptor (mGluR) agonists, or simply uncaging Ca^{2+} within the astrocyte were sufficient to induce SICs in nearby neurons (Angulo et al., 2004; Fellin et al., 2004; Tian et al., 2005; Fellin et al., 2006). From these data it was instead concluded that astrocyte Ca^{2+}-dependent neurotransmitter release was necessary for SIC generation. This conclusion was not compatible with hypoosmolar-induced SICs, which persisted even in transgenic mice which were incapable of astrocyte Ca^{2+} elevations (Fiacco et al., 2007). Perhaps most confusingly of all, one group found that neuronal SICs were produced following astrocytic Ca^{2+} elevations induced by activation of one receptor, but not by another (Shigetomi et al., 2008). Given these conflicting studies, it is quite interesting to note that VRAC, apart from being activated by membrane stretch, are also strongly potentiated by ATP activation of $P2Y_1$ receptors (which elevate intracellular Ca^{2+} as part of their signaling cascade), and could thus be activated by both Ca^{2+}-dependent and Ca^{2+}-independent means (Mongin and Kimelberg, 2005). Taken together, these studies raise the possibility that most or all astrocytic glutamate mediating SICs is released through VRAC opening.

SICs are unique in their relationship to seizure activity. A single astrocyte within the hippocampal CA1 area is can cover nearly 66,000 μm^3 of neuropil, ensheathing over 100,000 synapses (Bushong et al., 2002), allowing a single astrocyte to influence many neurons simultaneously. Accordingly, SICs have

been shown to be synchronous between neurons within ~100 μm, occurring in up to 12 neurons simultaneously (Angulo et al., 2004; Fellin et al., 2004). While such small synchronized populations of neurons may seem inconsequential, it is the gradual fusion of smaller synchronized populations into larger, "hypersynchronous" groups which eventually results in a seizure (Bikson et al., 2003; Jiruska et al., 2010).

1.7. A model for astrocytic involvement in seizures

Given that seizures are associated with astrocyte swelling, and swollen astrocytes release glutamate through volume-regulated channels, it seems likely that both play a pivotal role in epileptic disorders. We hypothesize that astrocyte swelling, and astrocyte glutamate release through swelling-activated channels, constitute primary factors in the initiation and maintenance of seizures. To study this overarching hypothesis, we have developed and utilized two models of astrocyte swelling and neuronal hyperexcitability in a hippocampal brain slice preparation. The basic tenets of these models are described below.

In the first of these two models (Figure 1.1A), excitability in CA1 neurons is elevated through the reduction of extracellular osmolarity (Lauderdale et al., 2015). Excess water (presumably) flows through AQP4 channels into astrocytes to produce astrocyte swelling. In the second model (Figure 1.1B), neuronal excitability is elevated through an increase in $[K^+]_o$. Potassium (presumably) flows across the astrocytic membrane through K_{ir} 4.1 channels, followed by osmotically-obligated water through AQP4. In both cases, astrocyte swelling

shrinks the extracellular space (increasing local concentrations of glutamate) and opens volume-regulated anion channels which release additional glutamate in the vicinity of adjacent extrasynaptic NMDA receptors, leading to SICs and neuronal synchrony (Figure 1.1C). We suggest that the firing of neurons within these local groups contributes to a positive feedback loop as additional K^+ and glutamate are released into the extracellular space, promoting further astrocyte swelling and thus further activation of VRAC. In addition, ephaptic interactions result in a gradual fusion of these smaller, SIC-driven neuronal populations. This feedback loop eventually results in synchronous bursting (the PDS) across the entirety of CA1, and seizures following thereafter.

In the following two studies, we utilize these two different models of neuronal hyperexcitability to explore the role of astrocyte swelling and glutamate release in seizure development. In the first, we use the hypoosmolar model of neuronal hyperexcitability as a "proof-of-principle" for rapid astrocyte swelling, determining the precise rate and degree of astrocyte swelling in relation to established effects on neuronal excitability, and exploring the role of AQP4 in hACSF-induced swelling. We also find some rather surprising effects on neuronal volume in hACSF, and investigate the possible causes. Our second study considers the role of astrocyte swelling and glutamate release in a high-$[K^+]_o$ model of epileptic seizure in a slice. Primary characteristics of this model are first discussed, including $[K^+]_o$ dose-dependence and pharmacology of observed epileptiform events. Further experiments are described which attempt to address

the contribution of astrocyte VRAC-dependent glutamate release, and astrocyte volume change, to high-$[K^+]_o$-induced epileptiform events. Finally, we address the possible caveats of these approaches and potential future directions.

1.8. References

Abdullaev IF, Rudkouskaya A, Schools GP, Kimelberg HK, Mongin AA (2006) Pharmacological comparison of swelling-activated excitatory amino acid release and Cl- currents in cultured rat astrocytes. J Physiol 572:677-689.

Akita T, Okada Y (2014) Characteristics and roles of the volume-sensitive outwardly rectifying (VSOR) anion channel in the central nervous system. Neuroscience 275:211-231.

Aldenkamp AP (2001) Cognitive and behavioural assessment in clinical trials: when should they be done? Epilepsy Res 45:155-157; discussion 159-161.

Aldenkamp AP, De Krom M, Reijs R (2003) Newer antiepileptic drugs and cognitive issues. Epilepsia 44 Suppl 4:21-29.

Amiry-Moghaddam M, Williamson A, Palomba M, Eid T, de Lanerolle NC, Nagelhus EA, Adams ME, Froehner SC, Agre P, Ottersen OP (2003) Delayed K+ clearance associated with aquaporin-4 mislocalization: phenotypic defects in brains of alpha-syntrophin-null mice. Proc Natl Acad Sci U S A 100:13615-13620.

Andrew RD (1991) Seizure and acute osmotic change: Clinical and neurophysiological aspects. In: Journal of the Neurological Sciences, pp 7-18.

Andrew RD, MacVicar BA (1994) Imaging cell volume changes and neuronal excitation in the hippocampal slice. Neuroscience 62:371-383.

Andrew RD, Lobinowich ME, Osehobo EP (1997) Evidence against volume regulation by cortical brain cells during acute osmotic stress. Exp Neurol 143:300-312.

Andrew RD, Labron MW, Boehnke SE, Carnduff L, Kirov SA (2007) Physiological evidence that pyramidal neurons lack functional water channels. Cereb Cortex 17:787-802.

Angulo MC, Kozlov AS, Charpak S, Audinat E (2004) Glutamate released from glial cells synchronizes neuronal activity in the hippocampus. J Neurosci 24:6920-6927.

Avoli M, Drapeau C, Perreault P, Louvel J, Pumain R (1990) Epileptiform activity induced by low chloride medium in the CA1 subfield of the hippocampal slice. J Neurophysiol 64:1747-1757.

Azouz R, Alroy G, Yaari Y (1997) Modulation of endogenous firing patterns by osmolarity in rat hippocampal neurones. J Physiol 502 (Pt 1):175-187.

Bedner P, Dupper A, Huttmann K, Muller J, Herde MK, Dublin P, Deshpande T, Schramm J, Haussler U, Haas CA, Henneberger C, Theis M, Steinhauser C (2015) Astrocyte uncoupling as a cause of human temporal lobe epilepsy. Brain 138:1208-1222.

Beghi E, Carpio A, Forsgren L, Hesdorffer DC, Malmgren K, Sander JW, Tomson T, Hauser WA (2010) Recommendation for a definition of acute symptomatic seizure. Epilepsia 51:671-675.

Behr C, Goltzene MA, Kosmalski G, Hirsch E, Ryvlin P (2016) Epidemiology of epilepsy. Revue neurologique 172:27-36.

Benfenati V, Ferroni S (2010) Water transport between CNS compartments: functional and molecular interactions between aquaporins and ion channels. Neuroscience 168:926-940.

Berg AT, Berkovic SF, Brodie MJ, Buchhalter J, Cross JH, van Emde Boas W, Engel J, French J, Glauser TA, Mathern GW, Moshe SL, Nordli D, Plouin P, Scheffer IE (2010) Revised terminology and concepts for organization of seizures and epilepsies: report of the ILAE Commission on Classification and Terminology, 2005-2009. Epilepsia 51:676-685.

Bikson M, Fox JE, Jefferys JG (2003) Neuronal aggregate formation underlies spatiotemporal dynamics of nonsynaptic seizure initiation. J Neurophysiol 89:2330-2333.

Binder DK, Oshio K, Ma T, Verkman AS, Manley GT (2004a) Increased seizure threshold in mice lacking aquaporin-4 water channels. NeuroReport 15:259-262.

Binder DK, Papadopoulos MC, Haggie PM, Verkman AS (2004b) In vivo measurement of brain extracellular space diffusion by cortical surface photobleaching. J Neurosci 24:8049-8056.

Binder DK, Yao X, Zador Z, Sick TJ, Verkman AS, Manley GT (2006) Increased seizure duration and slowed potassium kinetics in mice lacking aquaporin-4 water channels. GLIA 53:631-636.

Bordey A, Sontheimer H (1998) Properties of human glial cells associated with epileptic seizure foci. Epilepsy Res 32:286-303.

Boylan LS, Flint LA, Labovitz DL, Jackson SC, Starner K, Devinsky O (2004) Depression but not seizure frequency predicts quality of life in treatment-resistant epilepsy. Neurology 62:258-261.

Broberg M, Pope KJ, Lewis T, Olsson T, Nilsson M, Willoughby JO (2008) Cell swelling precedes seizures induced by inhibition of astrocytic metabolism. Epilepsy Res 80:132-141.

Bushong EA, Martone ME, Jones YZ, Ellisman MH (2002) Protoplasmic astrocytes in CA1 stratum radiatum occupy separate anatomical domains. J Neurosci 22:183-192.

Caspi A, Benninger F, Yaari Y (2009) KV7/M channels mediate osmotic modulation of intrinsic neuronal excitability. J Neurosci 29:11098-11111.

Cavelier P, Attwell D (2005) Tonic release of glutamate by a DIDS-sensitive mechanism in rat hippocampal slices. J Physiol 564:397-410.

Cavus I, Kasoff WS, Cassaday MP, Jacob R, Gueorguieva R, Sherwin RS, Krystal JH, Spencer DD, Abi-Saab WM (2005) Extracellular metabolites in the cortex and hippocampus of epileptic patients. Ann Neurol 57:226-235.

Chamberlin ME, Strange K (1989) Anisosmotic cell volume regulation: a comparative view. Am J Physiol 257:C159-173.

Chebabo SR, Hester MA, Aitken PG, Somjen GG (1995a) Hypotonic exposure enhances synaptic transmission and triggers spreading depression in rat hippocampal tissue slices. Brain Res 695:203-216.

Chebabo SR, Hester MA, Jing J, Aitken PG, Somjen GG (1995b) Interstitial space, electrical resistance and ion concentrations during hypotonia of rat hippocampal slices. J Physiol 487 (Pt 3):685-697.

Chever O, Djukic B, McCarthy KD, Amzica F (2010) Implication of Kir4.1 channel in excess potassium clearance: an in vivo study on anesthetized glial-conditional Kir4.1 knock-out mice. J Neurosci 30:15769-15777.

Choi DW (1992) Excitotoxic cell death. Journal of neurobiology 23:1261-1276.

Cohen I, Navarro V, Clemenceau S, Baulac M, Miles R (2002) On the origin of interictal activity in human temporal lobe epilepsy in vitro. Science 298:1418-1421.

Commission on Classification and Terminology of the International League Against Epilepsy (1981) Proposal for revised clinical and

electroencephalographic classification of epileptic seizures. Epilepsia 22:489-501.

Commission on Classification and Terminology of the International League Against Epilepsy (1989) Proposal for revised classification of epilepsies and epileptic syndromes. Epilepsia 30:389-399.

Connors NC, Adams ME, Froehner SC, Kofuji P (2004) The potassium channel Kir4.1 associates with the dystrophin-glycoprotein complex via alpha-syntrophin in glia. J Biol Chem 279:28387-28392.

Curia G, Longo D, Biagini G, Jones RS, Avoli M (2008) The pilocarpine model of temporal lobe epilepsy. J Neurosci Methods 172:143-157.

D'Ambrosio R, Gordon DS, Winn HR (2002) Differential role of KIR channel and Na(+)/K(+)-pump in the regulation of extracellular K(+) in rat hippocampus. J Neurophysiol 87:87-102.

Devinsky O (2004) Effects of Seizures on Autonomic and Cardiovascular Function. Epilepsy Curr 4:43-46.

Dichter M, Spencer WA (1969) Penicillin-induced interictal discharges from the cat hippocampus. I. Characteristics and topographical features. J Neurophysiol 32:649-662.

Dietzel I, Heinemann U, Hofmeier G, Lux HD (1980) Transient changes in the size of the extracellular space in the sensorimotor cortex of cats in relation to stimulus-induced changes in potassium concentration. Exp Brain Res 40:432-439.

Djukic B, Casper KB, Philpot BD, Chin LS, McCarthy KD (2007) Conditional knock-out of Kir4.1 leads to glial membrane depolarization, inhibition of potassium and glutamate uptake, and enhanced short-term synaptic potentiation. J Neurosci 27:11354-11365.

Dudek FE, Snow RW, Taylor CP (1986) Role of electrical interactions in synchronization of epileptiform bursts. Adv Neurol 44:593-617.

Dudek FE, Obenaus A, Tasker JG (1990) Osmolality-induced changes in extracellular volume alter epileptiform bursts independent of chemical synapses in the rat: importance of non-synaptic mechanisms in hippocampal epileptogenesis. Neurosci Lett 120:267-270.

During MJ, Spencer DD (1993) Extracellular hippocampal glutamate and spontaneous seizure in the conscious human brain. Lancet 341:1607-1610.

Eid T, Thomas MJ, Spencer DD, Runden-Pran E, Lai JC, Malthankar GV, Kim JH, Danbolt NC, Ottersen OP, de Lanerolle NC (2004) Loss of glutamine synthetase in the human epileptogenic hippocampus: possible mechanism for raised extracellular glutamate in mesial temporal lobe epilepsy. Lancet 363:28-37.

Eid T, Lee TS, Thomas MJ, Amiry-Moghaddam M, Bjornsen LP, Spencer DD, Agre P, Ottersen OP, de Lanerolle NC (2005) Loss of perivascular aquaporin 4 may underlie deficient water and K+ homeostasis in the human epileptogenic hippocampus. Proc Natl Acad Sci U S A 102:1193-1198.

Eriksson PS, Nilsson M, Wagberg M, Ronnback L, Hansson E (1992) Volume regulation of single astroglial cells in primary culture. Neurosci Lett 143:195-199.

Evanko DS, Zhang Q, Zorec R, Haydon PG (2004) Defining pathways of loss and secretion of chemical messengers from astrocytes. GLIA 47:233-240.

Fellin T, Pascual O, Gobbo S, Pozzan T, Haydon PG, Carmignoto G (2004) Neuronal synchrony mediated by astrocytic glutamate through activation of extrasynaptic NMDA receptors. Neuron 43:729-743.

Fellin T, Gomez-Gonzalo M, Gobbo S, Carmignoto G, Haydon PG (2006) Astrocytic glutamate is not necessary for the generation of epileptiform neuronal activity in hippocampal slices. J Neurosci 26:9312-9322.

Fiacco TA, Agulhon C, Taves SR, Petravicz J, Casper KB, Dong X, Chen J, McCarthy KD (2007) Selective stimulation of astrocyte calcium in situ does not affect neuronal excitatory synaptic activity. Neuron 54:611-626.

Fields RD, Ni Y (2010) Nonsynaptic communication through ATP release from volume-activated anion channels in axons. Sci Signal 3:ra73.

Fisher RS, Pedley TA, Moody WJ, Jr., Prince DA (1976) The role of extracellular potassium in hippocampal epilepsy. Arch Neurol 33:76-83.

Fisher RS, van Emde Boas W, Blume W, Elger C, Genton P, Lee P, Engel J, Jr. (2005) Epileptic seizures and epilepsy: definitions proposed by the International League Against Epilepsy (ILAE) and the International Bureau for Epilepsy (IBE). Epilepsia 46:470-472.

Fisher RS, Acevedo C, Arzimanoglou A, Bogacz A, Cross JH, Elger CE, Engel J, Jr., Forsgren L, French JA, Glynn M, Hesdorffer DC, Lee BI, Mathern GW, Moshe SL, Perucca E, Scheffer IE, Tomson T, Watanabe M, Wiebe S (2014a) ILAE official report: a practical clinical definition of epilepsy. Epilepsia 55:475-482.

Fisher RS, Scharfman HE, deCurtis M (2014b) How can we identify ictal and interictal abnormal activity? Advances in experimental medicine and biology 813:3-23.

Franco R, Quesada O, Pasantes-Morales H (2000) Efflux of osmolyte amino acids during isovolumic regulation in hippocampal slices. J Neurosci Res 61:701-711.

Goldstein J, Slomski J (2008) Epileptic spasms: a variety of etiologies and associated syndromes. Journal of child neurology 23:407-414.

Heuser K, Eid T, Lauritzen F, Thoren AE, Vindedal GF, Tauboll E, Gjerstad L, Spencer DD, Ottersen OP, Nagelhus EA, de Lanerolle NC (2012) Loss of perivascular Kir4.1 potassium channels in the sclerotic hippocampus of patients with mesial temporal lobe epilepsy. J Neuropathol Exp Neurol 71:814-825.

Hirrlinger PG, Wurm A, Hirrlinger J, Bringmann A, Reichenbach A (2008) Osmotic swelling characteristics of glial cells in the murine hippocampus, cerebellum, and retina in situ. J Neurochem 105:1405-1417.

Hirtz D, Thurman DJ, Gwinn-Hardy K, Mohamed M, Chaudhuri AR, Zalutsky R (2007) How common are the "common" neurologic disorders? Neurology 68:326-337.

Hoffmann EK, Lambert IH, Pedersen SF (2009) Physiology of cell volume regulation in vertebrates. Physiol Rev 89:193-277.

Holthoff K, Witte OW (1996) Intrinsic optical signals in rat neocortical slices measured with near-infrared dark-field microscopy reveal changes in extracellular space. J Neurosci 16:2740-2749.

Huang R, Bossut DF, Somjen GG (1997) Enhancement of whole cell synaptic currents by low osmolarity and by low [NaCl] in rat hippocampal slices. J Neurophysiol 77:2349-2359.

Hyzinski-Garcia MC, Rudkouskaya A, Mongin AA (2014) LRRC8A protein is indispensable for swelling-activated and ATP-induced release of excitatory amino acids in rat astrocytes. J Physiol 592:4855-4862.

Illarionova NB, Gunnarson E, Li Y, Brismar H, Bondar A, Zelenin S, Aperia A (2010) Functional and molecular interactions between aquaporins and Na,K-ATPase. Neuroscience 168:915-925.

Iwasa K, Tasaki I, Gibbons RC (1980) Swelling of nerve fibers associated with action potentials. Science 210:338-339.

Jefferys JG, Haas HL (1982) Synchronized bursting of CA1 hippocampal pyramidal cells in the absence of synaptic transmission. Nature 300:448-450.

Jensen MS, Yaari Y (1988) The relationship between interictal and ictal paroxysms in an in vitro model of focal hippocampal epilepsy. Ann Neurol 24:591-598.

Jensen MS, Yaari Y (1997) Role of intrinsic burst firing, potassium accumulation, and electrical coupling in the elevated potassium model of hippocampal epilepsy. J Neurophysiol 77:1224-1233.

Jiruska P, Csicsvari J, Powell AD, Fox JE, Chang WC, Vreugdenhil M, Li X, Palus M, Bujan AF, Dearden RW, Jefferys JG (2010) High-frequency network activity, global increase in neuronal activity, and synchrony expansion precede epileptic seizures in vitro. J Neurosci 30:5690-5701.

Kilb W, Dierkes PW, Sykova E, Vargova L, Luhmann HJ (2006) Hypoosmolar conditions reduce extracellular volume fraction and enhance epileptiform activity in the CA3 region of the immature rat hippocampus. J Neurosci Res 84:119-129.

Kimelberg HK, Goderie SK, Higman S, Pang S, Waniewski RA (1990) Swelling-induced release of glutamate, aspartate, and taurine from astrocyte cultures. J Neurosci 10:1583-1591.

Kimelberg HK (1995) Current concepts of brain edema. Review of laboratory investigations. J Neurosurg 83:1051-1059.

Kimelberg HK (2005) Astrocytic swelling in cerebral ischemia as a possible cause of injury and target for therapy. GLIA 50:389-397.

Kitaura H, Tsujita M, Huber VJ, Kakita A, Shibuki K, Sakimura K, Kwee IL, Nakada T (2009) Activity-dependent glial swelling is impaired in aquaporin-4 knockout mice. Neurosci Res 64:208-212.

Kivi A, Lehmann TN, Kovacs R, Eilers A, Jauch R, Meencke HJ, von Deimling A, Heinemann U, Gabriel S (2000) Effects of barium on stimulus-induced

rises of [K+]o in human epileptic non-sclerotic and sclerotic hippocampal area CA1. Eur J Neurosci 12:2039-2048.

Kreisman NR, Olson JE (2003) Taurine enhances volume regulation in hippocampal slices swollen osmotically. Neuroscience 120:635-642.

Kwan P, Brodie MJ (2000) Early identification of refractory epilepsy. N Engl J Med 342:314-319.

Kwan P, Brodie MJ (2001a) Neuropsychological effects of epilepsy and antiepileptic drugs. Lancet 357:216-222.

Kwan P, Brodie MJ (2001b) Effectiveness of first antiepileptic drug. Epilepsia 42:1255-1260.

Kwan P, Sills GJ, Brodie MJ (2001) The mechanisms of action of commonly used antiepileptic drugs. Pharmacology & Therapeutics 90:21-34.

Lagae L (2006) Cognitive side effects of anti-epileptic drugs. The relevance in childhood epilepsy. Seizure 15:235-241.

Larsen BR, Assentoft M, Cotrina ML, Hua SZ, Nedergaard M, Kaila K, Voipio J, MacAulay N (2014) Contributions of the Na(+)/K(+)-ATPase, NKCC1, and Kir4.1 to hippocampal K(+) clearance and volume responses. GLIA 62:608-622.

Lauderdale K, Murphy T, Tung T, Davila D, Binder DK, Fiacco TA (2015) Osmotic Edema Rapidly Increases Neuronal Excitability Through Activation of NMDA Receptor-Dependent Slow Inward Currents in Juvenile and Adult Hippocampus. ASN Neuro 7.

Laxer KD, Trinka E, Hirsch LJ, Cendes F, Langfitt J, Delanty N, Resnick T, Benbadis SR (2014) The consequences of refractory epilepsy and its treatment. Epilepsy Behav 37:59-70.

Le Meur K, Galante M, Angulo MC, Audinat E (2007) Tonic activation of NMDA receptors by ambient glutamate of non-synaptic origin in the rat hippocampus. J Physiol 580:373-383.

Lee JM, Zipfel GJ, Choi DW (1999) The changing landscape of ischaemic brain injury mechanisms. Nature 399:A7-14.

Levesque M, Avoli M (2013) The kainic acid model of temporal lobe epilepsy. Neuroscience and biobehavioral reviews 37:2887-2899.

Macaulay N, Zeuthen T (2012) Glial K(+) clearance and cell swelling: key roles for cotransporters and pumps. Neurochem Res 37:2299-2309.

Matsumoto H, Marsan CA (1964a) Cortical Cellular Phenomena in Experimental Epilepsy: Ictal Manifestations. Exp Neurol 9:305-326.

Matsumoto H, Marsan CA (1964b) Cortical Cellular Phenomena in Experimental Epilepsy: Interictal Manifestations. Exp Neurol 9:286-304.

Meeks JP, Mennerick S (2007) Astrocyte membrane responses and potassium accumulation during neuronal activity. Hippocampus 17:1100-1108.

Mody I, Lambert JD, Heinemann U (1987) Low extracellular magnesium induces epileptiform activity and spreading depression in rat hippocampal slices. J Neurophysiol 57:869-888.

Mongin AA, Kimelberg HK (2005) ATP regulates anion channel-mediated organic osmolyte release from cultured rat astrocytes via multiple Ca2+-sensitive mechanisms. American journal of physiology Cell physiology 288:C204-213.

Moody WJ, Futamachi KJ, Prince DA (1974) Extracellular potassium activity during epileptogenesis. Exp Neurol 42:248-263.

Morimoto K, Fahnestock M, Racine RJ (2004) Kindling and status epilepticus models of epilepsy: rewiring the brain. Prog Neurobiol 73:1-60.

Nagelhus EA, Mathiisen TM, Ottersen OP (2004) Aquaporin-4 in the central nervous system: cellular and subcellular distribution and coexpression with KIR4.1. Neuroscience 129:905-913.

Ngugi AK, Bottomley C, Kleinschmidt I, Sander JW, Newton CR (2010) Estimation of the burden of active and life-time epilepsy: a meta-analytic approach. Epilepsia 51:883-890.

Olson JE, Alexander C, Feller DA, Clayman ML, Ramnath EM (1995) Hypoosmotic volume regulation of astrocytes in elevated extracellular potassium. J Neurosci Res 40:333-342.

Olsson T, Broberg M, Pope KJ, Wallace A, Mackenzie L, Blomstrand F, Nilsson M, Willoughby JO (2006) Cell swelling, seizures and spreading depression: an impedance study. Neuroscience 140:505-515.

Papadopoulos MC, Verkman AS (2007) Aquaporin-4 and brain edema. Pediatric nephrology 22:778-784.

Papadopoulos MC, Verkman AS (2013) Aquaporin water channels in the nervous system. Nat Rev Neurosci 14:265-277.

Pasantes-Morales H, Lezama RA, Ramos-Mandujano G, Tuz KL (2006) Mechanisms of cell volume regulation in hypo-osmolality. Am J Med 119:S4-11.

Pasantes-Morales H, Cruz-Rangel S (2010) Brain volume regulation: osmolytes and aquaporin perspectives. Neuroscience 168:871-884.

Proper EA, Hoogland G, Kappen SM, Jansen GH, Rensen MG, Schrama LH, van Veelen CW, van Rijen PC, van Nieuwenhuizen O, Gispen WH, de Graan PN (2002) Distribution of glutamate transporters in the hippocampus of patients with pharmaco-resistant temporal lobe epilepsy. Brain 125:32-43.

Qiu Z, Dubin AE, Mathur J, Tu B, Reddy K, Miraglia LJ, Reinhardt J, Orth AP, Patapoutian A (2014) SWELL1, a plasma membrane protein, is an essential component of volume-regulated anion channel. Cell 157:447-458.

Risher WC, Andrew RD, Kirov SA (2009) Real-time passive volume responses of astrocytes to acute osmotic and ischemic stress in cortical slices and in vivo revealed by two-photon microscopy. GLIA 57:207-221.

Roper SN, Obenaus A, Dudek FE (1992) Osmolality and nonsynaptic epileptiform bursts in rat CA1 and dentate gyrus. Ann Neurol 31:81-85.

Rosen AS, Andrew RD (1990) Osmotic effects upon excitability in rat neocortical slices. Neuroscience 38:579-590.

Rowntree LG (1926) The effects on mammals of the administration of excessive quantities of water. Journal of Pharmacology and Experimental Therapeutics 29:135-159.

Rungta RL, Choi HB, Tyson JR, Malik A, Dissing-Olesen L, Lin PJ, Cain SM, Cullis PR, Snutch TP, MacVicar BA (2015) The cellular mechanisms of neuronal swelling underlying cytotoxic edema. Cell 161:610-621.

Rutecki PA, Lebeda FJ, Johnston D (1985) Epileptiform activity induced by changes in extracellular potassium in hippocampus. J Neurophysiol 54:1363-1374.

Rutecki PA, Lebeda FJ, Johnston D (1987) 4-Aminopyridine produces epileptiform activity in hippocampus and enhances synaptic excitation and inhibition. J Neurophysiol 57:1911-1924.

Rutecki PA, Lebeda FJ, Johnston D (1990) Epileptiform activity in the hippocampus produced by tetraethylammonium. J Neurophysiol 64:1077-1088.

Rutledge EM, Aschner M, Kimelberg HK (1998) Pharmacological characterization of swelling-induced D-[3H]aspartate release from primary astrocyte cultures. Am J Physiol 274:C1511-1520.

Saly V, Andrew RD (1993) CA3 neuron excitation and epileptiform discharge are sensitive to osmolality. J Neurophysiol 69:2200-2208.

Shigetomi E, Bowser DN, Sofroniew MV, Khakh BS (2008) Two forms of astrocyte calcium excitability have distinct effects on NMDA receptor-mediated slow inward currents in pyramidal neurons. J Neurosci 28:6659-6663.

Song Y, Gunnarson E (2012) Potassium dependent regulation of astrocyte water permeability is mediated by cAMP signaling. PLoS ONE 7:e34936.

Stafstrom CE, Carmant L (2015) Seizures and epilepsy: an overview for neuroscientists. Cold Spring Harbor perspectives in medicine 5.

Staley K, Hellier JL, Dudek FE (2005) Do interictal spikes drive epileptogenesis? Neuroscientist 11:272-276.

Stephen LJ, Kwan P, Brodie MJ (2001) Does the cause of localisation-related epilepsy influence the response to antiepileptic drug treatment? Epilepsia 42:357-362.

Strohschein S, Huttmann K, Gabriel S, Binder DK, Heinemann U, Steinhauser C (2011) Impact of aquaporin-4 channels on K+ buffering and gap junction coupling in the hippocampus. GLIA 59:973-980.

Tancredi V, Avoli M (1987) Control of spontaneous epileptiform discharges by extracellular potassium: an "in vitro" study in the CA1 subfield of the hippocampal slice. Exp Brain Res 67:363-372.

Tancredi V, Hwa GG, Zona C, Brancati A, Avoli M (1990) Low magnesium epileptogenesis in the rat hippocampal slice: electrophysiological and pharmacological features. Brain Res 511:280-290.

Tang X, Taniguchi K, Kofuji P (2009) Heterogeneity of Kir4.1 channel expression in glia revealed by mouse transgenesis. GLIA 57:1706-1715.

Thrane AS, Rangroo Thrane V, Nedergaard M (2014) Drowning stars: reassessing the role of astrocytes in brain edema. Trends Neurosci 37:620-628.

Tian G-F, Azmi H, Takano T, Xu Q, Peng W, Lin J, Oberheim N, Lou N, Wang X, Zielke HR, Kang J, Nedergaard M (2005) An astrocytic basis of epilepsy. Nature medicine 11:973-981.

Traynelis SF, Dingledine R (1988) Potassium-induced spontaneous electrographic seizures in the rat hippocampal slice. J Neurophysiol 59:259-276.

Traynelis SF, Dingledine R (1989) Role of extracellular space in hyperosmotic suppression of potassium-induced electrographic seizures. J Neurophysiol 61:927-938.

Vitarella D, DiRisio DJ, Kimelberg HK, Aschner M (1994) Potassium and taurine release are highly correlated with regulatory volume decrease in neonatal primary rat astrocyte cultures. J Neurochem 63:1143-1149.

Walz W, Hinks EC (1985) Carrier-mediated KCl accumulation accompanied by water movements is involved in the control of physiological K+ levels by astrocytes. Brain Res 343:44-51.

Walz W (2000) Role of astrocytes in the clearance of excess extracellular potassium. Neurochem Int 36:291-300.

Wetherington J, Serrano G, Dingledine R (2008) Astrocytes in the Epileptic Brain. In: Neuron, pp 168-178.

Yaari Y, Konnerth A, Heinemann U (1986) Nonsynaptic epileptogenesis in the mammalian hippocampus in vitro. II. Role of extracellular potassium. J Neurophysiol 56:424-438.

Yamamoto C (1972) Intracellular study of seizure-like afterdischarges elicited in thin hippocampal sections in vitro. Exp Neurol 35:154-164.

Zhang H, Cao HJ, Kimelberg HK, Zhou M (2011) Volume regulated anion channel currents of rat hippocampal neurons and their contribution to oxygen-and-glucose deprivation induced neuronal death. PLoS ONE 6:e16803.

Zhang Y, Zhang H, Feustel PJ, Kimelberg HK (2008) DCPIB, a specific inhibitor of volume regulated anion channels (VRACs), reduces infarct size in MCAo and the release of glutamate in the ischemic cortical penumbra. Exp Neurol 210:514-520.
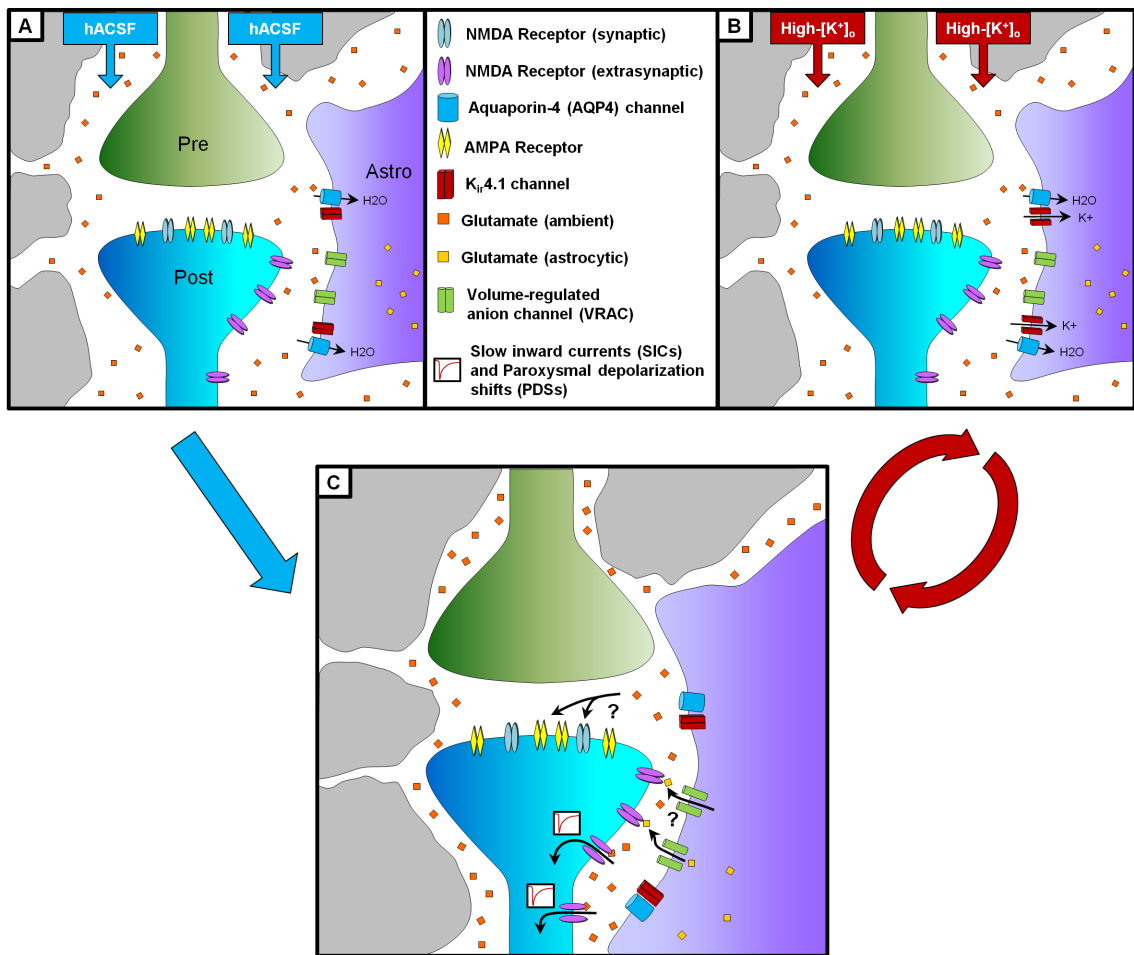
Figure 1.1. Hypothesized model of astrocyte swelling and glutamate release in two different models of neuronal hyperexcitability.
In a hypoosmolar model of neuronal hyperexcitability (A), astrocytes swell through direct water influx facilitated by the water channel AQP4. By contrast, the high-$[K^+]_o$ model (B) causes astrocyte swelling through initial influx of K^+ through K_{ir} 4.1 channels, followed by osmotically-obligated water through nearby AQP4 channels. In both cases (C), astrocyte swelling leads to a decrease in extracellular space (which increases local glutamate concentrations and enhances neuronal excitability), and opening of astrocytic VRAC, resulting in locally-synchronous currents (SICs) in neurons within the domain of a given astrocyte. Neuronal firing results in a positive feedback loop as glutamate and additional K^+ are released into the extracellular space, causing additional astrocyte swelling and subsequent VRAC activation. As ephaptic interactions cause neuronal firing to become synchronized, this system is driven from locally-synchronous activity (SICs) to global hypersynchrony (PDSs) and finally into a seizure.

Chapter 2: Hippocampal astrocytes and neurons exhibit similar swelling profiles in a hypoosmolar model of neuronal hyperexcitability

2.1. Abstract

Normal functioning of the nervous system is critically dependent on the balance of water and ions in the extracellular space. Pathological reductions in brain interstitial osmolarity result in osmotically-driven flux of water into cells, causing cellular edema which reduces the extracellular space and increases neuronal excitability, increasing the risk of seizures. In general, astrocytes are thought to be the most susceptible to cellular edema due to their expression of the water channel aquaporin-4 (AQP4), which is not expressed by neurons. The apparent resistance of pyramidal neurons to osmotic swelling has been attributed to their lack of functional water channels, but there is some disagreement as to whether neurons are entirely osmoresistant. Studies which have examined astrocyte or neuron volume in hypoosmolar conditions have generally lacked the temporal resolution to examine volume changes over the first few minutes. In this study we filled this gap by examining the volume responses of both astrocytes and neurons in hypoosmolar ACSF (hACSF). Whole-cell patch clamp, SR-101 dye loading, or transgenic expression of eGFP was used to fluorescently label stratum radiatum (s.r.) astrocytes or CA1 pyramidal neurons in acute mouse hippocampal slices. Soma area was measured by taking rapid image stacks through individual cells at 1-minute intervals during exposure to 17% or 40%

hypoosmolar artificial cerebrospinal fluid (hACSF). Astrocytes and neurons swelled significantly within 1 minute of 17 or 40% hACSF application, in both juvenile and adult hippocampal slices. Interestingly, genetic deletion of AQP4 did not inhibit, but rather augmented, astrocyte swelling. Our results indicate that neurons are just as osmosensitive as astrocytes in hypoosmolar conditions, contrary to a widely-accepted literature. Neuronal swelling was neither inhibited by TTX, nor by antagonists of NMDA or AMPA receptors, suggesting that neuronal swelling was not occurring as a result of excitotoxicity. Finally, isoosmolar elevation of $[K^+]_o$ to 6.5 mM was found to induce selective swelling of astrocytes. These data suggest that neurons are not osmoresistant as previously reported, and that osmotic swelling is driven by an AQP4-independent mechanism.

2.2. Introduction

Acute reduction of plasma osmolarity in humans is a medical emergency, often resulting in seizures and sometimes coma or even death (Andrew, 1991; Castilla-Guerra et al., 2006). Such deleterious effects on the CNS can be attributed to the sudden change in osmotic pressure within the interstitial space of the brain, which causes cells to take on water and swell, otherwise known as "cellular" or "cytotoxic" edema (Kimelberg, 1995). Tissue swelling resulting from cellular edema has been observed in many studies examining the effect of hypoosmolar conditions on excitability (Andrew and MacVicar, 1994; Chebabo et al., 1995b; Kilb et al., 2006). Given that cell swelling necessarily shrinks the extracellular space (ECS) and increases tissue resistance, hypoosmolar conditions amplify nonsynaptic excitability in neurons and increase susceptibility to seizure (Rosen and Andrew, 1990; Roper et al., 1992; Lauderdale et al., 2015).

Most cellular edema in the brain is thought to be driven by water influx through aquaporin-4 (AQP4) channels, which are expressed primarily by astrocytes (Nagelhus et al., 2004). Knockout of AQP4 inhibits the tissue swelling normally associated with seizures (Binder et al., 2004b), stroke (Katada et al., 2014), and other models of cytotoxic edema (Papadopoulos and Verkman, 2013). In normal physiology, AQP4 is important for water homeostasis in the brain, and appears to be required for the activity-dependent influxes of water which occur alongside potassium uptake and buffering (Amiry-Moghaddam et al.,

2003; Eid et al., 2005; Illarionova et al., 2010; Strohschein et al., 2011) Thus, astrocytic swelling via AQP4-mediated water uptake is well-established as both a physiological and pathological phenomenon.

Neuronal volume changes, by contrast, are considered to be almost solely pathological. Neuronal somata will rapidly swell in cases of excitotoxic damage (Choi, 1992; Andrew et al., 2007; Liang et al., 2007; Risher et al., 2009) but appear very resilient to hypoosmolar swelling, an expected consequence of nonfunctional water channels (Andrew et al., 2007; Caspi et al., 2009). This has led to the conclusion that hypoosmolar conditions result in glial swelling alone (Andrew et al., 2007; Risher et al., 2009). However, this conclusion is opposed by earlier reports showing swelling under hypoosmolar stress in isolated neurons in culture (Aitken et al., 1998; Somjen, 1999; Borgdorff et al., 2000). In addition, studies which have directly examined hypoosmolar swelling of neurons or astrocytes (Andrew et al., 2007; Hirrlinger et al., 2008; Risher et al., 2009) often lack temporal resolution below approximately 5 minutes. We have recently found that neuronal excitability increases significantly within 2 minutes of hypoosmolar ACSF (hACSF) exposure, suggesting that constriction of the ECS occurs rapidly during hACSF application (Lauderdale et al., 2015). Determining the precise contribution of the cellular swelling and reduction of the ECS to these rapid changes requires an equally rapid measurement of cell volume.

In the present study, we used confocal imaging to quantify stratum radiatum (s.r.) astrocyte and CA1 pyramidal neuron volume during repeated 5-7

minute hypoosmolar ACSF (hACSF) applications, at 1-minute resolution. Despite literature to the contrary, we found that CA1 neurons and s.r. astrocytes swell almost equally in both 17% and 40% hACSF over this time course, only differing slightly in their rate of swelling. Neuronal swelling did not differ between adult and juvenile animals, nor was it blocked by NMDA receptor antagonists, AMPA/Kainate receptor antagonists, or TTX. In $AQP4^{-/-}$ animals, we found that astrocyte hACSF-induced volume increases were augmented rather than inhibited. Finally, we show that astrocytes can be <u>selectively</u> swollen by raising $[K^+]_o$ to 6.5 mM, with no apparent change in neuronal volume. These data call into question the idea that neurons are osmoresistant and suggest that neurons and astrocytes may share a common, AQP4-independent swelling pathway in hypoosmolar conditions, whereas swelling in elevated K^+ conditions is astrocyte selective.

2.3. Methods

All animals and protocols used in the following experiments were approved by the Institutional Animal Care and Use Committee at UCR.

2.3.1. Slice preparation in juveniles

Hippocampal slices were prepared from juvenile (15-21 day old) C57Bl/6J mice as previously described (Xie et al., 2014). In some experiments, $AQP4^{-/-}$ or

Thy1-eGFP mice were used; both of these genotypes were on a C57Bl/6J background and did not exhibit any obvious phenotypic or behavioral differences from wild-type. Animals were deeply anesthetized under isofluorane and decapitated, and brains were quickly removed into ice-cold "slicing buffer" containing (in mM): 125 NaCl, 2.5 KCl, 3.8 $MgCl_2$, 1.25 NaH_2PO_4, 26 $NaHCO_3$, 25 glucose, and 1.3 ascorbic acid, bubbled continuously with carbogen (95% O_2/5% CO_2). Parasagittal hippocampal slices (350 μm thick) were prepared using a Leica VT1200S vibratome and transferred to a recovery chamber containing standard artificial cerebrospinal fluid (sACSF), which was composed of (in mM): 125 mM NaCl, 2.5 KCl, 2.5 $CaCl_2$, 1.3 mM $MgCl_2$, 1.25 NaH_2PO_4, 26 $NaHCO_3$, and 15 glucose, bubbled continuously with carbogen (~299-303 mOsm). Slices were incubated in ACSF at 35º C for 45 minutes, then allowed to cool to room temperature for a minimum of 15 minutes before being transferred to a recording chamber for experiments.

In some cases, SR-101 was used during incubation to selectively stain astrocytes (Schnell et al., 2015). Incubation was adjusted as follows (Xie et al., 2014): After preparation, slices were transferred to a recovery chamber containing 1 μM SR-101, dissolved in a modified ACSF composed of (in mM): 125 NaCl, 2.5 KCl, 0.5 $CaCl_2$, 6 $MgCl_2$, 1.25 NaH_2PO_4, 26 $NaHCO_3$, 15 glucose and 1.3 ascorbic acid, bubbled continuously with carbogen, and incubated at 35º C for 35 minutes. Slices were subsequently transferred to the same modified ACSF without SR-101 for 10 more minutes at 35º C. Finally, slices were allowed

to cool to room temperature for 15 minutes before being transferred to sACSF. Slices were equilibrated in sACSF for at least 15 minutes prior to use.

2.3.2. Slice preparation in adults

Adult (2-5 month old) hippocampal slices were prepared from C57Bl/6J or Thy1-eGFP mice as previously described (Lauderdale et al., 2015). Adult slicing buffer contained (in mM): 87 NaCl, 75 sucrose, 2.5 KCl, 0.5 $CaCl_2$, 7 $MgCl_2$, 1.25 NaH_2PO_4, 25 $NaHCO_3$, 10 glucose, 1.3 ascorbic acid, 3.5 MOPS, and 100 µM kynurenic acid, bubbled continuously with carbogen, and was partially frozen to form an icy "slush". Slices were prepared as described above, and transferred to a recovery chamber containing adult slicing buffer at 35º C, bubbled with carbogen. After 45 minutes, slices were removed to room temperature and allowed to cool for 15 minutes before being transferred to a recovery chamber containing sACSF. Slices were allowed to equilibrate in sACSF for a minimum of 20 minutes before being used for experiments.

The SR-101 protocol was adapted for use in adults initially by simply adding SR-101 to the adult slicing buffer (which had a similar composition to the modified ACSF normally used in SR-101 loading). For unknown reasons, however, adult astrocytes proved far more resistant to SR-101 loading than did juvenile astrocytes, and often would show nearly no staining at all. This may have been partially a result of the different incubation ACSF, although a series of trials suggested the composition of this ACSF did not substantially impact loading

success. We eventually found moderate success through the combined effects of increasing SR-101 concentration (2-fold or more), and increasing SR-101 incubation time (up to 45 minutes). This would sometimes increase background fluorescence, but overall tended to result in deeper staining of astrocytes.

2.3.3. Solutions and drugs

"Normosmolar ACSF" (nACSF, ~298 mOsm) was used for baselines and wash periods, and was prepared the same as sACSF but without Mg^{2+}. 17% and 40% "hypoosmolar ACSF" (hACSF) were prepared by using deionized water to dilute nACSF by 17% (final osmolarity: ~250 mOsm) or 40% (final osmolarity: ~180 mOsm). "NaCl-reduced" hACSF (hACSF-N) was made by omitting 25 mM NaCl from nACSF. High-$[K^+]_o$ ACSF was prepared by addition of 4 mM KCl to nACSF, with an equimolar removal of NaCl. All nACSF, hACSF, hACSF-N and high-$[K^+]_o$ ACSF solutions contained 1 µM TTX (to block voltage-gated Na^+ channels) and 10 µM NBQX (to block AMPA/Kainate receptors) (Lauderdale et al., 2015). In some experiments, 50 µM AP5 (an NMDA-receptor antagonist) or 6 mM Mg^{2+} (sufficient to block NMDA receptors in the slice) were also added to the experimental solutions.

A series of experiments was also performed using a more "physiological" set of solutions, in which standard (or diluted) Mg^{2+} is included and TTX and NBQX are omitted. In these experiments, sACSF was instead used for the

baseline and wash periods, and diluted by 17% or 40% to generate hypoosmolar versions.

2.3.4. Patch-clamp of neurons and astrocytes

Hippocampal slices were transferred to a recording chamber and continuously perfused with room-temperature, oxygenated sACSF. CA1 pyramidal neurons and passive stratum radiatum (s.r.) astrocytes were patch clamped in whole-cell mode using a Multiclamp 700B amplifier and Digidata 1550 digitizer, connected to a computer running pClamp software version 10.4 or above and Multiclamp commander software. Patch pipettes were pulled from borosilicate glass using a Narshige PC-10 vertical micropipette puller. Neuronal patch pipettes had a resistance of ~3-6 MΩ when filled with an internal solution containing (in mM): 140 K-gluconate, 4 MgCl2, 0.4 EGTA, 4 Mg-ATP, 0.2 Na-GTP, 10 HEPES, and 10 phosphocreatine, pH 7.3 with KOH. Neuronal patch pipettes also contained the fluorophores Alexa 488 hydrazide (100-200 µM) or Alexa 594 hydrazide. Astrocytic patch pipettes had a resistance of ~5-8 MΩ when filled with an internal solution containing (in mM): 130 K-gluconate, 4 MgCl2, 10 HEPES, 10 glucose, 1.185 Mg-ATP, 10.55 phosphocreatine, and 0.1315 mg/ml creatine phosphokinase, pH 7.3 by KOH. Astrocytic pipettes also contained Alexa Fluor 488 dextran or Oregon Green 488 dextran, both 10 kDa in size to prevent their spread to neighboring astrocytes via gap junctions.

CA1 pyramidal neurons and passive stratum radiatum (s.r.) astrocytes were identified first by location and morphology under DIC optics, and confirmed via voltage step immediately upon whole-cell configuration. Pyramidal neurons generally rested at approximately -60.1 ± 0.6 mV and exhibited characteristic voltage-gated Na^+ and K^+ currents in response to a voltage step. Astrocytes were identified as passive if they exhibited a characteristically low input resistance, low resting membrane potential (-78.0 ± 1.2 mV) and lack of voltage-gated conductances in response to a voltage-step.

2.3.5. Dye loading and laser settings

Slices were visualized on an Olympus BX61 WI upright microscope equipped with UMPLFLN 10x (N.A. 0.3) and LUMFLN 60x (N.A. 1.1) water-immersion objectives and DIC optics, controlled by a PC with Fluoview software. After attaining whole-cell configuration and running voltage steps, astrocytes and neurons were voltage-clamped at -90 mV and -70 mV respectively (see chapter 3 methods), and allowed to rest for ≤ 5 minutes to allow for dye to diffuse into the cytoplasm. In the interest of limiting the amount of cytoplasm which was dialyzed by the internal solution, this time was kept to a minimum by occasional, quick confocal scans to check cell brightness. In many cases (mostly in neurons), the cell was bright enough almost immediately upon break-in, and the pipette could be withdrawn shortly after checking the voltage step. A smooth, stable "off-cell" and formation of a > 1GΩ seal during pipette removal was considered an

indicator of good cell health. In later experiments, we omitted patch clamp from our protocols and instead imaged from SR-101 labeled astrocytes (see above), or eGFP-expressing neurons. In these cases, cells were chosen based on their depth in the tissue, lack of obvious morphological abnormalities, and their brightness under our standard imaging settings (see below).

Alexa Fluor 488 dextran, Oregon green 488 dextran, Alexa Fluor 488, and eGFP were excited using a 488 nm argon laser and detected with a 503-548 nm bandpass filter, controlled through Olympus Fluoview software. Laser power was generally held at 2.0% or lower to limit photoxocitiy and photobleaching, with acquisition time = 8 μs/pixel (for astrocytes, which often loaded poorly with dextrans) or 4 μs/pixel (for neurons), and PMT voltage = 830. Gain and offset were occasionally adjusted to minor degrees to improve brightness, but were generally avoided for their unknown effects on later image analysis (below). Alexa Fluor 594 and SR-101 were excited using a 559 nm semiconductor laser and detected via 624-724 nm bandpass filter. PMT voltage and acquisition times for astrocytes and neurons (8 μs/pixel and 4 μs/pixel, respectively) were kept the same as above for consistency. Laser power, as above, was limited to avoid bleaching or cell damage (~1.5% or lower).

2.3.6. Experimental design

In a typical experiment, nACSF was washed into the slice for 10 minutes starting immediately after a successful outside-out patch (for patch-loaded cells),

or after identification of the cell to be imaged in the case of SR-101 or eGFP cells. In addition to washing Mg^{2+} out of the slice, this 10 minute period provided recovery time for patched cells prior to osmotic stress. At the end of this period, a baseline z-stack was taken. We have found that single images are insufficient for gathering the full extent of the cell body in the x-y plane (which is necessary for soma area measurements, our proxy for cell volume), and capturing the same plane of section within a cell repeatedly across time points is difficult due to swelling-induced shifts in the z-axis of a slice. Therefore, we instead opted for rapid z-stacks through the soma, at 1.0 µm intervals and a zoom level of 3.5x. To increase acquisition speed, the "clip scan" function was used to scan a rectangular ROI encompassing little more than the soma. With these settings, we could obtain full z-stacks through a cell soma within 15 seconds or less. For simplicity, a z-stack will hereafter be referred to as an "image".

After a baseline image was obtained, hACSF was applied for 5 minutes, during which an additional image was obtained at the end of each minute. HACSF was then "washed out" by re-application of nACSF for 5 minutes, at the end of which an additional image was taken. This sequence was repeated an additional 2 times to determine repeatability of effects on cell volume. Each subsequent application and wash was lengthened by 1 minute due to our observations (unpublished) that SIC activity required longer periods of hACSF over time.

2.3.7. Volume analysis protocol

Analysis of neuron and astrocyte volumes were performed in FIJI/ImageJ as previously described (Lauderdale et al., 2015). Our basic analysis protocol is diagrammed in Figure 2.1. Image stacks collected at each time point were z-adjusted to correct for cell "drift" caused by slice swelling during hypoosmolar treatment. Stacks were then concatenated into an x-y-z-t hyperstack (Figure 2.1B), and filtered to remove noise (median filter, 2 pixel diameter). A max-intensity z-projection was next made through this hyperstack, producing a 2D time series (Figure 2.1C), where each frame showed the full extent of the soma in the x-y plane at a given time point. This time series was then aligned (to correct for cell x-y drift), followed by cropping to remove blank areas left behind by the alignment step, and background subtracted using FIJI's built-in background subtraction tool (radius 50 pixels, sliding paraboloid). Finally, this time series was binarized using the "mean" thresholding algorithm (Figure 2.1D). An elliptical ROI was drawn such that it just encompassed the soma across all time points in the series, and thresholded pixels in this region were measured. Soma area was quantified as a percent of baseline for each cell, and measured as percent change over baseline for each time point in hACSF and wash.

2.3.8. Statistical Analysis

Statistical analysis was performed with SPSS Statistics 22 software (IBM). Mixed-design ANOVA was used for all tests of difference over time (within-

subject factor) and between treatments, genotypes or cell types (between-subject factor). Outliers were removed extremely rarely and on a case-by-case basis. Only a single outlier was removed from any particular group, and only (a) if its removal improved the reliability of ANOVA results (making group N more equal, reducing normality or homogeneity of variance violations, etc); and (b) if it was clearly a result of measurement error or another unknown problem. Outliers were not examined if neither normality nor homogeneity of variance assumptions were violated. Following a mixed ANOVA, a significant effect for time point would be further investigated by pairwise comparisons of each time point group to baseline. Multiple comparison adjustments for time point were performed by the Holm-Bonferroni method, a stepwise procedure with the same assumptions as the Bonferroni correction, but substantially more power for larger numbers of comparisons. Significant effects for group were further investigated (if more than 2 groups) using pairwise comparisons, with Bonferroni or Dunnett (Fig 2 only) corrections for multiple comparisons. Significant interactions were investigated in two steps. First, between-group simple effects were tested at each time point using Student's t-test (for 2 groups) or one-way ANOVA with pairwise comparisons, adjusted with Bonferroni correction (for 3 or more groups). In the rare cases when a group at a particular time point violated the normality assumption of the above tests, the Mann-Whitney U or Kruskal-Wallis H tests were used as the respective alternatives. Second, the within-subjects simple effects for an interaction were determined by splitting the file by group and

running each as an individual one-way repeated measures ANOVA, with Holm-Bonferroni-corrected pairwise comparisons as described above. This "split-file" method has the effect of splitting the error terms by group and was deemed to be more accurate than obtaining simple main effects within the original mixed ANOVA, as the latter uses a pooled error in its calculations. Significant differences are indicated at the $p < 0.05$ (*), $p < 0.01$ (**), and $p < 0.001$ (***) levels.

2.4. Results

In a previous study, we found heightened neuronal excitability occurring immediately after initiation of glial swelling, within minutes of exposing hippocampal slices to 17% or 40% hypoosmolar ACSF (Lauderdale et al., 2015). The primary focus of the current study was to examine in depth the volume changes exhibited by neural cells over this time period. Although some previous studies had indicated that hypoosmolarity should affect only astrocyte volume (Andrew et al., 2007; Caspi et al., 2009; Risher et al., 2009), conflicting reports suggested this may not always be the case (Aitken et al., 1998; Borgdorff et al., 2000; Boss et al., 2013). Therefore, we chose to examine volume responses by stratum radiatum (s.r.) astrocytes as well as CA1 pyramidal neurons. Standard hypoosmolar solutions (denoted hACSF for simplicity) were made by 17% or 40% dilution of standard ACSF with distilled water, and included TTX (1 µM),

NBQX (10 µM) and 0 mM Mg^{2+} by default. These conditions were chosen to match our previous work demonstrating significant stimulation of NMDA receptor currents by hACSF in CA1 pyramidal neurons (Lauderdale et al., 2015). The use of TTX to block neuronal firing also reduced the likelihood of spreading depression, a wave of depolarization and subsequent synaptic silencing which has sometimes been observed in hypoosmolar conditions (Chebabo et al., 1995a). Normal ACSF (nACSF), used for "wash" solutions, was not diluted but was otherwise identical to the above.

2.4.1. Astrocytes and neurons swell to approximately equal degrees in hypoosmolar ACSF

We first examined the volume responses of CA1 pyramidal neurons and stratum radiatum (s.r.) astrocytes to 17% and 40% hACSF (Figure 2.2). Neurons and astrocytes were initially labeled by patch-clamp dialysis of the fluorescent indicators Alexa Fluor 568 hydrazide or fluorescein dextran, respectively, and imaged using confocal microscopy (see Methods). As in our previous study, image stacks were taken through cell somata at 1-minute intervals starting at baseline ("0" minutes hACSF) and proceeding through 5 minutes of hACSF exposure, with a final image stack acquired after an additional 5 minutes in normosmolar ACSF (nACSF). Cell area was then quantified as percentage change from baseline for each time point (see Figure 2.1 and associated methods for additional details). In contrast with previous studies showing

neuronal osmoresistance in these conditions (Andrew et al., 2007; Caspi et al., 2009), we found that neurons rapidly swelled in response to both 17% and 40% hACSF, and this swelling was similar in both magnitude and timecourse to volume changes in astrocytes (Figure 2.2A, B). Neuronal soma area significantly increased above baseline within 1 minute in 17% (102.04 ± 0.33%, $p < 0.001$) or 40% (102.09 ± 0.72%, $p = 0.044$) hACSF, and continued to gradually increase to a maximum of 104.72 ± 0.41% in 17% hACSF and 110.51 ± 0.93% in 40% hACSF (Figure 2.2B). Neuronal swelling mostly (but not fully) recovered to baseline after a 5 minute wash period in nACSF (101.27 ± 0.39% in 17%, 102.70 ± 0.92% in 40% hACSF, $p < 0.05$ each). These data bore a remarkable similarity to our observations of s.r. astrocytes in the same conditions (Figure 2.2C, D). As reported in Lauderdale et al (2015), astrocytes also rapidly swelled in both doses of hACSF within the first minute ($p < 0.01$) and in a dose-dependent manner. In contrast to neurons, astrocytes fully recovered to baseline volume upon return to nACSF for 5 minutes.

Swelling of both neurons and astrocytes was also rapidly re-evokable by multiple applications of 40% (Figure 2.2E) or 17% hACSF (Figure 2.2F). No significant interaction was observed between cell type and time point (40% hACSF, $F_{(2.66, 34.64)} = 1.12$, $p = 0.351$; 17% hACSF, $F_{(4.11, 65.73)} = 1.12$, $p = 0.355$), suggesting largely identical swelling characteristics between the two cell types. The only apparent differences between neuron vs. astrocyte volume change seemed to be the rate of swelling (during the first few minutes of 40%

hACSF) and the rate of shrinking (following a 5 minute nACSF wash period). To examine rate of swelling, the response of both cell types during the first 3 minutes was averaged across all 3 trials. Percent changes were calculated relative to the nACSF application that immediately preceded each hACSF application. Comparison of average percent difference over these 3 minutes revealed a small, but significantly faster rate of astrocyte swelling compared to neurons ($F(1,13) = 5.81$, p = 0.032; Figure 2.2E, inset).

2.4.2. Neuronal swelling is not an artifact of excitotoxic damage

The unexpected finding that neurons swell with nearly identical characteristics as astrocytes was initially thought to be an artifact of our experimental conditions or technique. We therefore performed a number of additional experiments to determine if an experimental variable was causing neuronal swelling. First, neuronal swelling is a well-established consequence of excitotoxic activation of NMDA receptors (Rothman and Olney, 1987; Choi, 1992). Given the absence of Mg^{2+} in our solutions and the large, NMDA receptor-dependent SICs occurring in hACSF during cell swelling (Fiacco et al., 2007; Lauderdale et al., 2015), we reasoned that excitotoxic activation of the NMDA receptor could be partially responsible for the observed neuronal swelling. This would also explain the similar speed of SIC generation and neuronal swelling in 40% hACSF (Figure 2.3B). However, we found that neither the selective NMDA receptor antagonist DL-2-Amino-5-phosphonopentanoic acid (DL-APV; 50 µM),

nor 6 mM Mg^{2+}, both of which entirely block NMDA receptor-dependent currents (Dissing-Olesen et al., 2014; Lauderdale et al., 2015), had any effect on neuronal swelling in 40% hACSF (Figure 2.3A). We also tested a more "physiological" 40% hACSF containing Mg^{2+} (1.3 mM diluted by 40%) and in which TTX and NBQX were omitted. Neuronal swelling was slightly, but nonsignificantly, reduced in these conditions compared to Mg^{2+}-free 40% hACSF with TTX and NBQX (p < 0.089). The slight differences observed may result from the simultaneous change in multiple factors between standard 40% hACSF and 40% hACSF without antagonists. Further investigation of the individual and combined effects of each of these factors (TTX, NBQX, partial Mg^{2+}) was beyond the scope of this study. However, it was clear from these tests that neuronal swelling in 40% hACSF did not require NMDA receptor activation and occurred to a similar extent in more physiologically-relevant conditions.

2.4.3. Neuronal swelling is not an artifact of patch clamp

In some previous studies, volume changes in neurons and astrocytes were measured using cell-specific transgenic expression of fluorescent markers (Andrew et al., 2007; Risher et al., 2009). Although we had no reason to suspect damage to the cell, we also considered the possibility that the simple act of patch clamping neurons may make them more susceptible to hACSF-induced swelling. We tested this by using hippocampal slices from transgenic Thy1-eGFP mice (Feng et al., 2000). These mice express GFP in a sparse, random population of

pyramidal neurons (Figure 2.4A), making them ideal for isolating a single neuron in the densely packed pyramidal layer of the hippcampal CA1 region (Andrew et al., 2007). Just as observed for patch clamp-loaded neurons, Thy1 neurons in 40% hACSF swelled rapidly to a maximum of ~10% above baseline, and did not differ significantly from patch-loaded neurons in magnitude of volume response ($F(1,16)$ = 0.98, p = 0.336; Figure 2.4B). Thy1 neurons also did not differ from patch clamped neurons in their response to 17% hACSF ($F(1,16)$ = 1.36, p = 0.26; Data not shown). These tests made it clear that neuronal swelling was not an artifact of whole-cell dialysis of neurons with fluorescent indicator.

We also compared patch clamp-loaded astrocytes against those loaded with sulforhodamine-101 (SR-101), a dye that has been used to selectively label astrocytes. SR-101 astrocytes did not differ from patched astrocytes in their response to 40% hACSF (SR-101, N = 10; Patched, N = 7; p = 0.401), although they did appear to increase more than Thy1 neurons in the same conditions (in contrast with patch clamped astrocytes and neurons, which had shown no difference at either dose of hACSF). This could suggest that dialysis of astrocytes somewhat dampens osmolarity-driven volume changes. However, it is also possible that the more limited and variable fluorescence achieved with fluorescein dextran was more troublesome to analyze using our thresholding technique, resulting in smaller perceived volume changes in patch clamped astrocytes. Because of these differences, we took the additional precaution of

55

using non-patch clamp methods (GFP-expressing neurons and SR101-labeled astrocytes) to image cells for further experiments.

2.4.4. Neither neuronal nor glial swelling is age-dependent

In our attempts to determine the cause of neuronal swelling in hACSF, we considered the possibility that it was an age-dependent effect. All of our experiments to this point had been performed in slices from juvenile mice, age 15-21 days. In contrast, previous work showing a lack of neuronal swelling used tissue from animals at least 4 weeks of age, well past weaning age and approaching adulthood (Andrew et al., 2007). To test the possibility that neuronal swelling was an age-dependent effect, we repeated our previous 40% hACSF experiments using adult (2-5 month old) mice (Figure 2.5). Once again, 40% hACSF was prepared without antagonists and with diluted Mg^{2+}, as it provided greater physiological relevance for our results and, in this particular experiment, allowed us to directly compare our results with those from previous studies (Andrew et al., 2007; Risher et al., 2009). Just as observed in juveniles, adult CA1 neurons and s.r. astrocytes both swelled rapidly in response to 40% hACSF application (Figure 2.5A), and did not differ significantly in their timecourse ($F(1,17) = 0.61$, p = 0.447). Comparisons of average percent change between adults and juveniles revealed a marginally-significant increase in swelling for adult neurons over juvenile ($F(1,15) = 4.90$, p = 0.043), but no significant difference for astrocytes between the two age groups ($F(1,16) = 0.00$, p = 0.974).

These data further confirmed that the neuronal swelling observed was not an artifact of our experimental conditions. They further suggested that adult neurons might even be more prone to hACSF-induced swelling compared to juvenile neurons.

2.4.5. Astrocytes are more prone to swelling than neurons in the low-NaCl model of hypoosmolarity

As an alternative to the simple dilution model, many groups have prepared hypoosmolar ACSF by removal of NaCl (Borgdorff et al., 2000; Kilb et al., 2006; Gunnarson et al., 2008; Hirrlinger et al., 2008). NaCl reduction (referred to as hACSF-N, for this section) and ACSF dilution (hACSF) have both been found to swell cells and elevate neuronal excitability (Fiacco et al., 2007; Lauderdale et al., 2015), and both are reliable models of osmotic edema in astrocytes (Hirrlinger et al., 2008; Risher et al., 2009). However, hACSF-N conditions have been reported to cause a "regulatory volume decrease" (RVD) over time, wherein tissue regains its normal volume even in the continued presence of hypoosmolar conditions (Andrew et al., 1997; Franco et al., 2000). We hypothesized that any acute changes in cell volume would also likely reflect these differences. Similar to what we observed in 17% hACSF, neurons in 17% hACSF-N swelled significantly above baseline by the first minute (Figure 2.6A; $101.52 \pm 0.39\%$, $p = 0.038$), reached a maximum of approximately 104% within 5 minutes ($p = 0.01$), and returned to baseline after 5 minutes in nACSF. This pattern was consistent

across all 3 hACSF-N applications. In contrast to their behavior in 17% hACSF, astrocytes exhibited a more robust initial response than neurons to hACSF-N. Astrocytes swelled approximately twofold more than neurons in the first minute (103.48 ± 0.41%, p = 0.003 vs. neurons) and remained nearly two-thirds larger than neurons after 5 minutes (106.13 ± 0.52%, p = 0.019). Differences between neurons and astrocytes were evident only during the first two applications of hACSF-N; during the third application, both cell types appeared to swell with equal speed and to equal degrees (Figure 2.6A). This fairly rapid change in swelling response between neurons and astrocytes may indicate the initial stages of an RVD in astrocytes. Interestingly, we found that neurons exposed to hACSF-N exhibited substantial RVD when they were dye-loaded via patch clamp (Figure 2.6B). While Thy1 neurons consistently swelled to 4-5% above baseline by the end of each hACSF-N application, neurons filled using patch-clamp techniques decreased in volume over time such that they did not differ from baseline even after 7 minutes in hACSF-N (100.45 ± 0.85%; p = 0.002 vs. Thy1). This marked the first (and only) time we observed a significant effect of patch clamp on neuronal cell volume. The specific mechanisms for this difference were not investigated further.

2.4.6. Hypoosmolar swelling is augmented in AQP4-/- astrocytes

In astrocytes, water permeability is thought to be regulated by the expression and gating of aquaporin 4 (AQP4) channels (Nagelhus et al., 2004;

Gunnarson et al., 2008; Song and Gunnarson, 2012). Functional water channels have not been found in pyramidal neurons, a proposed reason behind their apparent resistance to changes in osmolarity (Andrew et al., 2007). We reasoned that if AQP4 plays a significant role in hACSF-induced cell swelling, then AQP4 knockout should severely impair astrocyte volume change in 40% hACSF but have little or no effect on pyramidal neurons. Therefore, we repeated our 40% hACSF experiments using hippocampal slices from AQP4$^{-/-}$ mice (Figure 2.7). To ensure a more physiologically-relevant response, 40% hACSF was applied without antagonists and with diluted Mg^{2+}. As anticipated, AQP4 knockout had no effect on neuronal swelling in 40% hACSF ($F(1,16) = 0.02$, p = 0.891; data not shown). Unexpectedly, astrocytes from AQP4-/- tissue swelled significantly more compared to wild-type astrocytes. In comparison to wild-type astrocytes (Figure 2.7B), AQP4$^{-/-}$ astrocyte volume was approximately one-third larger by the end of the first hACSF application (Figure 2.7C; AQP4$^{-/-}$, 113.63 ± 1.15%; WT, 109.67 ± 0.82%; p = 0.016), with similar increases above wild-type astrocyte volume in subsequent hACSF applications. AQP4$^{-/-}$ astrocytes did not differ from wild-type astrocytes in volume during any of the wash periods in nACSF. These data seemed to indicate that AQP4 expression, far from being required for intracellular accumulation of water in hACSF, may actually be essential for *limiting* the degree of swelling during hypoosmolar stress.

2.4.7. Astrocytes are selectively swollen by 6.5 mM $[K^+]_o$

Studying neuronal excitability and its relationship to astrocytic swelling requires a selective method of swelling astrocytes. As it was clear that hypoosmolar solutions were not cell-type specific, we considered alternative methods. Astrocytes are known to swell in high-$[K^+]_o$ as a result of potassium uptake through K_{ir} 4.1 channels whose activity is linked to water influx through AQP4. This would suggest a more astrocyte-specific mechanism than hACSF, which appeared to act independently of AQP4. However, astrocyte swelling in high-$[K^+]_o$ has been mostly described in the context of extremely high (generally non-physiological) levels of $[K^+]_o$ (Walz, 1992; Risher et al., 2009), which are also known to swell neurons (Andrew et al., 2007; Zhou et al., 2010). To determine whether more physiological elevations of $[K^+]_o$ would induce astrocyte-specific swelling, we imaged juvenile neurons and astrocytes in ACSF containing 6.5 mM $[K^+]_o$. This level of $[K^+]_o$ is well within the ~10-12 mM peak concentration observed during seizure activity (Moody et al., 1974; Fisher et al., 1976; Yaari et al., 1986; Jensen and Yaari, 1997), but importantly is also sufficient to induce spontaneous epileptiform events in CA1 neurons (Rutecki et al., 1985; Tancredi and Avoli, 1987; see also Chapter 3). To facilitate comparison to our hACSF data, high-$[K^+]_o$ ACSF also contained 0 mM Mg^{2+}, 1 µM TTX and 10 µM NBQX. In stark contrast to the effects of hACSF, high-$[K^+]_o$ appeared to specifically swell only astrocytes at 6.5 mM concentration (Figure 2.9 A,B). Repeated applications of high-$[K^+]_o$ ACSF revealed no discernible change in neuron volume ($F(6,42) =$

1.48, p = 0.209), but astrocytes reliably swelled to at least 4% above baseline within 5 minutes of high-$[K^+]_o$ application (p < 0.001 vs. neurons at 5 minutes). This closely approximated the level of astrocyte swelling observed in 17% hACSF. High-$[K^+]_o$-induced astrocyte swelling was not accompanied by a neuronal volume increase. Interestingly, astrocytes swollen using high-$[K^+]_o$ ACSF did not fully return to baseline upon return to nACSF.

Overall, these data strongly suggest that water influx resulting from hypoosmolar ACSF application is not selective to astrocytes, and is not mediated by AQP4. However, $[K^+]_o$ elevations (within a moderate range) appear to selectively swell astrocytes (presumably due to the effect of $[K^+]_o$ on AQP4 activity), and may represent a more effective method of studying the effects of astrocyte swelling on neuronal excitability.

2.5. Discussion

In this study, we have shown that astrocytes (as anticipated) are rapidly swollen in hypoosmolar conditions, increasing their volume significantly above baseline even within the first minute of hACSF application. These data are in line with previous reports of the high osmosensitivity of astrocytes and astrocyte-like glial cells (Hirrlinger et al., 2008; Risher et al., 2009). However, we found that CA1 pyramidal neurons exhibited nearly identical osmosensitivity as glial cells, in spite of their lack of AQP4 water channels, and in direct contrast to previous work

showing a lack of volume response to hypoosmolar conditions (Andrew et al., 2007; Caspi et al., 2009). Neither glial nor neuronal swelling was found to be dependent upon AQP4 expression. These data cast doubt over the commonly-accepted roles of neurons and astrocytes in brain water regulation.

It is difficult to resolve the discrepancy in neuronal volume response between our results and those of Andrew et al (2007), the study most widely cited as concrete evidence of neuronal osmoresistance. One possibility is that neuronal volume changes are extremely sensitive to subtle differences in methodology. For example, experiments in the 2007 study (Andrew et al., 2007) were performed at a higher temperature than in the current study. Elevated temperature substantially increased the efficiency with which regulatory volume decrease (RVD) occured in a slice exposed to isoosmolar NaCl reduction (Andrew et al., 1999). Although RVD was not observed in hACSF-treated slices, there was a noticeable decrease in slice swelling at higher temperature (Andrew et al., 1997) which may suggest instead a more efficient isovolumetric regulation (IVR). IVR is thought to involve similar mechanisms as RVD and is characterized by an apparent resistance to volume change (Pasantes-Morales and Tuz, 2006). Isovolumetric regulation is observed only during gradual (but not sudden) shifts in osmolarity (Franco et al., 2000; Tuz et al., 2001; Pasantes-Morales and Tuz, 2006). Neurons imaged in deeper tissue than ours, as used by Andrew and colleagues (2007), would likely be exposed to more gradual solution exchanges and thus, more gradual changes in osmolarity which would facilitate IVR.

Interestingly, earlier studies in culture observed neuronal swelling resulting from hypoosmolar solutions, which correlated with intracellular Ca^{2+} elevations within the neuron (Aitken et al., 1998; Borgdorff et al., 2000). In astrocytes, intracellular Ca^{2+} elevations have been shown to augment the amino acid effluxes important for RVD, including taurine (Mongin et al., 1999; Mongin and Kimelberg, 2005), which may be released by neurons as part of their RVD/IVR in hypoosmolar conditions (Pasantes-Morales et al.; Franco et al., 2000; Kreisman and Olson, 2003; Haskew-Layton et al., 2008). Thus, the disparity in neuronal swelling between our work and that of Andrew et al (2007) could be due to differences in neuronal taurine content, and/or differences in neuronal calcium elevations. It should also be noted that, in contrast to Andrew et al, our standard hACSF contained TTX and NBQX – preventing firing and reducing tissue excitability. With TTX and NBQX removed, we observed a rather surprising reduction in neuronal swelling which suggested that neuronal firing was important for neuronal volume regulation. Voltage-gated Ca^{2+} channels would be a prime target for further examination of this topic.

The discussion above comes with the important caveat that, with the exception of the studies by Andrew and colleagues, all of the studies listed above (and most others in the field) exclusively used reductions of NaCl to produce hypoosmolar conditions. Isolation of the precise effects of hypoosmolarity and NaCl could be considered difficult if not impossible with such a model, although attempts have been made (Huang et al., 1997; Somjen, 1999; Borgdorff et al.,

63

2000; Haskew-Layton et al., 2008). Few studies exist which attempt to truly isolate the effect of hypoosmolarity from NaCl reductions (Andrew et al., 1997; Andrew et al., 1999; Andrew et al., 2007; Caspi et al., 2009). This discrepancy complicates discussion of osmotic edema, as the "dilution" model and the "low-NaCl" model are not equivalent. In the present study, we noted two important differences between these models. First, we found that despite having identical swelling profiles in 17% hACSF, astrocytes swelled considerably more than neurons in the first 2 applications of 17% hACSF-N and appeared to exhibit a reduced volume response by the third application. This would appear to be an obvious indicator of RVD (Andrew et al., 1997), which is not observed in astrocytes swollen by hACSF (Risher et al., 2009; see also figure 1 in this chapter). Secondly and perhaps more importantly, we noted a rapid and persistent reduction in neuronal volume across multiple hACSF-N applications, but only when fluorescent indicator was delivered to neurons via whole-cell patch clamp. This rapid time course is reminiscent of the so-called "apoptotic volume decrease" (AVD), a process which can be induced in hypoosmolar conditions in some circumstances and operates through RVD pathways (Maeno et al., 2000). Whether this process is responsible for the shrinking of patch-clamped neurons observed in our hACSF-N conditions is unclear. However, this possibility must be considered when interpreting earlier studies which used patch clamp in combination with hACSF-N (e.g. Huang et al., 1997).

It is worth noting that our image analysis, although based on established methods (Hirrlinger et al., 2008; Risher et al., 2009), was intentionally conservative and likely underestimates the actual change in cell volume. For example, we chose to examine cell soma area as a proxy for overall volume changes, as direct measures of cell volume were not feasible for our conditions. If one assumes that cell volume is changing equally in all directions, it can be inferred that our measurements reflect only about two-thirds of the true change in volume. We also observed that the precise method of image processing had a surprisingly strong impact on measured volume. While procedures among groups remained generally similar, the overall magnitude of volume change could be increased twofold or more simply through the use of different thresholding methods. These apparent increases in signal-to-noise ratio often came at the expense of "cell" and "background" pixels being incorrectly classified, and the thresholded images inconsistent with what could be observed "by eye" pre-processing (unpublished observations). We therefore rejected these methods in favor of the more conservative "mean" threshold method, which more consistently returned an image in which the cell body could be clearly identified.

If neurons are indeed swelling in hACSF, then what is the route of water influx? Clues to this answer may lie in other conditions which cause neuronal swelling. While hypoosmolar swelling has generally been reported only in dissociated neurons *in vitro* (Aitken et al., 1998; Somjen, 1999; Inoue et al., 2005; Boss et al., 2013), pyramidal neurons have long been known to swell in

excitotoxic conditions (Choi, 1992; Risher et al., 2009; Zhou et al., 2010). Massive intracellular sodium influx (as observed in cases of continuous neuronal firing or excessive NMDA receptor activation) can depolarize the membrane enough to open a voltage-gated Cl^- channel, with the resulting increase in intracellular osmolarity (from both Na^+ and Cl^-) producing an osmotic gradient into the cell (Rungta et al., 2015). This highlights the possibility that, despite lacking functional water channels, neurons are capable of taking on water through alternate means quite rapidly. Consistent with this, spreading depression (a wave of depolarization, excessively high K^+ and glutamate in the extracellular space) has been reported in hypoosmolar conditions (Chebabo et al., 1995a; Huang et al., 1995) and can induce excitotoxic neuronal swelling (Zhou et al., 2010). We have little reason to believe an excitotoxic mechanism is directly responsible for the observed neuronal swelling in our model, as we have previously found no evidence of spreading depression in hACSF (Lauderdale et al., 2015). Furthermore, in the present study we found that blocking NMDA receptors had no effect on neuronal swelling. Instead we propose that the osmotic gradient in excitotoxicity, which drives water into a neuron following excessive Na^+ and Cl^- influx, is similar to the gradient imposed by hACSF on a neuron with normal intracellular ion concentrations. Unfortunately, the routes for such water influx into neurons are not well-defined. Two possible routes might be inferred from the known or hypothesized (non-AQP4-dependent) pathways for water influx into astrocytes: simple water diffusion across the plasma membrane

or water movement through a commonly-expressed cotransporter such as the Na$^+$,K$^+$,2Cl$^-$ cotransporter NKCC1 (Kimelberg, 2005; Macaulay and Zeuthen, 2012). Neither of these water pathways is likely to be exclusive to astrocytes, and the similarity in swelling profiles between neurons and astrocytes in our standard hACSF conditions could suggest a common mechanism independent of AQP4.

Supporting the idea that neurons and astrocytes share a common swelling mechanism in hACSF, we could find no evidence for AQP4-mediated water influx into astrocytes exposed to hACSF. On the contrary, AQP4$^{-/-}$ astrocyte volume in hACSF increased more rapidly and to a greater extent than in wild-type animals. AQP4 has been well-established to play an important role in astrocyte water permeability and brain water homeostasis as a whole (Papadopoulos and Verkman, 2007) and removal of the channel in transgenic animals would be expected to block astrocyte swelling. Perhaps the simplest explanation for our results is that AQP4 is more important for allowing water <u>efflux</u>, and removal of AQP4 removes an important efflux pathway for water. AQP4 is enriched at perivascular endfeet and thought to be functionally coupled to K$_{ir}$ 4.1 activity (Nagelhus et al., 2004). Blocking K$_{ir}$ 4.1 (which should inhibit AQP4 activity as well) significantly swells astrocyte processes even in isoosmolar conditions (Hirrlinger et al., 2008), suggesting that the inhibition of AQP4 activity prevents water efflux from the astrocyte. Recent studies, however, suggest that the precise role of AQP4 may even be more complicated. In one study, knockout of the anchoring protein α-syntrophin, which removes perivascular AQP4 (Amiry-

Moghaddam et al., 2004), significantly inhibited swelling in severe (~33%) hACSF, but had no effect on swelling in mild (~17%) hACSF (Anderova et al., 2014). With a full knockout of AQP4^{-/-}, another study found nearly the opposite effect; little or no change in volume in 30% hACSF, but significant reduction in volume at 20% hACSF (Thrane et al., 2011). The reason for this discrepancy is unclear, but these two studies suggest that AQP4 is not the only route for water influx into astrocytes in hACSF. It is also interesting to note that in both studies (more obviously in the latter), the dose of hACSF determined whether astrocyte volume regulation occurred, regardless of genotype. The differences between hACSF doses in terms of RVD and AQP4 influence may reflect the emerging role of AQP4 in astrocyte volume regulation. In Müller glia (an "astrocyte-like" glial cell type in the retina), rapid water influx through AQP4 produces membrane stretch, which then activates nearby stretch-activated TRPV4 channels to permit Ca^{2+} entry and promote RVD (Jo et al., 2015; Iuso and Krizaj, 2016). While the requirement of TRPV4 opening and Ca^{2+} influx in RVD has been recently questioned (Mola et al., 2016), it seems clear that rapid water influx through AQP4 is an important trigger, whether direct or indirect, for subsequent volume regulation (Benfenati et al., 2011; Mola et al., 2016). Consequently, knockout of AQP4^{-/-} could produce progressive swelling without a counterbalancing RVD, resulting in an apparent enhancement of hACSF-induced swelling as seen in the present study. It must be stressed, as in the earlier discussion, that the studies mentioned above were performed in hACSF made by NaCl reduction, and thus

their applicability to our own results may be questionable. Finally, it is interesting to note that AQP4$^{-/-}$ animals show nearly a 30% increase in extracellular space as compared to wild-type animals (Yao et al., 2008) which would logically increase the volume of space available for astrocyte swelling and could explain the speed and degree of AQP4$^{-/-}$ astrocyte swelling in our conditions. This would not explain the lack of increased swelling in neurons, however. It is also unlikely that astrocyte volume changes in our 40% hACSF were limited by the extracellular space in wild-type animals, as tissue continues to swell at far more severe doses (Chebabo et al., 1995b).

The finding that astrocytes selectively swell in high-K^{+}, on the other hand, is strongly suggestive of an AQP4-dependent mechanism. Astrocytic swelling in high-K^{+} has been long-established (Walz and Hinks, 1985; MacVicar et al., 2002; Risher et al., 2009), and multiple studies point to a direct interaction between astrocyte potassium uptake and AQP4-mediated water influx (Amiry-Moghaddam et al., 2003; Nagelhus et al., 2004; Binder et al., 2006; Strohschein et al., 2011). Water permeability through AQP4 may even be partially gated by extracellular K^{+} (Song and Gunnarson, 2012). Curiously, most prior studies of astrocyte volume in high K^{+} have used concentrations well above the physiological range of ~3-10 mM (Heinemann and Lux, 1977). At these high levels of extracellular K^{+} neurons have also been shown to swell, likely as a consequence of spreading depression (Andrew et al., 2007; Zhou et al., 2010). We observed no obvious neuronal swelling in our conditions, suggesting that astrocyte swelling could be isolated by

this technique. Since TTX was included in our 6.5 mM K$^+$ condition, we cannot presently determine if 6.5 mM K$^+$ remains selective to astrocytes when neurons are allowed to generate action potentials. Further experiments will be needed to address these issues.

2.6. References

Aitken PG, Borgdorff AJ, Juta AJ, Kiehart DP, Somjen GG, Wadman WJ (1998) Volume changes induced by osmotic stress in freshly isolated rat hippocampal neurons. Pflugers Archiv : European journal of physiology 436:991-998.

Amiry-Moghaddam M, Williamson A, Palomba M, Eid T, de Lanerolle NC, Nagelhus EA, Adams ME, Froehner SC, Agre P, Ottersen OP (2003) Delayed K+ clearance associated with aquaporin-4 mislocalization: phenotypic defects in brains of alpha-syntrophin-null mice. Proc Natl Acad Sci U S A 100:13615-13620.

Amiry-Moghaddam M, Frydenlund DS, Ottersen OP (2004) Anchoring of aquaporin-4 in brain: molecular mechanisms and implications for the physiology and pathophysiology of water transport. Neuroscience 129:999-1010.

Anderova M, Benesova J, Mikesova M, Dzamba D, Honsa P, Kriska J, Butenko O, Novosadova V, Valihrach L, Kubista M, Dmytrenko L, Cicanic M, Vargova L (2014) Altered astrocytic swelling in the cortex of alpha-syntrophin-negative GFAP/EGFP mice. PLoS ONE 9:e113444.

Andrew RD (1991) Seizure and acute osmotic change: Clinical and neurophysiological aspects. In: Journal of the Neurological Sciences, pp 7-18.

Andrew RD, MacVicar BA (1994) Imaging cell volume changes and neuronal excitation in the hippocampal slice. Neuroscience 62:371-383.

Andrew RD, Lobinowich ME, Osehobo EP (1997) Evidence against volume regulation by cortical brain cells during acute osmotic stress. Exp Neurol 143:300-312.

Andrew RD, Jarvis CR, Obeidat AS (1999) Potential sources of intrinsic optical signals imaged in live brain slices. Methods 18:185-196, 179.

Andrew RD, Labron MW, Boehnke SE, Carnduff L, Kirov SA (2007) Physiological evidence that pyramidal neurons lack functional water channels. Cereb Cortex 17:787-802.

Benfenati V, Caprini M, Dovizio M, Mylonakou MN, Ferroni S, Ottersen OP, Amiry-Moghaddam M (2011) An aquaporin-4/transient receptor potential vanilloid 4 (AQP4/TRPV4) complex is essential for cell-volume control in astrocytes. Proc Natl Acad Sci U S A 108:2563-2568.

Binder DK, Papadopoulos MC, Haggie PM, Verkman AS (2004b) In vivo measurement of brain extracellular space diffusion by cortical surface photobleaching. J Neurosci 24:8049-8056.

Binder DK, Yao X, Zador Z, Sick TJ, Verkman AS, Manley GT (2006) Increased seizure duration and slowed potassium kinetics in mice lacking aquaporin-4 water channels. GLIA 53:631-636.

Borgdorff AJ, Somjen GG, Wadman WJ (2000) Two mechanisms that raise free intracellular calcium in rat hippocampal neurons during hypoosmotic and low NaCl treatment. J Neurophysiol 83:81-89.

Boss D, Kuhn J, Jourdain P, Depeursinge C, Magistretti PJ, Marquet P (2013) Measurement of absolute cell volume, osmotic membrane water permeability, and refractive index of transmembrane water and solute flux by digital holographic microscopy. Journal of biomedical optics 18:036007.

Caspi A, Benninger F, Yaari Y (2009) KV7/M channels mediate osmotic modulation of intrinsic neuronal excitability. J Neurosci 29:11098-11111.

Castilla-Guerra L, del Carmen Fernandez-Moreno M, Lopez-Chozas JM, Fernandez-Bolanos R (2006) Electrolytes disturbances and seizures. Epilepsia 47:1990-1998.

Chebabo SR, Hester MA, Aitken PG, Somjen GG (1995a) Hypotonic exposure enhances synaptic transmission and triggers spreading depression in rat hippocampal tissue slices. Brain Res 695:203-216.

Chebabo SR, Hester MA, Jing J, Aitken PG, Somjen GG (1995b) Interstitial space, electrical resistance and ion concentrations during hypotonia of rat hippocampal slices. J Physiol 487 (Pt 3):685-697.

Choi DW (1992) Excitotoxic cell death. Journal of neurobiology 23:1261-1276.

Dissing-Olesen L, LeDue JM, Rungta RL, Hefendehl JK, Choi HB, MacVicar BA (2014) Activation of neuronal NMDA receptors triggers transient ATP-mediated microglial process outgrowth. J Neurosci 34:10511-10527.

Eid T, Lee TS, Thomas MJ, Amiry-Moghaddam M, Bjornsen LP, Spencer DD, Agre P, Ottersen OP, de Lanerolle NC (2005) Loss of perivascular aquaporin 4 may underlie deficient water and K+ homeostasis in the human epileptogenic hippocampus. Proc Natl Acad Sci U S A 102:1193-1198.

Feng G, Mellor RH, Bernstein M, Keller-Peck C, Nguyen QT, Wallace M, Nerbonne JM, Lichtman JW, Sanes JR (2000) Imaging neuronal subsets in transgenic mice expressing multiple spectral variants of GFP. Neuron 28:41-51.

Fiacco TA, Agulhon C, Taves SR, Petravicz J, Casper KB, Dong X, Chen J, McCarthy KD (2007) Selective stimulation of astrocyte calcium in situ does not affect neuronal excitatory synaptic activity. Neuron 54:611-626.

Fisher RS, Pedley TA, Moody WJ, Jr., Prince DA (1976) The role of extracellular potassium in hippocampal epilepsy. Arch Neurol 33:76-83.

Franco R, Quesada O, Pasantes-Morales H (2000) Efflux of osmolyte amino acids during isovolumic regulation in hippocampal slices. J Neurosci Res 61:701-711.

Gunnarson E, Zelenina M, Axehult G, Song Y, Bondar A, Krieger P, Brismar H, Zelenin S, Aperia A (2008) Identification of a molecular target for glutamate regulation of astrocyte water permeability. GLIA 56:587-596.

Haskew-Layton RE, Rudkouskaya A, Jin Y, Feustel PJ, Kimelberg HK, Mongin AA (2008) Two distinct modes of hypoosmotic medium-induced release of excitatory amino acids and taurine in the rat brain in vivo. PLoS ONE 3:e3543.

Heinemann U, Lux HD (1977) Ceiling of stimulus induced rises in extracellular potassium concentration in the cerebral cortex of cat. Brain Res 120:231-249.

Hirrlinger PG, Wurm A, Hirrlinger J, Bringmann A, Reichenbach A (2008) Osmotic swelling characteristics of glial cells in the murine hippocampus, cerebellum, and retina in situ. J Neurochem 105:1405-1417.

Huang R, Aitken PG, Somjen GG (1995) The extent and mechanism of the loss of function caused by strongly hypotonic solutions in rat hippocampal slices. Brain Res 695:195-202.

Huang R, Bossut DF, Somjen GG (1997) Enhancement of whole cell synaptic currents by low osmolarity and by low [NaCl] in rat hippocampal slices. J Neurophysiol 77:2349-2359.

Illarionova NB, Gunnarson E, Li Y, Brismar H, Bondar A, Zelenin S, Aperia A (2010) Functional and molecular interactions between aquaporins and Na,K-ATPase. Neuroscience 168:915-925.

Inoue H, Mori S, Morishima S, Okada Y (2005) Volume-sensitive chloride channels in mouse cortical neurons: characterization and role in volume regulation. Eur J Neurosci 21:1648-1658.

Iuso A, Krizaj D (2016) TRPV4-AQP4 interactions 'turbocharge' astroglial sensitivity to small osmotic gradients. Channels:1-3.

Jensen MS, Yaari Y (1997) Role of intrinsic burst firing, potassium accumulation, and electrical coupling in the elevated potassium model of hippocampal epilepsy. J Neurophysiol 77:1224-1233.

Jo AO, Ryskamp DA, Phuong TT, Verkman AS, Yarishkin O, MacAulay N, Krizaj D (2015) TRPV4 and AQP4 Channels Synergistically Regulate Cell Volume and Calcium Homeostasis in Retinal Muller Glia. J Neurosci 35:13525-13537.

Katada R, Akdemir G, Asavapanumas N, Ratelade J, Zhang H, Verkman AS (2014) Greatly improved survival and neuroprotection in aquaporin-4-knockout mice following global cerebral ischemia. FASEB journal : official publication of the Federation of American Societies for Experimental Biology 28:705-714.

Kilb W, Dierkes PW, Sykova E, Vargova L, Luhmann HJ (2006) Hypoosmolar conditions reduce extracellular volume fraction and enhance epileptiform activity in the CA3 region of the immature rat hippocampus. J Neurosci Res 84:119-129.

Kimelberg HK (1995) Current concepts of brain edema. Review of laboratory investigations. J Neurosurg 83:1051-1059.

Kimelberg HK (2005) Astrocytic swelling in cerebral ischemia as a possible cause of injury and target for therapy. GLIA 50:389-397.

Kreisman NR, Olson JE (2003) Taurine enhances volume regulation in hippocampal slices swollen osmotically. Neuroscience 120:635-642.

Lauderdale K, Murphy T, Tung T, Davila D, Binder DK, Fiacco TA (2015) Osmotic Edema Rapidly Increases Neuronal Excitability Through Activation of NMDA Receptor-Dependent Slow Inward Currents in Juvenile and Adult Hippocampus. ASN Neuro 7.

Liang D, Bhatta S, Gerzanich V, Simard JM (2007) Cytotoxic edema: mechanisms of pathological cell swelling. Neurosurg Focus 22:E2.

Macaulay N, Zeuthen T (2012) Glial K(+) clearance and cell swelling: key roles for cotransporters and pumps. Neurochem Res 37:2299-2309.

MacVicar BA, Feighan D, Brown A, Ransom B (2002) Intrinsic optical signals in the rat optic nerve: role for K(+) uptake via NKCC1 and swelling of astrocytes. GLIA 37:114-123.

Maeno E, Ishizaki Y, Kanaseki T, Hazama A, Okada Y (2000) Normotonic cell shrinkage because of disordered volume regulation is an early prerequisite to apoptosis. Proc Natl Acad Sci U S A 97:9487-9492.

Mola MG, Sparaneo A, Gargano CD, Spray DC, Svelto M, Frigeri A, Scemes E, Nicchia GP (2016) The speed of swelling kinetics modulates cell volume regulation and calcium signaling in astrocytes: A different point of view on the role of aquaporins. GLIA 64:139-154.

Mongin AA, Cai Z, Kimelberg HK (1999) Volume-dependent taurine release from cultured astrocytes requires permissive [Ca(2+)](i) and calmodulin. Am J Physiol 277:C823-832.

Mongin AA, Kimelberg HK (2005) ATP regulates anion channel-mediated organic osmolyte release from cultured rat astrocytes via multiple Ca2+-sensitive mechanisms. American journal of physiology Cell physiology 288:C204-213.

Moody WJ, Futamachi KJ, Prince DA (1974) Extracellular potassium activity during epileptogenesis. Exp Neurol 42:248-263.

Nagelhus EA, Mathiisen TM, Ottersen OP (2004) Aquaporin-4 in the central nervous system: cellular and subcellular distribution and coexpression with KIR4.1. Neuroscience 129:905-913.

Papadopoulos MC, Verkman AS (2007) Aquaporin-4 and brain edema. Pediatric nephrology 22:778-784.

Papadopoulos MC, Verkman AS (2013) Aquaporin water channels in the nervous system. Nat Rev Neurosci 14:265-277.

Pasantes-Morales H, Maar TE, Moran J (1993) Cell volume regulation in cultured cerebellar granule neurons. J Neurosci Res 34:219-224.

Pasantes-Morales H, Tuz K (2006) Volume changes in neurons: hyperexcitability and neuronal death. Contrib Nephrol 152:221-240.

Risher WC, Andrew RD, Kirov SA (2009) Real-time passive volume responses of astrocytes to acute osmotic and ischemic stress in cortical slices and in vivo revealed by two-photon microscopy. GLIA 57:207-221.

Roper SN, Obenaus A, Dudek FE (1992) Osmolality and nonsynaptic epileptiform bursts in rat CA1 and dentate gyrus. Ann Neurol 31:81-85.

Rosen AS, Andrew RD (1990) Osmotic effects upon excitability in rat neocortical slices. Neuroscience 38:579-590.

Rothman SM, Olney JW (1987) Excitotoxicity and the Nmda Receptor. Trends in Neurosciences 10:299-302.

Rungta RL, Choi HB, Tyson JR, Malik A, Dissing-Olesen L, Lin PJ, Cain SM, Cullis PR, Snutch TP, MacVicar BA (2015) The cellular mechanisms of neuronal swelling underlying cytotoxic edema. Cell 161:610-621.

Rutecki PA, Lebeda FJ, Johnston D (1985) Epileptiform activity induced by changes in extracellular potassium in hippocampus. J Neurophysiol 54:1363-1374.

Schnell C, Shahmoradi A, Wichert SP, Mayerl S, Hagos Y, Heuer H, Rossner MJ, Hulsmann S (2015) The multispecific thyroid hormone transporter OATP1C1 mediates cell-specific sulforhodamine 101-labeling of hippocampal astrocytes. Brain Struct Funct 220:193-203.

Somjen GG (1999) Low external NaCl concentration and low osmolarity enhance voltage-gated Ca currents but depress K currents in freshly isolated rat hippocampal neurons. Brain Res 851:189-197.

Song Y, Gunnarson E (2012) Potassium dependent regulation of astrocyte water permeability is mediated by cAMP signaling. PLoS ONE 7:e34936.

Strohschein S, Huttmann K, Gabriel S, Binder DK, Heinemann U, Steinhauser C (2011) Impact of aquaporin-4 channels on K+ buffering and gap junction coupling in the hippocampus. GLIA 59:973-980.

Tancredi V, Avoli M (1987) Control of spontaneous epileptiform discharges by extracellular potassium: an "in vitro" study in the CA1 subfield of the hippocampal slice. Exp Brain Res 67:363-372.

Thrane AS, Rappold PM, Fujita T, Torres A, Bekar LK, Takano T, Peng W, Wang F, Rangroo Thrane V, Enger R, Haj-Yasein NN, Skare O, Holen T, Klungland A, Ottersen OP, Nedergaard M, Nagelhus EA (2011) Critical

role of aquaporin-4 (AQP4) in astrocytic Ca2+ signaling events elicited by cerebral edema. Proc Natl Acad Sci U S A 108:846-851.

Tuz K, Ordaz B, Vaca L, Quesada O, Pasantes-Morales H (2001) Isovolumetric regulation mechanisms in cultured cerebellar granule neurons. J Neurochem 79:143-151.

Walz W, Hinks EC (1985) Carrier-mediated KCl accumulation accompanied by water movements is involved in the control of physiological K+ levels by astrocytes. Brain Res 343:44-51.

Walz W (1992) Mechanism of rapid K(+)-induced swelling of mouse astrocytes. Neurosci Lett 135:243-246.

Xie AX, Lauderdale K, Murphy T, Myers TL, Fiacco TA (2014) Inducing plasticity of astrocytic receptors by manipulation of neuronal firing rates. J Vis Exp:1-13.

Yaari Y, Konnerth A, Heinemann U (1986) Nonsynaptic epileptogenesis in the mammalian hippocampus in vitro. II. Role of extracellular potassium. J Neurophysiol 56:424-438.

Yao X, Hrabetova S, Nicholson C, Manley GT (2008) Aquaporin-4-deficient mice have increased extracellular space without tortuosity change. J Neurosci 28:5460-5464.

Zhou N, Gordon GR, Feighan D, MacVicar BA (2010) Transient swelling, acidification, and mitochondrial depolarization occurs in neurons but not astrocytes during spreading depression. Cereb Cortex 20:2614-2624.
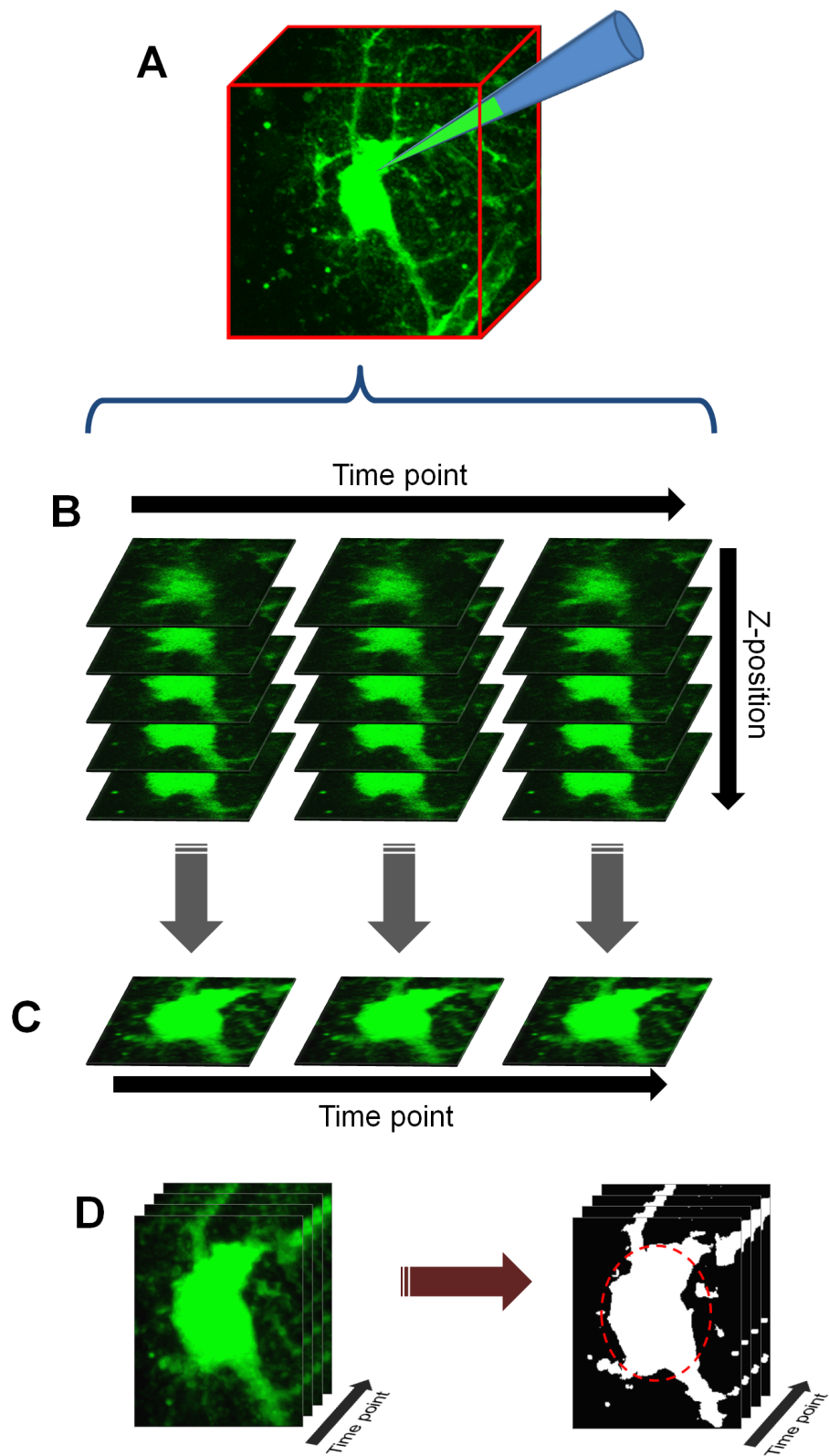
Figure 2.1. Basic protocol for cell volume analysis
(A) Astrocytes or neurons are fluorescently labeled, by patch clamp or other means. Starting with baseline, z-stacks are taken through the soma at each time point. During analysis, these stacks (x-y-z) are concatenated into a time-series (x-y-z-t) hyperstack (B). The hyperstack is filtered and collapsed in the z-plane to produce a time series (x-y-t) composed of max-intensity projections (C). The resulting time series stack is aligned, cropped and background subtracted, before finally being binarized using the "mean" thresholding algorithm (D). An elliptical ROI is drawn around the soma, and any pixels above threshold within this ROI are quantified.
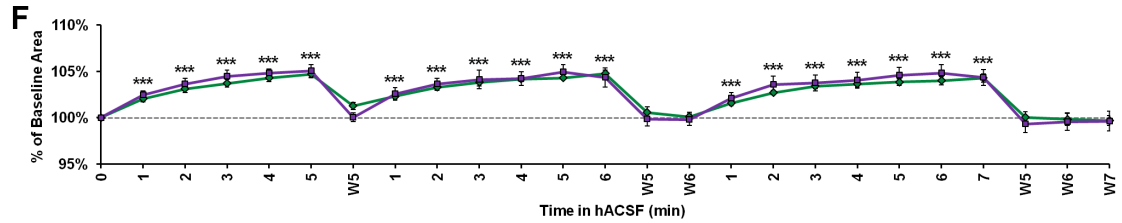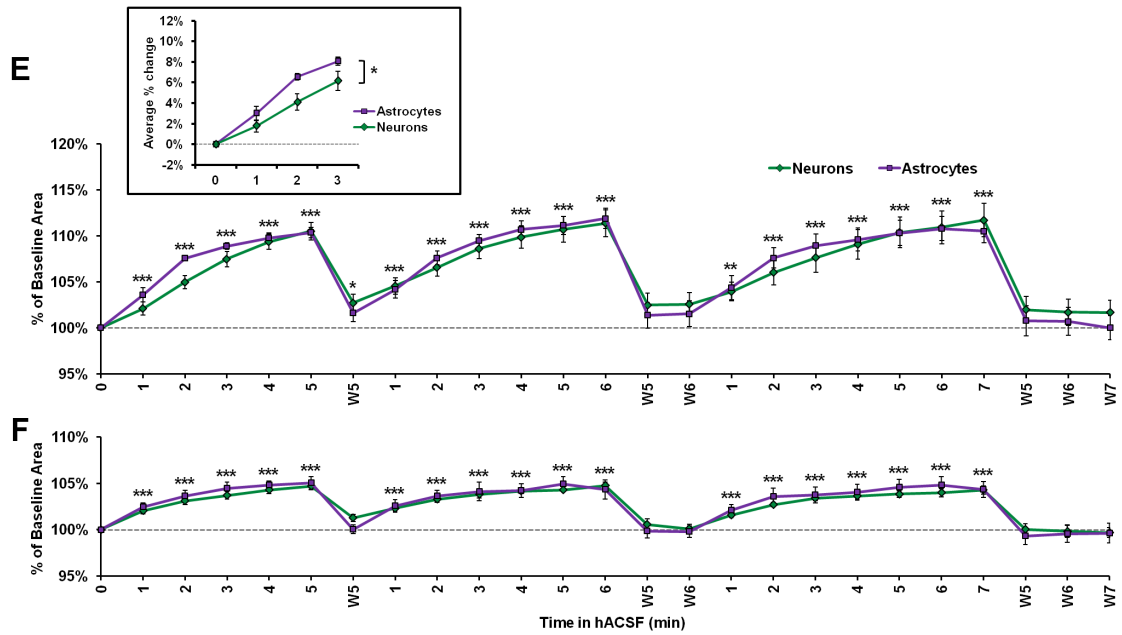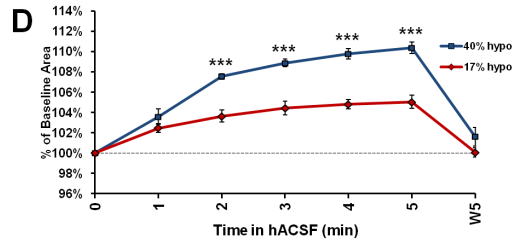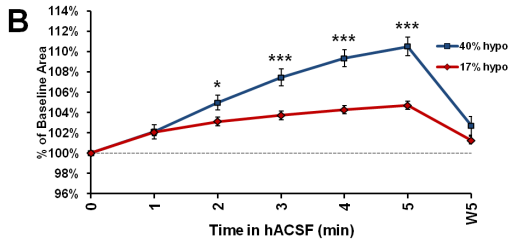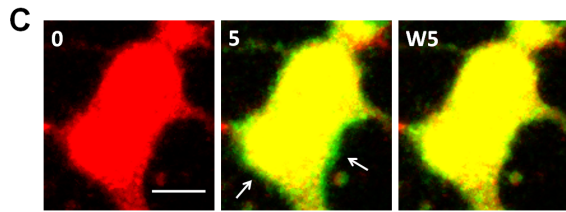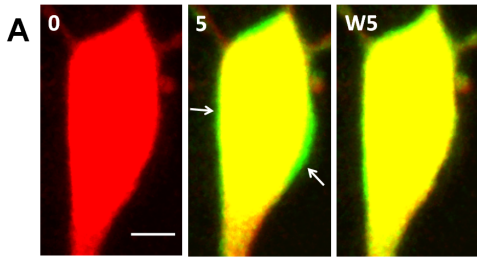
80

Figure 2.2. Neurons and astrocytes both swell in hypoosmotic conditions
(A) Representative images of a CA1 pyramidal neuron loaded with Alexa Fluor 488 dye (pseudocolored here for clarity) taken at baseline (0), after 5 minutes in 40% hACSF (5), and after 5 minutes of washout (W5). Merged images at (5) and (W5) time points illustrate expansion of soma in hACSF (white arrows), and subsequent shrinkage following wash. Scale bar = 5 µm. (B) Quantification of neuronal soma area as a percent of baseline in 17% and 40% hACSF conditions over a single 5-minute application. Time points 0, 5 and W5 correspond to images in A. (C) Representative images of astrocytes loaded with Alexa Fluor 488 dextran (10,000 MW) in 40% hACSF condition, same time points as in (A). White arrows indicate expansion of soma in hACSF. Scale bar = 5 µm. (D) Quantification of astrocyte soma area as a percentage of baseline in 17% and 40% hACSF conditions. *$p < 0.05$ and ***$p < 0.001$ for 17% vs. 40% at each time point in B and D. (E) Neuron and astrocyte volume changes are quantified over multiple re-applications of 40% hACSF. Inset shows subtle difference in average rate of swelling between neurons and astrocytes across first 3 minutes of each evoke. (F) Same as E, but in 17% hACSF. No interaction was found between time point and cell type for either dose of ACSF. *$p < 0.05$, **$p < 0.01$, and ***$p < 0.001$, percent area versus 100% (baseline) in E and F. N = 7-9 cells per group.
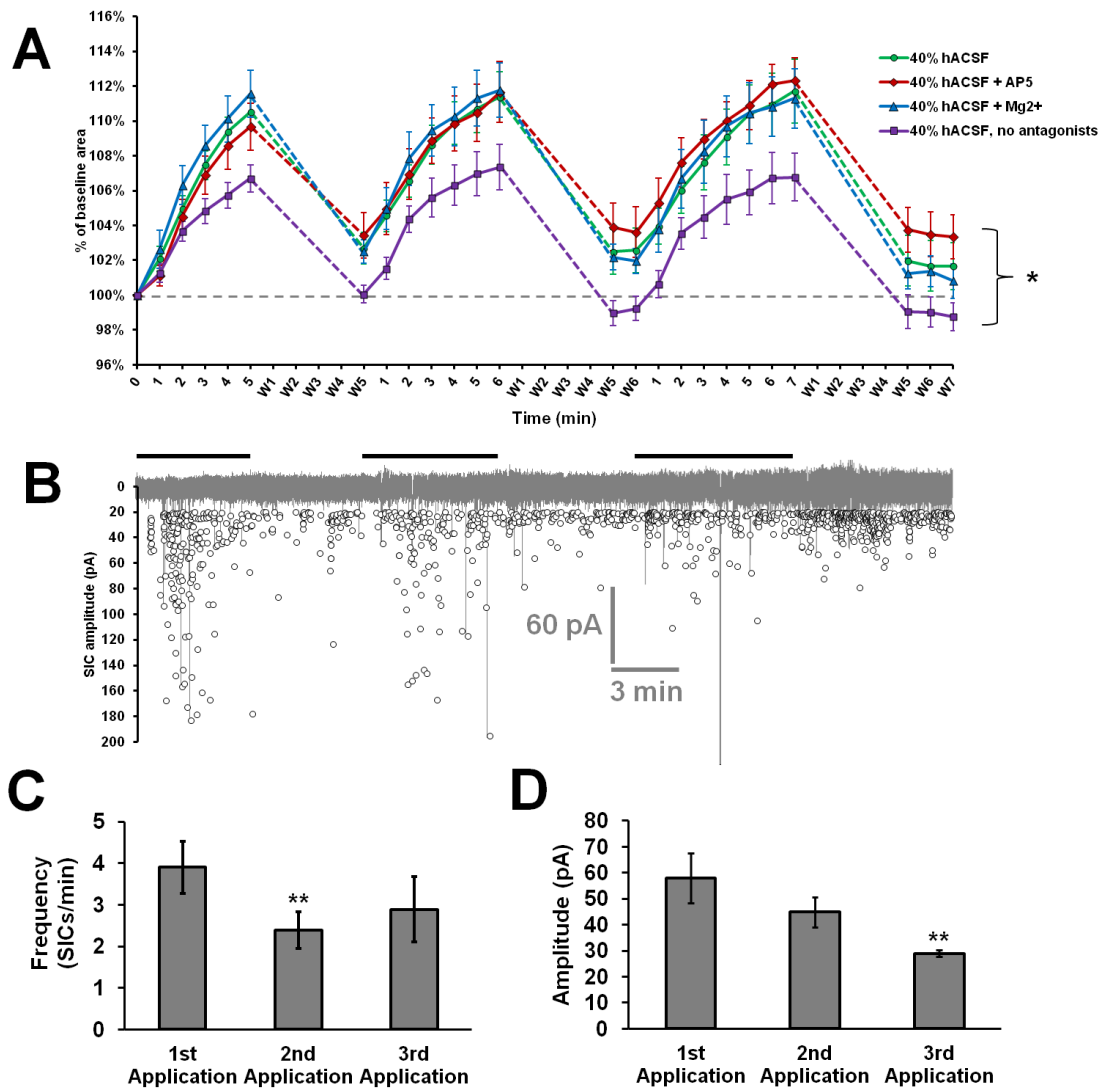
Figure 2.3 Neuronal swelling occurs simultaneously with, but independently of, slow inward currents

(A) Neuron soma area measured as a percentage of baseline during multiple applications of standard 40% hACSF (positive control), 40% hACSF + AP5, 40% hACSF + 6 mM Mg^{2+}, or 40% hACSF without antagonists. *p < 0.05, main effect of group; pairwise comparisons (Dunnett post-hoc) indicate a nonsignificant trend (p = 0.089) between 40% hACSF without antagonists and the positive control; N = 7-9 cells per group. (B) SIC activity in neurons during the same time points as in A. Black bars above trace indicate periods of 40% hACSF. Background trace (grey) shows a typical neuron during 40% hACSF, while foreground scatterplot shows the overall distribution of SIC activity across all neurons. (C, D) Average SIC frequency and amplitude in each application of 40% hACSF; **p < 0.01 versus 1st application.
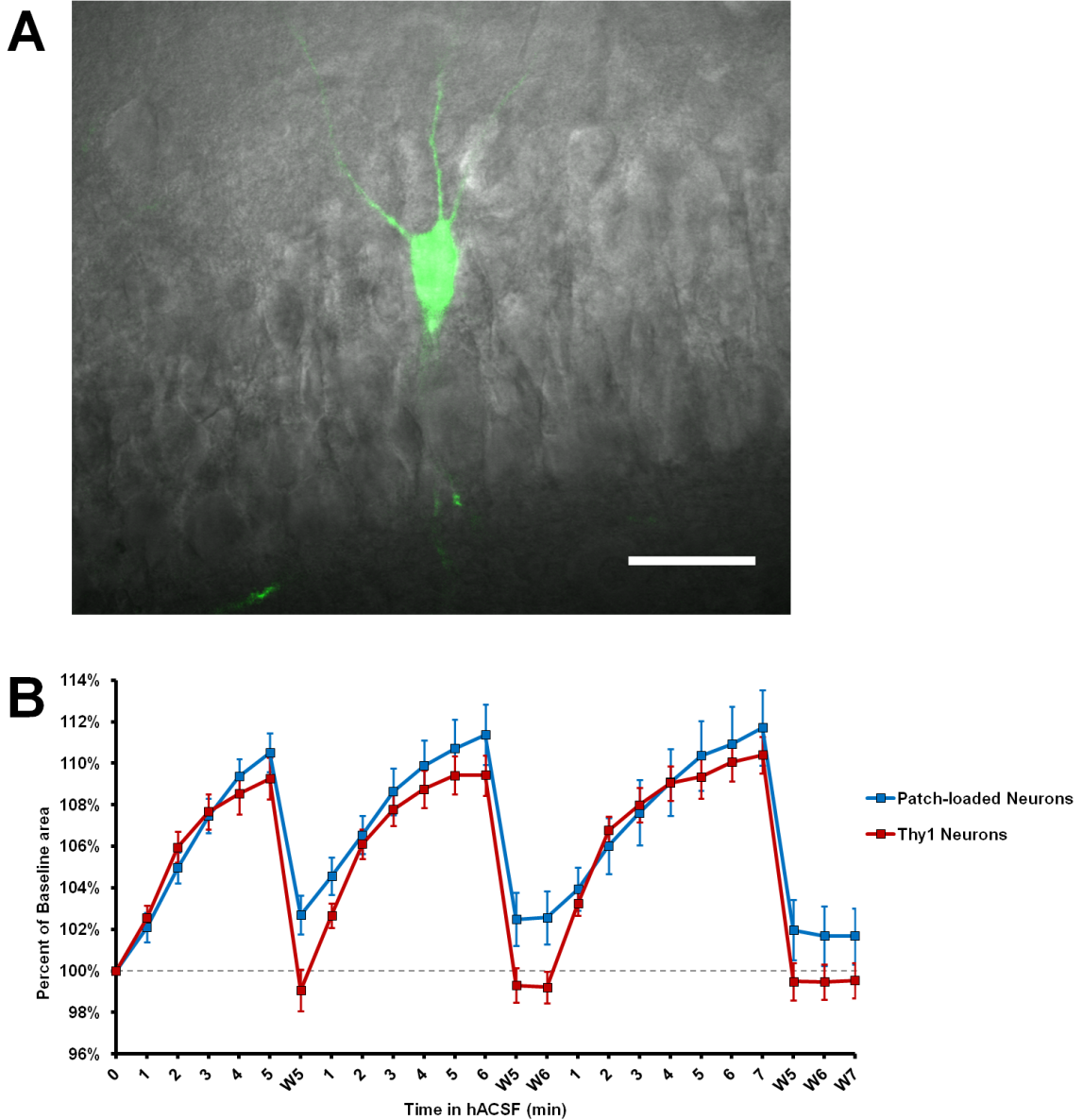
Figure 2.4. Neuronal swelling is not a consequence of patch-clamp
(A) Merged infrared (IR) and fluorescent images from a section of the CA1 field in a typical Thy1 hippocampal slice. Labeled neurons are random and usually very sparse, as shown here. Scale bar, 30 μm. (B) Comparison of swelling characteristics in 40% hACSF for Thy1 neurons versus wild-type neurons loaded with dye by patch clamp. Wash periods suggest patch-loaded cells may be impaired in returning to baseline as compared to Thy1; however, mixed ANOVA revealed no significant main effect or interaction effect of genotype. N = 8 patched, 10 Thy1 neurons.
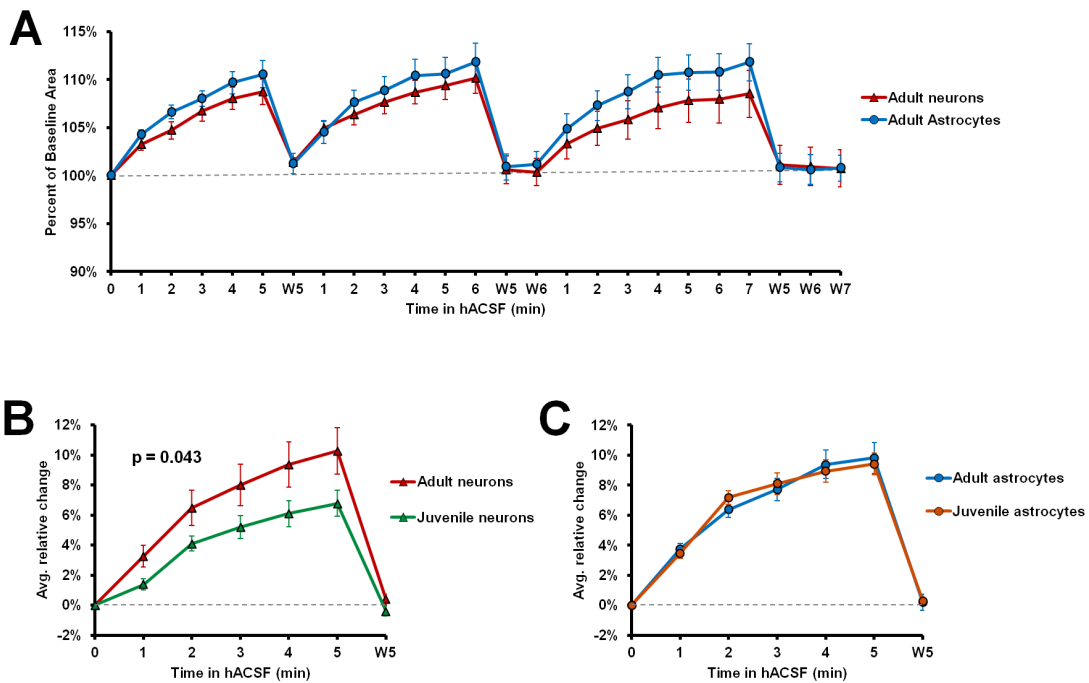
Figure 2.5. Neuron and astrocyte volume changes in 40% hACSF do not differ between adults and juveniles

(A) Rapid neuron and astrocyte swelling was observed in adult hippocampal slices when repeatedly exposed to 40% hACSF without antagonists. As with juveniles, adult astrocytes and neurons did not differ significantly in their response to hACSF. (B) Average percent change across 3 hACSF applications for adult and juvenile CA1 pyramidal neurons. (C) Average percent change across 3 hACSF applications for adult and juvenile s.r. astrocytes. Adults and juveniles did not differ in average percent change for either cell type shown in B and C. N = 8-10 cells per group.
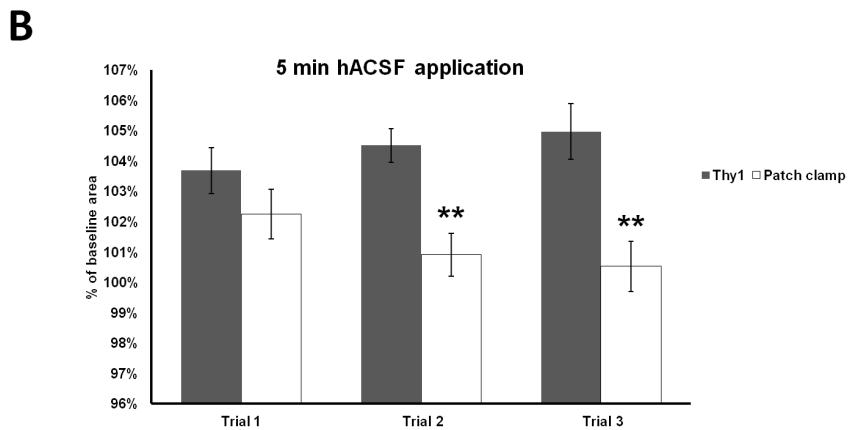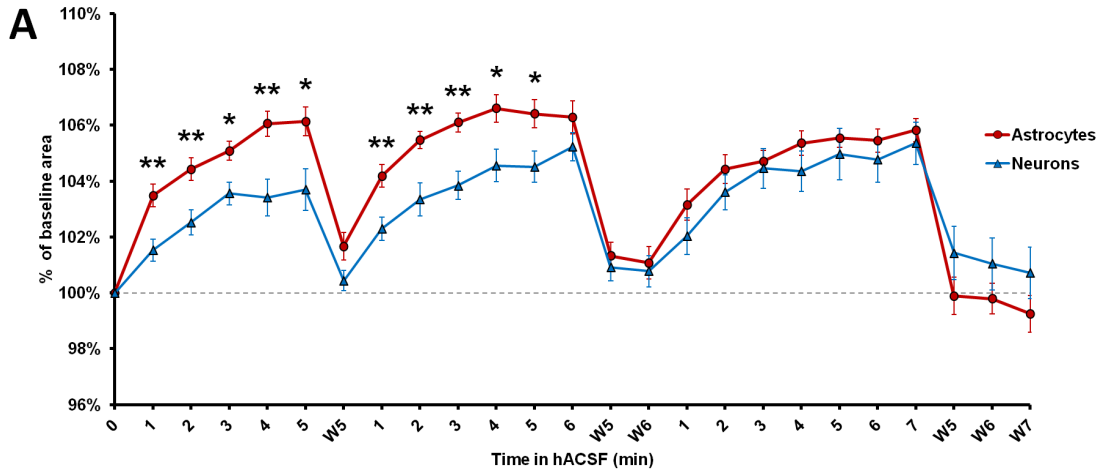
Figure 2.6. Neurons and astrocytes swell similarly in low-NaCl hACSF
(A) Soma volume of astrocytes (black line) and neurons (grey line), measured as a percentage of baseline, in ACSF made 17% hypoosmotic by removal of 25 mM NaCl. Baseline (100%) is indicated by the dashed grey line. Neurons exhibit a similar time course and degree of swelling as in 17% hACSF made by dilution (see Figure 1). Neurons swell more gradually than astrocytes during the first 2 hACSF applications, but no significant difference is observed by the 3rd application. (B) Thy1 neurons versus patch clamp dye-loaded neurons after 5 minutes in NaCl-reduced hACSF, across all 3 trials. Patch clamped neurons appear to undergo a regulatory volume decrease (RVD) over time which is not observed in Thy1 neurons. RVD was not observed in any other conditions, whether or not patch clamp was used for dye loading. N = 9 cells per group.
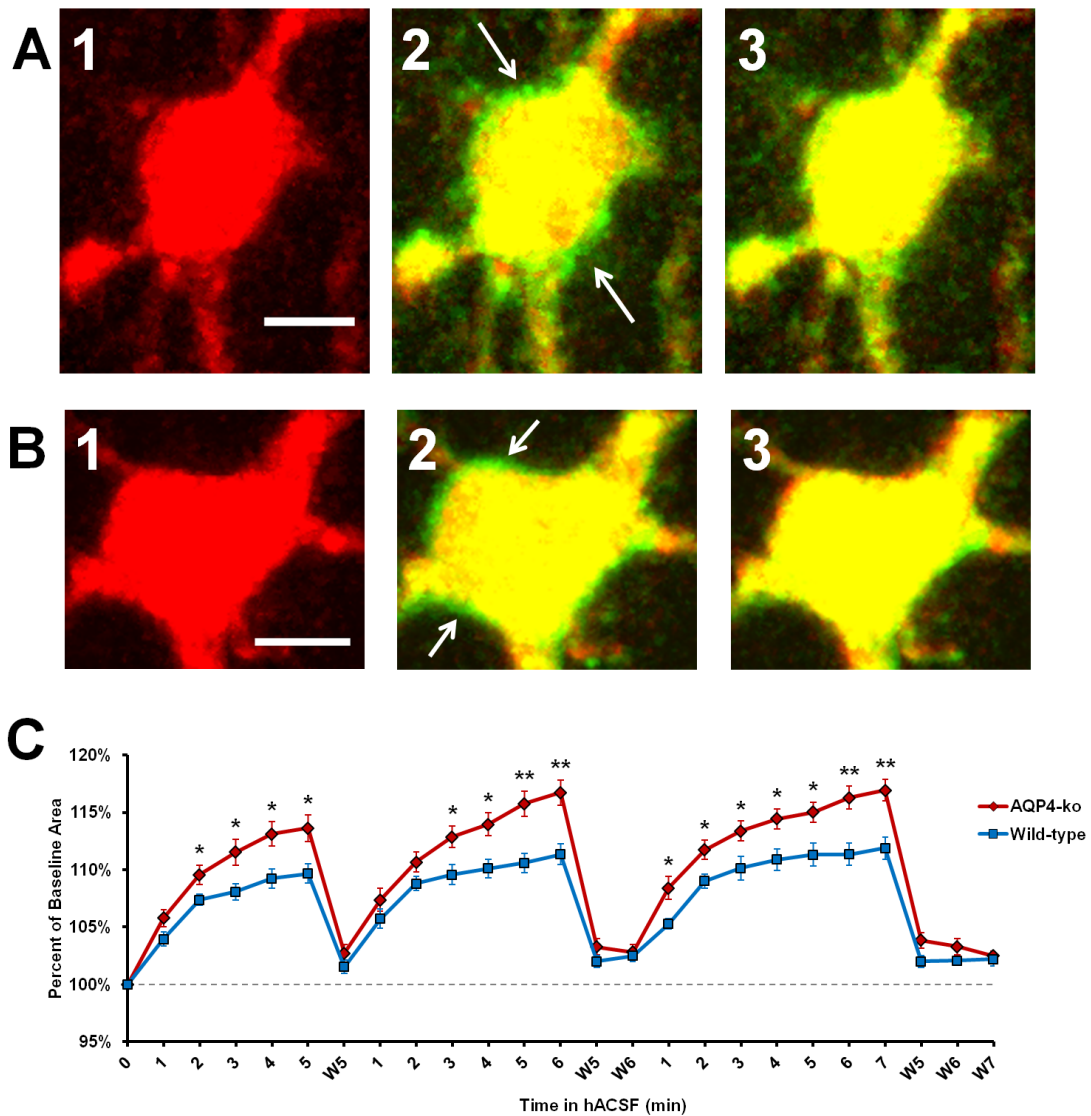
Figure 2.7. AQP4 knockout enhances astrocyte volume change in 40% hACSF

(A) Representative images of an AQP4-/- astrocyte soma at baseline (A1), after 5 minutes in 40% hACSF (A2), and after a 5 minute washout (A3). Baseline image is overlaid with A2 and A3 images to highlight swelling over baseline, indicated by white arrows. (B) Representative images of a wild-type astrocyte and its volume responses in 40% hACSF, at time points matching those in 5A above. Scale bars = 5 µm for A and B. (C) Soma area quantified as a percentage of baseline in AQP4-/- and wild-type astrocytes. Neurons (N = 9 per group, not shown) did not exhibit any difference in swelling between the two genotypes. *p < 0.05, **p < 0.01 versus wild-type; N = 7 astrocytes per group.
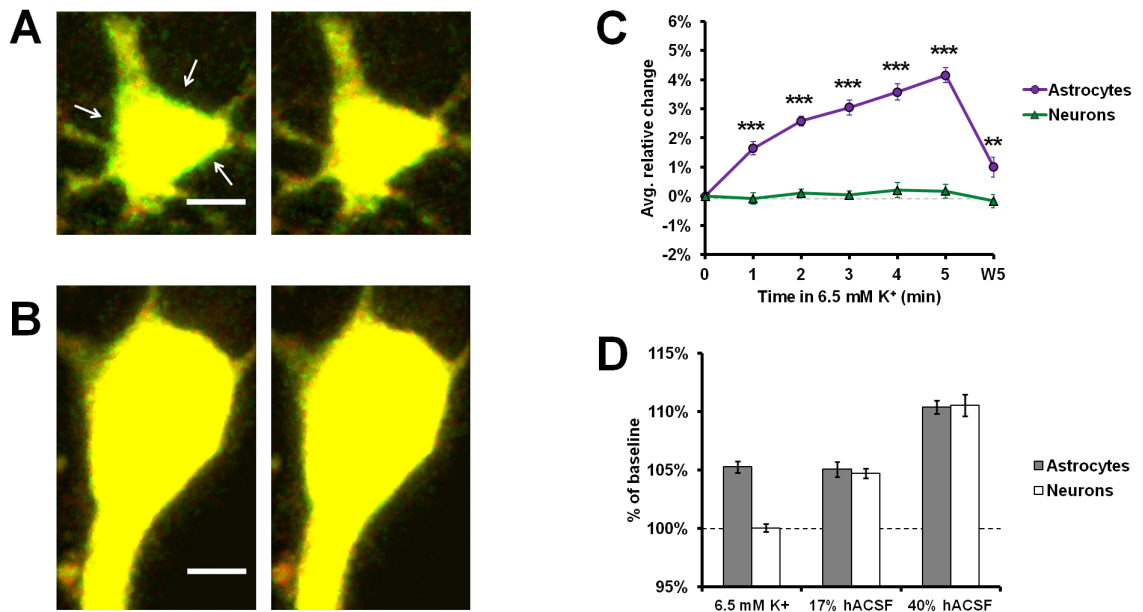
Figure 2.8. Astrocytes swell selectively in response to a physiological elevation in [K$^+$]$_o$

(A) Representative images of an astrocyte after 5 minutes of 6.5 mM [K$^+$]$_o$ (left) and 5 minutes washout (right), overlaid with baseline image to highlight volume changes. Expansions of the soma during high-[K$^+$]$_o$ are visible as green borders around the soma and are indicated directly by white arrows. (B) Overlays of neuronal volume at the same time points show a complete lack of volume change. Scale bars = 5 μm each for A and B. (C) Relative changes in astrocyte and neuron cell volume during exposure to 6.5 mM [K$^+$]$_o$, averaged across 3 consecutive applications. Dashed line indicates baseline level. Note that astrocytes do not return to baseline during the wash, as "baseline" astrocyte soma size increased with each high-[K$^+$]$_o$ application. **P < 0.01, ***P < 0.001 vs. neuron relative change; N = 8 cells per group. (D) Comparisons of astrocyte and neuron volume change after 5 minutes in 17% hACSF, 40% hACSF or 6.5 mM [K$^+$]$_o$. Astrocyte volume in 6.5 mM [K$^+$]$_o$ is roughly equivalent to that of 17% hACSF, but is not accompanied by the neuronal swelling observed in the latter.

Chapter 3: Astrocyte swelling and glutamate release in a high-$[K^+]_o$ model of epileptiform activity

3.1. Abstract

Epilepsy is a collection of disorders affecting an estimated 65 million people worldwide, and is broadly characterized by unprovoked, unpredictable recurrence of seizures. Most current therapies have negative effects on cognition, and are ineffective in approximately 1/3 of epilepsy cases. In recent years, astrocytes have been suggested to play a critical role in the development of disorders such as epilepsy. Astrocytes remove and redistribute potassium ions following neuronal synaptic transmission, which requires a corresponding water influx through the astrocyte-specific water channel aquaporin-4 (AQP4). Thus, astrocyte potassium buffering does lead to transient swelling. Astrocytes (like most cells) also express a class of volume-regulated anion channels (VRAC) which are permeable to excitatory amino acids including glutamate, and which are known to open in conditions of hypoosmolar or high-$[K^+]_o$-induced swelling. Thus, the possibility exists that astrocyte swelling could contribute to neuronal excitability by reducing extracellular space and releasing glutamate through VRAC. To determine the contribution of astrocyte swelling and glutamate release to epileptiform activity, we utilized the well-established high-$[K^+]_o$ model of epilepsy to record effects of astrocyte manipulations on neuronal epileptiform (seizure-like) activity in hippocampal slices. We found that paroxysmal

depolarizing shifts (PDSs), a type of epileptiform activity, could be readily evoked by physiological elevations of $[K^+]_o$. PDS amplitude and frequency were inversely proportional and dependent on $[K^+]_o$ dose. PDSs could be entirely blocked by the NMDA receptor antagonist AP5, but not the AMPA/Kainate receptor antagonist NBQX. Importantly, PDS amplitude was significantly reduced by ~50% over time by the astrocyte-specific VRAC antagonist DCPIB. Preliminary experiments indicate that astrocytes swell rapidly in the presence of elevated-$[K^+]_o$. We also found that individual astrocytes swell continuously (and selectively) when patch-clamped using a hyperosmolar internal solution. This selective manipulation of astrocyte volume will be used in future experiments to address the role of astrocyte swelling on neuronal excitability and seizures.

3.2. Introduction

Epilepsy is a seizure disorder affecting 65 million people worldwide (www.epilepsy.com), and is characterized by recurrent, unprovoked seizures in a patient. For approximately 30% of epilepsy patients, seizures cannot be controlled with current antiepileptic drugs (Brodie and Dichter, 1996; Kwan and Brodie, 2000; Brodie et al., 2012), and require more invasive surgical procedures (Thom et al., 2010). For those with non-refractory epilepsies, quality of life remains substantially reduced by the cognitive side effects of extant AEDs (Kwan and Brodie, 2001a; Aldenkamp et al., 2003) which mostly target neurons directly to reduce firing (Rogawski and Loscher, 2004; Stafstrom, 2010; Abdelsayed and Sokolov, 2013). This lack of effective treatments reflects, in part, an incomplete understanding of the underlying causes for many epilepsies and seizures (Eadie, 2012).

In recent years, glial cells such as astrocytes have come to the forefront as potential targets for a number of neurological disorders, including epilepsy (Seifert et al., 2006; Wetherington et al., 2008; Hubbard et al., 2013). Considerable evidence suggests that astrocyte swelling, in particular, may contribute to seizure development. Tissue swelling and reduction of the extracellular space (ECS) is well-documented to increase susceptibility to seizure (Traynelis and Dingledine, 1989; Dudek et al., 1990; Andrew, 1991; Roper et al., 1992; Kilb et al., 2006) and tends to precede a seizure *in vivo,* but is significantly reduced in animals lacking the astrocytic water channel aquaporin-4 (AQP4)

(Binder et al., 2004b). AQP4$^{-/-}$ animals also show a significant increase in seizure threshold (Binder et al., 2004a). AQP4 is also one of several surface channels/receptors mis-expressed in astrocytes from epileptic tissue (Binder and Steinhauser, 2006).

Apart from increasing ephaptic interactions and ECS concentrations of K$^+$ and glutamate through swelling, astrocytes may also trigger epileptiform activity by releasing their own intracellular glutamate. Hypoosmotic swelling of astrocytes in culture consistently results in the release of excitatory amino acids, including glutamate (Kimelberg et al., 1990; Kimelberg et al., 1995) through volume-regulated anion channels (VRAC) (Rutledge et al., 1998; Abdullaev et al., 2006). In intact tissue, astrocytic glutamate release may be responsible for the generation of slow inward currents (SICs), which can be synchronous among neurons up to ~100 μm apart (Angulo et al., 2004; Fellin et al., 2004; Fiacco et al., 2007). These small groups of neurons firing in synchrony could aggregate into larger groups over time under epileptogenic conditions, eventually leading to a seizure (Bikson et al., 2003; Jiruska et al., 2010). Both swelling and channel-mediated glutamate release by astrocytes could therefore contribute to the generation of seizures.

In this study, we use a high-[K$^+$]$_o$ model of epileptiform activity (Korn et al., 1987; Traynelis and Dingledine, 1988; Jensen and Yaari, 1997; Frohlich et al., 2008) to test the hypothesis that astrocyte swelling, and astrocytic glutamate release, are significant contributors to the development and maintenance of

epileptiform activity. We begin with the establishment of the high-$[K^+]_o$ model in our lab, discussing the basic properties and pharmacology of evoked epileptiform activity. Evidence will be presented to suggest that high-$[K^+]_o$-induced astrocytic swelling alone is not sufficient to induce epileptiform activity; however, astrocytic glutamate release may be a significant contributor.

3.3.   Materials and Methods

All animals and protocols used in the following experiments were approved by the Institutional Animal Care and Use Committee at UCR.

3.3.1. Slice preparation

Hippocampal slices were prepared from juvenile (12-21 day old) C57Bl/6J mice as previously described (Xie et al., 2014, and Chapter 2). Animals were deeply anesthetized under isofluorane and decapitated, and brains were quickly removed into ice-cold "slicing buffer" containing (in mM): 125 NaCl, 2.5 KCl, 3.8 $MgCl_2$, 1.25 NaH_2PO_4, 26 $NaHCO_3$, 25 glucose, 1.3 ascorbic acid and 3.5 MOPS, bubbled continuously with carbogen (95% O_2/5% CO_2). Parasagittal hippocampal slices (300-350 µm thick) were prepared as described in chapter 2, and recovered in standard ACSF containing (in mM): 125 mM NaCl, 2.5 KCl, 1.5 $CaCl_2$, 1.5 mM $MgCl_2$, 1.25 NaH_2PO_4, 26 $NaHCO_3$, and 15 glucose, bubbled continuously with carbogen (~299-303 mOsm). The reduced $CaCl_2$ (and slightly

increased MgCl$_2$) match concentrations used by Traynelis and Dingledine (1988), whose work was used as the basis of our high-[K$^+$]$_o$ model. Slices were incubated in ACSF at 35º C for 45 minutes, then allowed to cool to room temperature for a minimum of 15 minutes before being transferred to a recording chamber for experiments.

For one experiment, SR-101 was used to specifically label astrocytes (Schnell et al., 2015). Incubation times and solutions for this procedure were identical to those described in Chapter 2.

3.3.2. Experimental solutions and drugs

Prior to starting an experiment, slices were bathed in standard ACSF by default. Over the course of an experiment, two types of "experimental" ACSF solutions would then be used. The first, "Mg^{2+}-free" ACSF was prepared the same as standard ACSF, but Mg^{2+} was omitted (~297-301 mOsm); this was described as the "baseline" or "wash" ACSF in the experiments below. The second, "High-[K$^+$]$_o$" ACSF, was prepared in one of two ways. For early experiments, high-[K$^+$]$_o$ ACSF was prepared by simple addition of KCl to Mg^{2+}-free ACSF (generally an additional 2-6 mM, depending on the experiment), which correspondingly raised solution osmolarity by 4-12 mOsm. As we became concerned about possible effects of this hyperosmolar shift (see Results), this method was replaced by a secondary "isoosmolar" method in which the addition of KCl was balanced by an equimolar reduction in NaCl. This amounted to a <5%

reduction in $[Na^+]_o$ content and would not be expected to significantly impact physiological responses. No difference was found in epileptiform responses between the two high-$[K^+]_o$ ACSF types.

All experimental solutions contained 10 µM D-serine, a required co-agonist for the glycine site on the NMDA receptor. Where indicated, experimental solutions also contained 10 µM NBQX (an AMPA/Kainate receptor antagonist), 1 µM TTX (a voltage-gated Na^+ channel antagonist) or 50 µM DL-AP5 (an NMDA receptor antagonist). For early VRAC antagonist experiments, a cocktail was prepared consisting of the VRAC antagonists NPPB (100 µM) and DCPIB (20 µM) and the VRAC/Cl^- channel blocker DIDS (200 µM). In later VRAC antagonist experiments, DCPIB alone was used as it blocks VRAC more selectively than NPPB or DIDS.

3.3.3. Electrophysiology

Whole-cell patch clamp recordings were obtained using either a Multiclamp 700B amplifier and Digidata 1550 digitizer, or an Axopatch 200B amplifier and Digidata 1320 amplifier, connected to a computer running pClamp software version 10.2 or above and Multiclamp software (if required). Patch pipettes were pulled from borosilicate glass using a Sutter P-97 Flaming/Brown horizontal or Narshige PC-10 vertical micropipette puller. Neuronal patch pipettes had a resistance of ~3-6 MΩ when filled with an internal solution containing (in mM): 140 K-gluconate, 4 MgCl2, 0.4 EGTA, 4 Mg-ATP, 0.2 Na-GTP, 10 HEPES,

and 10 phosphocreatine, pH 7.3 with KOH. Astrocytic patch pipettes had a resistance of ~5-8 MΩ when filled with an internal solution containing (in mM): 130 K-gluconate, 4 MgCl2, 10 HEPES, 10 glucose, 1.185 Mg-ATP, 10.55 phosphocreatine, and 0.1315 mg/ml creatine phosphokinase, pH 7.3 by KOH. Astrocytes and neurons were identified as described in Chapter 2 methods. Neurons were voltage-clamped at -70 mV, the approximate reversal potential of chloride in our conditions, to help limit confounding effects of IPSCs on observed epileptiform activity. Neuronal currents were recorded in gap-free mode at 5 kHz and lowpass filtered at 2 kHz. Astrocytes, when recorded for a long term (as in the dual-patch clamp experiments), were held at -90 mV (the approximate reversal potential for K^+, which drives most of the astrocyte membrane potential) and recorded in gap-free mode alongside neurons.

3.3.4. PDS generation in high-$[K^+]_o$ conditions

In general, an experiment began with patch clamp of a CA1 pyramidal neuron. Following voltage step and recording of the membrane potential to confirm cell health, neurons were voltage-clamped at -70 mV. This is approximately equal to the reversal potential of Cl^- in our conditions and thus helps prevent IPSCs from confounding the observed epileptiform currents. Mg^{2+}-free ACSF was subsequently applied for a minimum of 8-10 minutes to remove the majority of the Mg^{2+} block from NMDA receptors in the slice. Neurons were then recorded in gap-free mode and exposed to high-$[K^+]_o$ ACSF for a minimum

of 5 minutes, with $[K^+]_o$ doses and drugs as required for a given experiment, before returning to Mg^{2+}-free ACSF for a 5 minute wash period. In most cases PDSs began occurring in the patched neuron within 2-3 minutes of high-$[K^+]_o$ application. Occasionally, PDSs would take significantly longer to occur (up to 8 minutes or more), or would not occur at all during the first high-$[K^+]_o$ application, but would occur normally during a second application (following a 5-minute wash). In these cases, PDSs occurring during the second application were treated as "baseline" PDS activity in high-$[K^+]_o$, and PDSs in the first application (if any) were ignored. Cells which failed to respond after multiple high-$[K^+]_o$ applications were generally discarded. Access resistance was checked before and after each application period (high-$[K^+]_o$ application + wash) for later use in PDS analysis.

3.3.5. Detecting and analyzing PDSs

PDSs were first recognizable by eye as generally being substantially larger than a typical miniature EPSC (often by an order of magnitude or more) with slow rise and decay slopes, often appearing highly similar to the NMDA receptor-dependent slow inward currents (SICs) we have observed in hypoosmolar conditions (Fiacco et al., 2007; Lauderdale et al., 2015). PDSs differed most visibly from SICs in their regularity, as PDSs would occur at a relatively constant, $[K^+]_o$ dose-dependent rate within a particular cell (see

96

Results). This is a general feature of interictal discharges/PDSs in various seizure models (Tancredi and Avoli, 1987; Fellin et al., 2006).

Although most PDSs were 100 pA or larger, we found that detection of smaller PDSs (particularly in the DCPIB study, where PDSs shrank sometimes to just above noise level) proved challenging for a standard threshold event search; too high a threshold would eliminate smaller PDSs, but too low a threshold picked up considerable mEPSC noise. Furthermore, threshold detection did not discriminate based on the "shape" of the current, one of the more recognizable features of a PDS. Therefore, PDSs were instead detected using clampfit's "template search". For each cell, the first ~5 clearly-recognizable PDSs were chosen from within the "baseline" high-$[K^+]_o$ application, and averaged together to create a template. PDSs containing un-clamped action potentials, or other anomalies to their standard shape were not considered "representative" PDSs and were thus skipped during template creation. For a given cell, a template search would then be run on each evoke using the template created from its baseline. In most cases, kinetics were reported for raw data. Kinetics could not be calculated for raw PDSs in which un-clamped action potentials were observed; instead, these events were separately detected and curve-fitted. Kinetics calculated based on these curve fits were used in place of the missing data.

Access resistance (see above) was used to determine usability of recording segments. PDS amplitudes and rise/decay kinetics were not used for

recordings in which access resistance changed more than 25% from the start of the recording, or from the end of the baseline recording. These criteria proved particularly difficult to meet for experiments involving DCPIB, which by their nature required patched cells to remain stable for at least 45 minutes. By Ohm's law ($I = V/R$) we know that measured current is inversely proportional to input resistance, R_{in}, which includes the access resistance R_a. Thus, with all else being equal, a change in R_a should cause PDS amplitude to change in the opposite direction. Conversely, if PDS amplitude changed in the *same direction* as R_a, we could be certain that R_a was not contributing to the observed change in amplitude. We therefore defined two exceptions to our original access resistance criteria, under which amplitude and kinetics could still be used from an initially "rejected" recording: First, if R_a and PDS amplitude both increased, and second, if R_a and PDS amplitude both decreased.

Event frequency was calculated for all recordings without regard to rejection criteria, since changes in R_a (possibly with some extreme exceptions) would not be expected to change the overall number of events in a recording.

3.3.6. High-$[K^+]_o$ and astrocyte volume

Astrocytes were loaded via patch clamp with 100-200 µM Fluorescein Dextran or Alexa Fluor 488 Dextran, 10,000 kDa. Following a successful outside-out patch, astrocytes were allowed to rest for 8-10 minutes, during which time Mg^{2+}-free ACSF was washed in. Fluorescein and Alexa Fluor 488 dextrans were

detected with a 488 nm laser, with excitation/emission settings and basic imaging protocol as described in Chapter 2. The first z-stack was obtained following the 8-10 minute recovery period, and another stack obtained every 1-2 minutes during high-$[K^+]_o$ application. A final stack was obtained at the end of the 5 minute washout period in Mg^{2+}-free ACSF. Analysis was performed as described in Chapter 2 methods and outlined in Figure 2.1.

3.3.7. Patch-clamp modulation of astrocyte volume

For preliminary experiments on direct astrocyte swelling, internal solutions were made hyperosmolar through the addition of 20-50 mM sucrose and contained Fluorescein dextran or Alexa Fluor 488 dextran. Astrocytes were then patch clamped as described above, and z-stacks were obtained at 5 minute intervals (starting at 5 minutes after whole-cell configuration). Volume clamp attempts were performed similarly, but relied on astrocyte internal solution which was either unmodified (~285 mOsm, slightly hypoosmotic to extracellular solution) or made ~20 mOsm hypoosmolar by dilution with deionized water.

Functional tests of astrocyte swelling (and to a lesser extent, volume clamp) were performed through simultaneous patch clamp of a neuron and astrocyte during PDS generation. To visually confirm the proximity of these cells, neuronal internal solutions contained 200 µM Alexa Fluor 568 or 594 hydrazide, which were detected with the same excitation and emission spectra as SR-101; Astrocyte internal solutions contained Fluorescein dextran or Alexa Fluor 488

99

dextran as described above. Multiple strategies were used in an attempt to optimize success of this procedure. By far the most successful was to apply Mg^{2+}-free ACSF for 10 minutes <u>first</u>, then seal onto both cells. After this, we could rupture the neuronal patch and record from the neuron as normal. Both the neuron and the astrocyte were continuously recorded in voltage-clamp mode, even before breaking into the astrocyte, as a method of monitoring the seal on the astrocyte; in some cases (albeit unintentionally) we found this was an excellent way of identifying the precise moment of we went whole-cell on an astrocyte, which itself could have utility in future experiments.

3.3.8. Statistics

Statistical analysis was generally as described in Chapter 2 Methods, including outlier detection/exclusion and mixed ANOVA procedures. In some cases, a mixed ANOVA was inappropriate due to missing time points in some groups (most notably in the DCPIB experiments, as described in Results), which would ordinarily result in the exclusion of the entire cell from analysis. To avoid this substantial loss of data, these sets were instead analyzed using the linear mixed models (LMM) approach in SPSS, a more flexible (if complicated) method of analyzing repeated measures which would not exclude cases with missing time points. Post-hoc tests, if required, were adjusted for multiple comparisons by the Bonferroni method. With the exception of scatterplots (Figures 3.3 and 3.4),

all graphs display data as mean ± S.E.M. Significant differences are displayed as $*p < 0.05$, $**p < 0.01$, and $***p < 0.001$.

3.4. Results

3.4.1. Establishing parameters of a high-$[K^+]_o$ model

In studying the effect of astrocyte swelling and glutamate release on neuronal epileptiform activity, we elected to use a high-$[K^+]_o$, 0 mM Mg^{2+} model of epilepsy in hippocampal slices. This model was developed from existing, well-described models of high-$[K^+]_o$-induced (Rutecki et al., 1985; Traynelis and Dingledine, 1988) and low-Mg^{2+}-induced epileptiform activity in the hippocampus (Walther et al., 1986; Tancredi et al., 1990; Derchansky et al., 2004). Elevated $[K^+]_o$ presented an attractive model for this study both for its well-established effects on neuronal excitability and seizure generation (Frohlich et al., 2008), and for its direct effect on astrocyte volume (Walz, 1987; MacVicar et al., 2002) and related volume changes in brain tissue (Traynelis and Dingledine, 1989; Holthoff and Witte, 2000).

We began by establishing the optimal parameters for our model. In previous studies, epileptiform activity was reliably recorded using ~5-8 mM $[K^+]_o$ (Rutecki et al., 1985; Tancredi and Avoli, 1987; Traynelis and Dingledine, 1988), suggesting that 5.5-8.5 mM $[K^+]_o$ (a 3-6 mM elevation above the baseline $[K^+]_o$ of 2.5 mM in our ACSF) would be sufficient to evoke epileptiform activity in our

hippocampal slices. Epileptiform activity has often been reported using either extracellular electrodes, or impaling electrodes for intracellular voltage recordings. We instead opted to record neuronal currents using whole-cell voltage clamp, with neurons held at -70 mV to reduce the contribution of IPSCs (see Methods). This setup aided us in recording the large, excitatory currents underlying epileptiform events, as well as allowing detection of slow inward currents (Lauderdale et al., 2015) if present.

Similar to previous groups, we found that elevation of $[K^+]_o$ to 6.5 mM or above was sufficient to reliably evoke epileptiform activity (Figure 1A). These events tended to be very large (generally >100 pA), fairly stereotypical in shape (Figure 3.1B, D), and occurred with a low, but relatively stable frequency in a given cell. The repetitive nature and abnormal size of such events (as well as the conditions in which they occurred) strongly resembled characteristics of the interictal discharges observed by other groups (Rutecki et al., 1985; Jensen and Yaari, 1988; Traynelis and Dingledine, 1988), recorded intracellularly as the "synchronous epileptiform discharge" (SED) observed by Tancredi and Avoli (1987), and more commonly referred to as the "paroxysmal depolarizing shift" or PDS (Hablitz, 1984; Johnston and Brown, 1984; Rutecki et al., 1985). Although our neurons were technically voltage-clamped (preventing the depolarizing shift), the intracellular events recorded were clearly the voltage-clamp correlate of the PDS (Rutecki et al., 1985; Fellin et al., 2006). This was further confirmed through limited experiments in which extracellular recordings were made of interictal

events, which closely matched the typical frequency of the putative PDS (Figure 3.1C). Thus, we chose the term "PDS" to describe the epileptiform events we observed, despite the technical misnomer. All subsequent discussion of such events in this study will refer to them as PDSs for the sake of clarity.

3.4.2. PDSs are dependent on neuronal firing and NMDAR activation

A central tenet of our early hypothesis was that if astrocytes are swelling in high-$[K^+]_o$ independently of neuronal firing (see Ch. 2), we might also expect astrocytic glutamate release through VRAC (Rutledge et al., 1998), leading to epileptiform activity independently of neuronal firing. In practice, we found that PDSs were never evoked in the presence of the Na^+_V channel antagonist tetrodotoxin (TTX; 1 μM), and were rapidly abolished when it was added mid-recording (not shown). These data suggested that, as reported previously, PDSs were "giant synaptic potentials" (Johnston and Brown, 1984) and dependent on neuronal firing (Fellin et al., 2006). This did not, however, preclude the possibility of astrocytic contribution to PDS generation. Despite their dependence on neuronal firing, PDSs bore a remarkable resemblance to the TTX-independent, NMDA-receptor-dependent slow inward currents (SICs) observed in hypoosmolar conditions (Fiacco et al., 2007; Lauderdale et al., 2015). To determine if PDSs shared a similar pharmacology, we performed a limited set of experiments in which PDSs were recorded before and after application of the NMDA receptor antagonist D,L-AP5 (50 μM), which in our previous study was sufficient to abolish

SIC activity (Lauderdale et al., 2015). In nearly every case, PDSs were completely abolished within 1 minute of AP5 application (Figure 3.2A, C). In contrast, addition of the AMPA/Kainate receptor antagonist NBQX (10 μM) had no significant effect on event frequency (Figure 3.2B, D). NBQX did have the effect of "cleaning up" the PDS, presumably as a consequence of removing the AMPA EPSCs normally observed below the overall PDS waveform (Figure 3.2B, insets), but had little apparent effect on PDS amplitude. As with high-$[K^+]_o$ alone, PDSs could be evoked and re-evoked indefinitely in the presence of NBQX (not shown).

3.4.3. PDS amplitude and frequency are inversely correlated

While determining the appropriate parameters for our model we observed that higher doses of K^+ seemed to evoke PDSs with higher frequency but lower amplitude. The gradual decline in PDS amplitude over time (see Figure 3.1) became more apparent in higher $[K^+]_o$, to the point that PDSs in $[K^+]_o$ above ~8 mM would sometimes disappear entirely within 2-3 minutes after their initiation. We wondered whether this counterintuitive result might be a consequence of the small hyperosmotic shift (~2-12 mOsm) conferred by addition of K^+ to our high-$[K^+]_o$ solutions. Neuronal excitability and seizure activity are both inversely correlated with extracellular osmolarity (Traynelis and Dingledine, 1989; Rosen and Andrew, 1990; Saly and Andrew, 1993; Azouz et al., 1997; Huang et al., 1997; Lauderdale et al., 2015); moreover, if astrocyte swelling was involved in

PDS generation, then increased osmolarity (which should shrink astrocytes) would result in smaller PDSs. We tested this possibility by preparing "isoosmotic" high-$[K^+]_o$ solutions, in which K^+ elevations were offset by equimolar reductions of Na^+. In both 6.5 mM and 7.5 mM K^+ (two of our most commonly used doses), we found no significant change in PDS amplitude or frequency resulting from isoosmotic high-$[K^+]_o$.

Combining these data together with PDSs evoked in NBQX, it became clear that of the factors tested, the best determinant of PDS activity was in fact the $[K^+]_o$ dose itself (Rutecki et al., 1985; Tancredi and Avoli, 1987). As we had observed, K^+ dose increases correlated with increasing PDS frequency (Figure 3.3A) and decreasing amplitude (Figure 3.3B). This inverse relationship between frequency and amplitude is easily observed when pooled across $[K^+]_o$ doses (Figure 3.3C).

3.4.4. PDSs are inhibited or blocked by VRAC antagonists

With the basic parameters of our model established, we set out to examine the role of astrocytic volume-dependent glutamate release on PDS activity. Astrocytes are known to express volume-regulated anion channels (VRAC) which are permeable to glutamate and other excitatory amino acids (EAAs), and antagonists of these channels are known to inhibit swelling-induced EAA release from astrocytes in culture (Akita and Okada, 2014). In the interest of blocking any possible VRAC contribution to PDS activity, we created a cocktail of

3 commonly-used VRAC antagonists: DCPIB (4-(2-butyl-6,7-dichlor-2-cyclopentyl-indan-1-on-5-yl), 20 µM; DIDS (4,4'-diisothiocyanatostilbene-2,2'-disulfonic acid), 200 µM; and NPPB (5-nitro-2-(3-phenylpropylamino)benzoic acid), 100 µM (Rutledge et al., 1998; Abdullaev et al., 2006; Liu et al., 2006). As before, PDSs were evoked in 8.5 mM $[K^+]_o$ prior to addition of antagonists and measured for several minutes afterwards (Figure 3.4A). As shown in Figure 3.4B (normalized to max amplitude per cell, due to low N), PDS amplitude sharply declined following addition of the antagonist cocktail and in most cases, eventually disappeared. In contrast to a cell in typical high-$[K^+]_o$ ACSF (Figure 3.4C), PDSs could not be re-evoked by the same dose of high-$[K^+]_o$ in antagonist-treated cells (Figure 3.4D), even after a 20-minute washout (not shown).

While the aforementioned experiment clearly showed strong block of PDSs, it also lacked specificity. Evidence suggests that some neurons also express VRAC subtypes which can be inhibited by many of the same antagonists as in astrocytes (Inoue et al., 2005; Inoue and Okada, 2007; Zhang et al., 2011). Additionally, both NPPB and DIDS have known nonspecific targets (Evanko et al., 2004). We therefore narrowed our focus to DCPIB alone, a highly selective VRAC blocker (Decher et al., 2001) which potently inhibits astrocytic, but not neuronal, VRAC at low concentrations (Abdullaev et al., 2006; Zhang et al., 2011). Performing the same experiment as with the full cocktail, it quickly became clear that DCPIB had a much slower effect than NPPB or DIDS and that

a single high-$[K^+]_o$ application (or even a second application) was insufficient to observe much of an effect. We therefore applied high-$[K^+]_o$ a total of 3 times for DCPIB-only experiments (Figure 3.5). A "baseline" application of 6.5 mM $[K^+]_o$ (High-$[K^+]_o$ Trial 1, 5 minute minimum; see Methods) was followed by a 5 minute return to baseline $[K^+]_o$; these steps were repeated 2 additional times in each cell. This general time course is displayed in figure 3.5A and B. Upon the first "wash" back to baseline $[K^+]_o$, either DCPIB (20 µM, dissolved in EtOH) or EtOH vehicle control (0.02% v/v) was added to the bath and left in until the end of the 2nd high-$[K^+]_o$ application (Figure 3.5A, B). Concerns about possible effects of EtOH on PDS behavior (Swartzwelder et al., 1995) led to the inclusion of a third, "untreated" control group, in which only elevated $[K^+]_o$ was applied. Effects of DCPIB alone were far more subtle than the VRAC antagonist cocktail. In stark contrast to the VRAC antagonist cocktail, DCPIB did not fully block PDS generation, and PDSs still initiated at or near full amplitude even in the 3rd high-$[K^+]_o$ application – more than 15 minutes after DCPIB application (Figure 3.5B). This longer time course may reflect differences in the mechanism of action for DCPIB as compared to NPPB or DIDS (see Discussion).

DCPIB's effects were generally most apparent in the minutes following the first several PDSs during the 3rd high-$[K^+]_o$ application, when PDS amplitude sharply declined and remained suppressed for the remainder of the application (Figure 3.5C). Comparisons of average PDS amplitude between DCPIB and EtOH further highlight the effect of DCPIB (Figure 3.6A). Unlike the EtOH control

condition in which PDSs grew significantly larger over time (N=8 cells, 1st through 3rd high-$[K^+]_o$ application), PDS amplitude in the presence of DCPIB decreased significantly across high-$[K^+]_o$ applications, reaching only ~50% of the amplitude of the EtOH controls (N=8 cells, 1st through 3rd high-$[K^+]_o$ application). Untreated controls (N=12 cells) did not vary significantly in PDS amplitude across the first 3 high-$[K^+]_o$ applications. For those few cells which could be held in voltage-clamp beyond the 3rd high-$[K^+]_o$ application, a 15-minute wash period was included ("Wash", Figure 3.6A). A nonsignificant trend (p=0.099) suggested that DCPIB's effects could not be washed out even after 15 minutes; unfortunately, the lack of viable cells by this time point (N=4, 4, and 5 cells for DCPIB, EtOH, and Untreated Control, respectively) precluded a more thorough analysis. PDS frequency (Figure 3.6B) generally decreased starting from the 2nd high-$[K^+]_o$ application, with no significant interaction between treatment and time point but notably in direct proportion to PDS amplitude in DCPIB and indirect proportion to PDS amplitude in EtOH. Rise time (Figure 3.6C) and decay tau (Figure 3.6D) were not significantly altered by DCPIB or by EtOH, although rise time overall tended to increase with subsequent evokes. Together, these data strongly suggest that volume-dependent glutamate release, at least some of it astrocytic, is important for the magnitude of PDS activity.

3.4.5. Astrocyte volume change in the high-$[K^+]_o$ model

If astrocyte volume-dependent glutamate release is indeed a contributor to

the PDS, we would expect to observe rapid astrocyte swelling in 6.5 mM $[K^+]_o$. Astrocytes were patch-loaded with fluorescent dextrans (10 kDa), or stained with SR-101, and exposed to 6.5 mM $[K^+]_o$ ACSF for at least 5 minutes (a typical time course for observing PDSs). Just as we observed in Mg^{2+}-free, high-$[K^+]_o$ ACSF with TTX and NBQX (Figure 3.7A, right; see also chapter 2), astrocytes swelled rapidly in 6.5 mM $[K^+]_o$ alone (Figure 3.7A, left) and in the presence of normal Mg^{2+} (Figure 3.7A, center). Preliminary analysis suggested that Mg^{2+}-free, high-$[K^+]_o$ alone was less effective at swelling astrocytes than high-$[K^+]_o$ without Mg^{2+} (Figure 3.7B; $p < 0.05$), but it is worth noting that the former astrocytes were patch-loaded with fluorescent dextrans and the latter loaded by SR-101. As established in Chapter 2, patch clamp tends to result in a small but significant reduction in cell volume change, at least when evoked using hypoosmolar ACSF. Therefore, the precise effect (if any) of Mg^{2+} on astrocyte high-$[K^+]_o$-induced swelling remains to be determined. It is, however readily apparent that none of these conditions blocked astrocyte swelling in high-$[K^+]_o$.

To further probe the possibility that astrocyte glutamate release could provoke or compound PDS activity, we required a method of selectively manipulating astrocytes. Most recent literature suggests hypoosmolar solution should be a viable method of swelling astrocytes (Andrew et al., 2007; Caspi et al., 2009; Risher et al., 2009), but we found this was not specific to astrocytes in our conditions (see chapter 2). Instead, we considered the possibility of individually patch-clamping astrocytes to manipulate their contents directly.

Preliminary experiments indicated that individual astrocytes could be directly swollen by patch clamp, through the use of a modified astrocyte internal solution. Using sucrose to increase the internal osmolarity of the astrocyte by ~50 mOsm, we found that a patch-clamped astrocyte swelled indefinitely until the pipette was removed, after which it would gradually regain its original volume (Figure 3.8A). Since passive astrocytes are widely coupled via gap junctions (Wallraff et al., 2004), we reasoned that sucrose (which is well within the ~1 kDa size limit for gap junction permeability should be able to swell a wide area of the astrocyte syncytium. However, we found this was not the case. Even when directly adjacent (Figure 3.8B) and thus highly likely to be coupled, nearby astrocytes steadfastly retained their volume while patched astrocytes swelled as expected (Figure 3.8C). The reason for this selectivity is not yet clear.

If a simple increase of internal osmolarity could produce such astrocyte swelling (and possibly volume-induced channel opening), we hypothesized that any effects of astrocyte volume-dependent glutamate release on PDS amplitude or frequency would be amplified by directly swelling astrocytes with a hyperosmolar internal solution. To test this, we recorded high-$[K^+]_o$ evoked PDSs from a neuron (Figure 3.9A, top cell and trace) while simultaneously patch clamping a nearby astrocyte with a 20-40 mOsm hyperosmotic internal solution (Figure 3.9A, bottom cell and trace). Cells in these experiments were chosen especially for their proximity to one another, as this increased the likelihood of interaction. Despite the astrocyte swelling caused by hyperosmolar internal

solution, preliminary experiments did not indicate any significant effect on PDS amplitude in nearby neurons (p = 0.466 vs baseline PDS amplitude, Two-tailed t-test, N = 28-41 events pooled across 2 cells), nor any obvious change in PDS frequency. We did note, however, that astrocytes were a remarkably good readout of PDS activity in the neuron (Figure 3.9A, B). Every large PDS was almost simultaneous with a large, presumably K^+-driven inward current in the associated astrocyte, while smaller PDSs (often those which didn't fit the overall "pattern" of PDS activity, as seen with the small event in Figure 3.9B) elicited no change in the astrocyte. This suggests that astrocyte currents could be a more accurate (if less direct) readout of epileptiform activity.

We also considered the opposite approach: if astrocyte swelling contributes to PDS activity, then blocking it should have a noticeable effect on PDS generation in nearby neurons. Since the pipette volume is enormous compared to the volume of the astrocyte itself, it effectively acts as a huge source and sink for water and ions, so patch clamping an astrocyte with a standard (isoosmolar or slightly hypoosmolar) internal solution should effectively "clamp" the volume. Whether this strategy is effective in clamping astrocyte volume is currently unknown; however, limited experiments indicated that, as above, PDSs in nearby neurons were not visibly affected by this astrocyte manipulation. These data remain preliminary and further experimentation will be required to determine the effect of manipulating astrocyte volume on PDS activity.

3.5. Discussion

In this study, we established a model of high-$[K^+]_o$-induced epileptiform activity in our lab, and utilized it to begin testing the hypothesis that astrocytic swelling and glutamate release are important contributors to the development of seizures. We found, as previous authors have, that PDSs (and by extension, interictal discharges) are dependent upon neuronal firing in hippocampal area CA1. However, we also found evidence of astrocyte volume-dependent glutamate release contributing to the PDS.

Multiple factors are thought to contribute to PDS generation and spread (de Curtis and Avanzini, 2001). Many studies (Rutecki et al., 1985; Mody et al., 1987; Jensen and Yaari, 1988; Jones and Heinemann, 1988; Traynelis and Dingledine, 1988) have demonstrated that PDSs are generally propagated by synaptic activity; this is particularly evident in the hippocampal slice model, where severing the Schaffer collaterals (and thereby disconnecting CA3 from CA1) abolishes PDSs in CA1 but not CA3 (Mody et al., 1987; Traynelis and Dingledine, 1988; Tancredi et al., 1990). As might be expected, PDS pharmacology also differs substantially between CA1 and CA3, with CA1 PDSs being far more sensitive to NMDA receptor antagonists than CA3 (Dingledine et al., 1986; Mody et al., 1987; Fellin et al., 2006). Consistent with both of these lines of evidence, blocking either neuronal firing or NMDA receptors abolished PDS activity in our model, but AMPA antagonists had little to no effect. PDS frequency increased and amplitude decreased with increasing $[K^+]_o$, as observed

112

in other studies (Rutecki et al., 1985; Tancredi and Avoli, 1987). Interestingly, this $[K^+]_o$ dependence remains even for PDSs evoked in the absence of synaptic transmission (Haas and Jefferys, 1984; Yaari et al., 1986). This suggests that in some models, and especially in CA1, PDSs may be dependent more on the nonsynaptic effects of $[K^+]_o$ elevations than on pure synaptic transmission.

Multiple studies have previously shown that nonsynaptic interactions such as ephaptic coupling and local changes in ion concentrations are capable of eliciting PDSs in the absence of synaptic transmission (Jefferys and Haas, 1982; Taylor and Dudek, 1984; Dudek et al., 1986; Konnerth et al., 1986). These effects become even more pronounced when the extracellular space, which is already particularly small in CA1, is reduced by high-$[K^+]_o$ or hypoosmolar cell swelling (McBain et al., 1990; Jensen and Yaari, 1997). Our observations of rapid astrocyte swelling would seem to agree with these studies, as such swelling occurred with a similar time course to PDS generation. Further, this high-$[K^+]_o$-induced astrocyte swelling was not substantially different from that observed in the presence of TTX, in agreement with data showing that astrocyte water permeability can be increased by either potassium or by glutamate (Gunnarson et al., 2008; Song and Gunnarson, 2012). Given that PDS activity *was* blocked by TTX, this suggests that astrocyte swelling alone is not sufficient to initiate or maintain PDSs. It must be noted that although neuronal swelling was not observed in the presence of TTX (see chapter 2), the question remains as to whether neurons swell when firing is not blocked. Neuronal activity has been

reported in some preparations not only to swell axons directly, but to induce neurotransmitter release from volume-regulated anion channels (Fields and Ni, 2010). This was a proposed mechanism for neuron-to-glial communication in the white matter.

The significant block of PDS activity by our cocktail of VRAC antagonists is suggestive of a significant contribution by nonsynaptic, volume-dependent glutamate release. It is important to recognize that, of the 3 antagonists used in this study, only DCPIB at low concentrations is specific to astrocytic VRAC (Zhang et al., 2011) despite the use of all 3 to block astrocytic VRAC in culture. Both NPPB and DIDS have been used to block swelling-activated Cl^- channels in neurons, which can become activated in excitotoxic or ischemic conditions when neurons typically swell (Inoue et al., 2005; Inoue et al., 2007; Inoue and Okada, 2007; Zhang et al., 2011). Neurons are also known to swell in extremely high levels of $[K^+]_o$, normally producing spreading depression (Andrew et al., 2007; Zhou et al., 2010) and sometimes seizures as well (Huang et al., 1995; Olsson et al., 2006). While neuronal swelling is not observed with more gradual increases in $[K^+]_o$ (Zhou et al., 2010), the possibility exists that this resistance to volume change is a result of continuous volume regulation which would almost certainly involve the opening of neuronal VRAC. Finally, one must keep in mind that both NPPB and DIDS are also considered rather broad chloride channel blockers, and concerns have been raised about their effects on chloride channels required for vesicular loading of neurotransmitter (Evanko et al., 2004). In sum, data involving

the use of NPPB and DIDS, whilst informative, must also be interpreted extremely carefully.

These data are most interesting when compared with the effects of DCPIB alone, which is generally thought to block only astrocytic VRAC in the CNS. Most obvious is the difference in time – while the antagonist cocktail acted almost immediately, DCPIB usually required over 15 minutes of application to exert a noticeable effect. This is considerably slower than previously reported (Best et al., 2004; Abdullaev et al., 2006). The simplest explanation is that DCPIB simply takes time to exert its effects, as Best and colleagues (2004) found was the case with lower concentrations of DCPIB. Given that DCPIB is hydrophobic and must diffuse through layers of intact tissue in our model, it would likely interact with cell membranes and may take considerably longer to reach an effective concentration at the depth of our recorded cells. However, this does not explain the specific pattern of DCPIB's effects when they do become apparent after 15-20 minutes. Its lack of effect on the initial PDSs in trial 3 suggests that the PDS itself is unlikely to be directly driven by glutamate release from VRAC. It could be speculated that astrocytic VRAC opening simply increases the extracellular glutamate concentration, increasing the likelihood of NMDA receptor activation. "Ambient" glutamate of non-synaptic origin has already been observed in hippocampal slices, presumed to be released via DIDS-sensitive channels on astrocytes (Cavelier and Attwell, 2005). Ambient glutamate of non-synaptic origin induces a tonic NMDA current in CA1 pyramidal neurons (Le Meur et al., 2007).

VRAC may serve to elevate extracellular glutamate in a similar manner, maintaining a basal level of neuronal excitability necessary for episodic release of glutamate to be effective. Interestingly, swollen astrocytes may maintain a relatively stable intracellular concentration of glutamate through continuous reuptake of glutamate, even as it is being released through volume-sensitive channels (Schober and Mongin, 2015). With the volume-sensitive release blocked by DCPIB, the continuous activity of astrocyte glutamate transporters might gradually reduce the ambient glutamate concentration, in turn reducing the amount which could contribute to the PDS. Finally, it must also be noted that even DCPIB is not perfectly selective. Recent studies in cultured astrocytes have shown that DCPIB activates a potassium conductance and reduces both glutamate uptake through GLT-1, and glutamate release through connexin hemichannels (a nonspecific effect it shares with NPPB; Ye et al., 2009), while in slices it induces an outward potassium current in pyramidal neurons (Bowens et al., 2013; Minieri et al., 2013). This latter nonspecific effect in particular would also be likely to reduce neuronal excitability.

The role of astrocytic swelling and swelling-induced glutamate release in epileptiform activity remains an open question. Recently, the molecular identity of VRAC in multiple cell types was finally discovered, a heteromeric combination of leucine-rich repeat containing 8 (LRRC8) proteins, with LRRC8A being required for VRAC activation and other members (B-E) modifying its kinetics (Hyzinski-Garcia et al., 2014; Qiu et al., 2014; Voss et al., 2014). With this new information,

astrocytic (and/or neuronal) VRAC can be more easily targeted through RNAi knockdown or new drugs to target LRRC8 proteins. These will likely be important tools in determining the specific role of VRAC in epileptiform activity. Development of more specific tools to manipulate astrocyte swelling and glutamate release is an ongoing goal for this project. As we have shown, it is possible to directly swell astrocytes through hyperosmotic internal solution, and to record from said astrocytes simultaneously with neurons during PDS generation. We also found that the astrocyte itself makes an excellent detector of epileptiform activity, as others have observed (Traynelis and Dingledine, 1988), which may obviate the need for a neuronal (or extracellular) electrode in some future experiments. It remains to be determined whether astrocyte swelling induced by this method is sufficient to induce astrocytic glutamate release and influence neuronal PDS activity. A direct way to test both questions would simply be to elevate intracellular glutamate concentrations by 20 mM or more, thereby increasing both the volume of the astrocyte, and the amount of glutamate available for release through VRAC. It should be noted, however, that the increase in ionic strength conferred by glutamate could possibly *inhibit* VRAC activation (Voets et al., 1999). Future experiments will determine the viability of this approach, and continue to provide increasingly-specific information about the role of astrocytic swelling and glutamate release in epileptiform activity.

3.6. References

Abdelsayed M, Sokolov S (2013) Voltage-gated sodium channels: pharmaceutical targets via anticonvulsants to treat epileptic syndromes. Channels 7:146-152.

Abdullaev IF, Rudkouskaya A, Schools GP, Kimelberg HK, Mongin AA (2006) Pharmacological comparison of swelling-activated excitatory amino acid release and Cl- currents in cultured rat astrocytes. J Physiol 572:677-689.

Akita T, Okada Y (2014) Characteristics and roles of the volume-sensitive outwardly rectifying (VSOR) anion channel in the central nervous system. Neuroscience 275:211-231.

Aldenkamp AP, De Krom M, Reijs R (2003) Newer antiepileptic drugs and cognitive issues. Epilepsia 44 Suppl 4:21-29.

Andrew RD (1991) Seizure and acute osmotic change: Clinical and neurophysiological aspects. In: Journal of the Neurological Sciences, pp 7-18.

Andrew RD, Labron MW, Boehnke SE, Carnduff L, Kirov SA (2007) Physiological evidence that pyramidal neurons lack functional water channels. Cereb Cortex 17:787-802.

Angulo MC, Kozlov AS, Charpak S, Audinat E (2004) Glutamate released from glial cells synchronizes neuronal activity in the hippocampus. J Neurosci 24:6920-6927.

Azouz R, Alroy G, Yaari Y (1997) Modulation of endogenous firing patterns by osmolarity in rat hippocampal neurones. J Physiol 502 (Pt 1):175-187.

Best L, Yates AP, Decher N, Steinmeyer K, Nilius B (2004) Inhibition of glucose-induced electrical activity in rat pancreatic beta-cells by DCPIB, a selective inhibitor of volume-sensitive anion currents. Eur J Pharmacol 489:13-19.

Bikson M, Fox JE, Jefferys JG (2003) Neuronal aggregate formation underlies spatiotemporal dynamics of nonsynaptic seizure initiation. J Neurophysiol 89:2330-2333.

Binder DK, Oshio K, Ma T, Verkman AS, Manley GT (2004a) Increased seizure threshold in mice lacking aquaporin-4 water channels. NeuroReport 15:259-262.

Binder DK, Papadopoulos MC, Haggie PM, Verkman AS (2004b) In vivo measurement of brain extracellular space diffusion by cortical surface photobleaching. J Neurosci 24:8049-8056.

Binder DK, Steinhauser C (2006) Functional changes in astroglial cells in epilepsy. GLIA 54:358-368.

Bowens NH, Dohare P, Kuo YH, Mongin AA (2013) DCPIB, the proposed selective blocker of volume-regulated anion channels, inhibits several glutamate transport pathways in glial cells. Mol Pharmacol 83:22-32.

Brodie MJ, Dichter MA (1996) Antiepileptic drugs. N Engl J Med 334:168-175.

Brodie MJ, Barry SJ, Bamagous GA, Norrie JD, Kwan P (2012) Patterns of treatment response in newly diagnosed epilepsy. Neurology 78:1548-1554.

Caspi A, Benninger F, Yaari Y (2009) KV7/M channels mediate osmotic modulation of intrinsic neuronal excitability. J Neurosci 29:11098-11111.

Cavelier P, Attwell D (2005) Tonic release of glutamate by a DIDS-sensitive mechanism in rat hippocampal slices. J Physiol 564:397-410.

de Curtis M, Avanzini G (2001) Interictal spikes in focal epileptogenesis. Prog Neurobiol 63:541-567.

Decher N, Lang HJ, Nilius B, Bruggemann A, Busch AE, Steinmeyer K (2001) DCPIB is a novel selective blocker of I(Cl,swell) and prevents swelling-induced shortening of guinea-pig atrial action potential duration. Br J Pharmacol 134:1467-1479.

Derchansky M, Shahar E, Wennberg RA, Samoilova M, Jahromi SS, Abdelmalik PA, Zhang L, Carlen PL (2004) Model of frequent, recurrent, and spontaneous seizures in the intact mouse hippocampus. Hippocampus 14:935-947.

Dingledine R, Hynes MA, King GL (1986) Involvement of N-methyl-D-aspartate receptors in epileptiform bursting in the rat hippocampal slice. J Physiol 380:175-189.

Dudek FE, Snow RW, Taylor CP (1986) Role of electrical interactions in synchronization of epileptiform bursts. Adv Neurol 44:593-617.

Dudek FE, Obenaus A, Tasker JG (1990) Osmolality-induced changes in extracellular volume alter epileptiform bursts independent of chemical

synapses in the rat: importance of non-synaptic mechanisms in hippocampal epileptogenesis. Neurosci Lett 120:267-270.

Eadie MJ (2012) Shortcomings in the current treatment of epilepsy. Expert review of neurotherapeutics 12:1419-1427.

Evanko DS, Zhang Q, Zorec R, Haydon PG (2004) Defining pathways of loss and secretion of chemical messengers from astrocytes. GLIA 47:233-240.

Fellin T, Pascual O, Gobbo S, Pozzan T, Haydon PG, Carmignoto G (2004) Neuronal synchrony mediated by astrocytic glutamate through activation of extrasynaptic NMDA receptors. Neuron 43:729-743.

Fellin T, Gomez-Gonzalo M, Gobbo S, Carmignoto G, Haydon PG (2006) Astrocytic glutamate is not necessary for the generation of epileptiform neuronal activity in hippocampal slices. J Neurosci 26:9312-9322.

Fiacco TA, Agulhon C, Taves SR, Petravicz J, Casper KB, Dong X, Chen J, McCarthy KD (2007) Selective stimulation of astrocyte calcium in situ does not affect neuronal excitatory synaptic activity. Neuron 54:611-626.

Fields RD, Ni Y (2010) Nonsynaptic communication through ATP release from volume-activated anion channels in axons. Sci Signal 3:ra73.

Frohlich F, Bazhenov M, Iragui-Madoz V, Sejnowski TJ (2008) Potassium dynamics in the epileptic cortex: new insights on an old topic. Neuroscientist 14:422-433.

Gunnarson E, Zelenina M, Axehult G, Song Y, Bondar A, Krieger P, Brismar H, Zelenin S, Aperia A (2008) Identification of a molecular target for glutamate regulation of astrocyte water permeability. GLIA 56:587-596.

Haas HL, Jefferys JG (1984) Low-calcium field burst discharges of CA1 pyramidal neurones in rat hippocampal slices. J Physiol 354:185-201.

Hablitz JJ (1984) Picrotoxin-induced epileptiform activity in hippocampus: role of endogenous versus synaptic factors. J Neurophysiol 51:1011-1027.

Holthoff K, Witte OW (2000) Directed spatial potassium redistribution in rat neocortex. GLIA 29:288-292.

Huang R, Aitken PG, Somjen GG (1995) The extent and mechanism of the loss of function caused by strongly hypotonic solutions in rat hippocampal slices. Brain Res 695:195-202.

Huang R, Bossut DF, Somjen GG (1997) Enhancement of whole cell synaptic currents by low osmolarity and by low [NaCl] in rat hippocampal slices. J Neurophysiol 77:2349-2359.

Hubbard JA, Hsu MS, Fiacco TA, Binder DK (2013) Glial cell changes in epilepsy: overview of the clinical problem and therapeutic opportunities. Neurochem Int 63:638-651.

Hyzinski-Garcia MC, Rudkouskaya A, Mongin AA (2014) LRRC8A protein is indispensable for swelling-activated and ATP-induced release of excitatory amino acids in rat astrocytes. J Physiol 592:4855-4862.

Inoue H, Mori S, Morishima S, Okada Y (2005) Volume-sensitive chloride channels in mouse cortical neurons: characterization and role in volume regulation. Eur J Neurosci 21:1648-1658.

Inoue H, Ohtaki H, Nakamachi T, Shioda S, Okada Y (2007) Anion channel blockers attenuate delayed neuronal cell death induced by transient forebrain ischemia. J Neurosci Res 85:1427-1435.

Inoue H, Okada Y (2007) Roles of volume-sensitive chloride channel in excitotoxic neuronal injury. J Neurosci 27:1445-1455.

Jefferys JG, Haas HL (1982) Synchronized bursting of CA1 hippocampal pyramidal cells in the absence of synaptic transmission. Nature 300:448-450.

Jensen MS, Yaari Y (1988) The relationship between interictal and ictal paroxysms in an in vitro model of focal hippocampal epilepsy. Ann Neurol 24:591-598.

Jensen MS, Yaari Y (1997) Role of intrinsic burst firing, potassium accumulation, and electrical coupling in the elevated potassium model of hippocampal epilepsy. J Neurophysiol 77:1224-1233.

Jiruska P, Csicsvari J, Powell AD, Fox JE, Chang WC, Vreugdenhil M, Li X, Palus M, Bujan AF, Dearden RW, Jefferys JG (2010) High-frequency network activity, global increase in neuronal activity, and synchrony expansion precede epileptic seizures in vitro. J Neurosci 30:5690-5701.

Johnston D, Brown TH (1984) The synaptic nature of the paroxysmal depolarizing shift in hippocampal neurons. Ann Neurol 16 Suppl:S65-71.

Jones RS, Heinemann U (1988) Synaptic and intrinsic responses of medical entorhinal cortical cells in normal and magnesium-free medium in vitro. J Neurophysiol 59:1476-1496.

Kilb W, Dierkes PW, Sykova E, Vargova L, Luhmann HJ (2006) Hypoosmolar conditions reduce extracellular volume fraction and enhance epileptiform activity in the CA3 region of the immature rat hippocampus. J Neurosci Res 84:119-129.

Kimelberg HK, Goderie SK, Higman S, Pang S, Waniewski RA (1990) Swelling-induced release of glutamate, aspartate, and taurine from astrocyte cultures. J Neurosci 10:1583-1591.

Kimelberg HK, Rutledge E, Goderie S, Charniga C (1995) Astrocytic swelling due to hypotonic or high K+ medium causes inhibition of glutamate and aspartate uptake and increases their release. J Cereb Blood Flow Metab 15:409-416.

Konnerth A, Heinemann U, Yaari Y (1986) Nonsynaptic epileptogenesis in the mammalian hippocampus in vitro. I. Development of seizurelike activity in low extracellular calcium. J Neurophysiol 56:409-423.

Korn SJ, Giacchino JL, Chamberlin NL, Dingledine R (1987) Epileptiform burst activity induced by potassium in the hippocampus and its regulation by GABA-mediated inhibition. J Neurophysiol 57:325-340.

Kwan P, Brodie MJ (2000) Early identification of refractory epilepsy. N Engl J Med 342:314-319.

Kwan P, Brodie MJ (2001a) Neuropsychological effects of epilepsy and antiepileptic drugs. Lancet 357:216-222.

Lauderdale K, Murphy T, Tung T, Davila D, Binder DK, Fiacco TA (2015) Osmotic Edema Rapidly Increases Neuronal Excitability Through Activation of NMDA Receptor-Dependent Slow Inward Currents in Juvenile and Adult Hippocampus. ASN Neuro 7.

Le Meur K, Galante M, Angulo MC, Audinat E (2007) Tonic activation of NMDA receptors by ambient glutamate of non-synaptic origin in the rat hippocampus. J Physiol 580:373-383.

Liu HT, Tashmukhamedov BA, Inoue H, Okada Y, Sabirov RZ (2006) Roles of two types of anion channels in glutamate release from mouse astrocytes under ischemic or osmotic stress. GLIA 54:343-357.

MacVicar BA, Feighan D, Brown A, Ransom B (2002) Intrinsic optical signals in the rat optic nerve: role for K(+) uptake via NKCC1 and swelling of astrocytes. GLIA 37:114-123.

McBain CJ, Traynelis SF, Dingledine R (1990) Regional variation of extracellular space in the hippocampus. Science 249:674-677.

Minieri L, Pivonkova H, Caprini M, Harantova L, Anderova M, Ferroni S (2013) The inhibitor of volume-regulated anion channels DCPIB activates TREK potassium channels in cultured astrocytes. Br J Pharmacol 168:1240-1254.

Mody I, Lambert JD, Heinemann U (1987) Low extracellular magnesium induces epileptiform activity and spreading depression in rat hippocampal slices. J Neurophysiol 57:869-888.

Olsson T, Broberg M, Pope KJ, Wallace A, Mackenzie L, Blomstrand F, Nilsson M, Willoughby JO (2006) Cell swelling, seizures and spreading depression: an impedance study. Neuroscience 140:505-515.

Qiu Z, Dubin AE, Mathur J, Tu B, Reddy K, Miraglia LJ, Reinhardt J, Orth AP, Patapoutian A (2014) SWELL1, a plasma membrane protein, is an essential component of volume-regulated anion channel. Cell 157:447-458.

Risher WC, Andrew RD, Kirov SA (2009) Real-time passive volume responses of astrocytes to acute osmotic and ischemic stress in cortical slices and in vivo revealed by two-photon microscopy. GLIA 57:207-221.

Rogawski MA, Loscher W (2004) The neurobiology of antiepileptic drugs. Nat Rev Neurosci 5:553-564.

Roper SN, Obenaus A, Dudek FE (1992) Osmolality and nonsynaptic epileptiform bursts in rat CA1 and dentate gyrus. Ann Neurol 31:81-85.

Rosen AS, Andrew RD (1990) Osmotic effects upon excitability in rat neocortical slices. Neuroscience 38:579-590.

Rutecki PA, Lebeda FJ, Johnston D (1985) Epileptiform activity induced by changes in extracellular potassium in hippocampus. J Neurophysiol 54:1363-1374.

Rutledge EM, Aschner M, Kimelberg HK (1998) Pharmacological characterization of swelling-induced D-[3H]aspartate release from primary astrocyte cultures. Am J Physiol 274:C1511-1520.

Saly V, Andrew RD (1993) CA3 neuron excitation and epileptiform discharge are sensitive to osmolality. J Neurophysiol 69:2200-2208.

Schnell C, Shahmoradi A, Wichert SP, Mayerl S, Hagos Y, Heuer H, Rossner MJ, Hulsmann S (2015) The multispecific thyroid hormone transporter OATP1C1 mediates cell-specific sulforhodamine 101-labeling of hippocampal astrocytes. Brain Struct Funct 220:193-203.

Schober AL, Mongin AA (2015) Intracellular levels of glutamate in swollen astrocytes are preserved via neurotransmitter reuptake and de novo synthesis: implications for hyponatremia. J Neurochem 135:176-185.

Seifert G, Schilling K, Steinhauser C (2006) Astrocyte dysfunction in neurological disorders: a molecular perspective. Nat Rev Neurosci 7:194-206.

Song Y, Gunnarson E (2012) Potassium dependent regulation of astrocyte water permeability is mediated by cAMP signaling. PLoS ONE 7:e34936.

Stafstrom CE (2010) Mechanisms of action of antiepileptic drugs: the search for synergy. Current opinion in neurology 23:157-163.

Swartzwelder HS, Wilson WA, Tayyeb MI (1995) Differential sensitivity of NMDA receptor-mediated synaptic potentials to ethanol in immature versus mature hippocampus. Alcoholism, clinical and experimental research 19:320-323.

Tancredi V, Avoli M (1987) Control of spontaneous epileptiform discharges by extracellular potassium: an "in vitro" study in the CA1 subfield of the hippocampal slice. Exp Brain Res 67:363-372.

Tancredi V, Hwa GG, Zona C, Brancati A, Avoli M (1990) Low magnesium epileptogenesis in the rat hippocampal slice: electrophysiological and pharmacological features. Brain Res 511:280-290.

Taylor CP, Dudek FE (1984) Excitation of hippocampal pyramidal cells by an electrical field effect. J Neurophysiol 52:126-142.

Thom M, Mathern GW, Cross JH, Bertram EH (2010) Mesial temporal lobe epilepsy: How do we improve surgical outcome? Ann Neurol 68:424-434.

Traynelis SF, Dingledine R (1988) Potassium-induced spontaneous electrographic seizures in the rat hippocampal slice. J Neurophysiol 59:259-276.

Traynelis SF, Dingledine R (1989) Role of extracellular space in hyperosmotic suppression of potassium-induced electrographic seizures. J Neurophysiol 61:927-938.

Voets T, Droogmans G, Raskin G, Eggermont J, Nilius B (1999) Reduced intracellular ionic strength as the initial trigger for activation of endothelial volume-regulated anion channels. Proc Natl Acad Sci U S A 96:5298-5303.

Voss FK, Ullrich F, Munch J, Lazarow K, Lutter D, Mah N, Andrade-Navarro MA, von Kries JP, Stauber T, Jentsch TJ (2014) Identification of LRRC8 heteromers as an essential component of the volume-regulated anion channel VRAC. Science 344:634-638.

Wallraff A, Odermatt B, Willecke K, Steinhauser C (2004) Distinct types of astroglial cells in the hippocampus differ in gap junction coupling. GLIA 48:36-43.

Walther H, Lambert JD, Jones RS, Heinemann U, Hamon B (1986) Epileptiform activity in combined slices of the hippocampus, subiculum and entorhinal cortex during perfusion with low magnesium medium. Neurosci Lett 69:156-161.

Walz W (1987) Swelling and potassium uptake in cultured astrocytes. Can J Physiol Pharmacol 65:1051-1057.

Wetherington J, Serrano G, Dingledine R (2008) Astrocytes in the Epileptic Brain. In: Neuron, pp 168-178.

Xie AX, Lauderdale K, Murphy T, Myers TL, Fiacco TA (2014) Inducing plasticity of astrocytic receptors by manipulation of neuronal firing rates. J Vis Exp:1-13.

Yaari Y, Konnerth A, Heinemann U (1986) Nonsynaptic epileptogenesis in the mammalian hippocampus in vitro. II. Role of extracellular potassium. J Neurophysiol 56:424-438.

Ye ZC, Oberheim N, Kettenmann H, Ransom BR (2009) Pharmacological "cross-inhibition" of connexin hemichannels and swelling activated anion channels. GLIA 57:258-269.

Zhang H, Cao HJ, Kimelberg HK, Zhou M (2011) Volume regulated anion channel currents of rat hippocampal neurons and their contribution to oxygen-and-glucose deprivation induced neuronal death. PLoS ONE 6:e16803.

Zhou N, Gordon GR, Feighan D, MacVicar BA (2010) Transient swelling, acidification, and mitochondrial depolarization occurs in neurons but not astrocytes during spreading depression. Cereb Cortex 20:2614-2624.
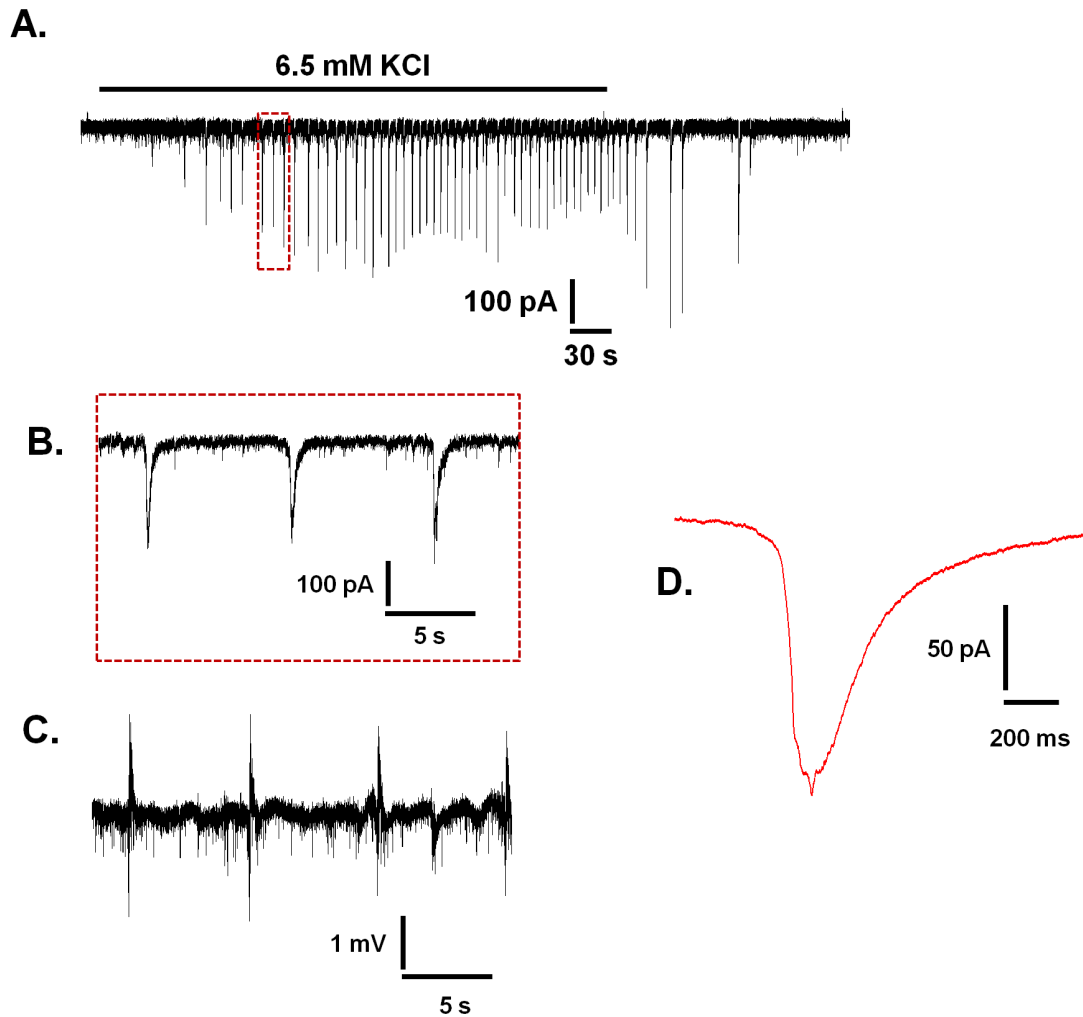
Figure 3.1. Basic features of epileptiform activity induced by high-$[K^+]_o$
(A) Sample voltage-clamp recording of a CA1 neuron in Mg^{2+}-free ACSF + D-serine, with 6.5 mM $[K^+]_o$ included as indicated. Paroxysmal depolarization shifts (PDSs) can be observed starting approximately 1 minute after application of 6.5 mM $[K^+]_o$. (B) Zoomed-in view of a small section in A, highlighting the characteristic shape and repetitive nature of PDSs which facilitates their detection. (C) Sample extracellular recording of PDSs in 6.5 mM K^+ (different experiment day). Similar frequency of events supports the idea that the recorded currents in A and B are the voltage-clamp correlate of the true PDS. (D) Averaged PDS current from the cell displayed in A and B (N=345 total events averaged over 6 applications of high K^+).
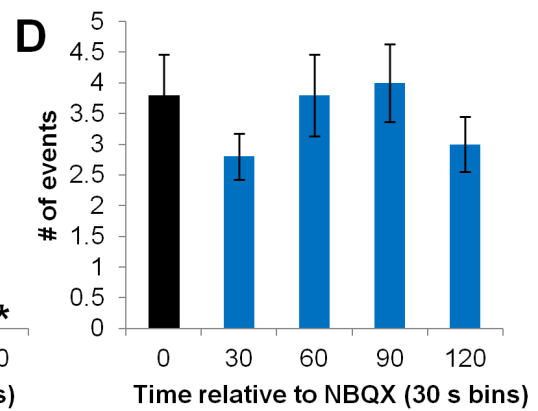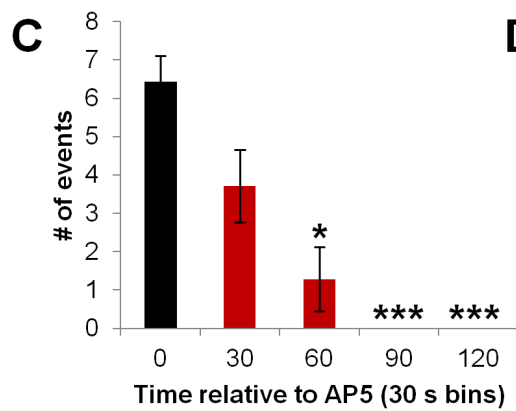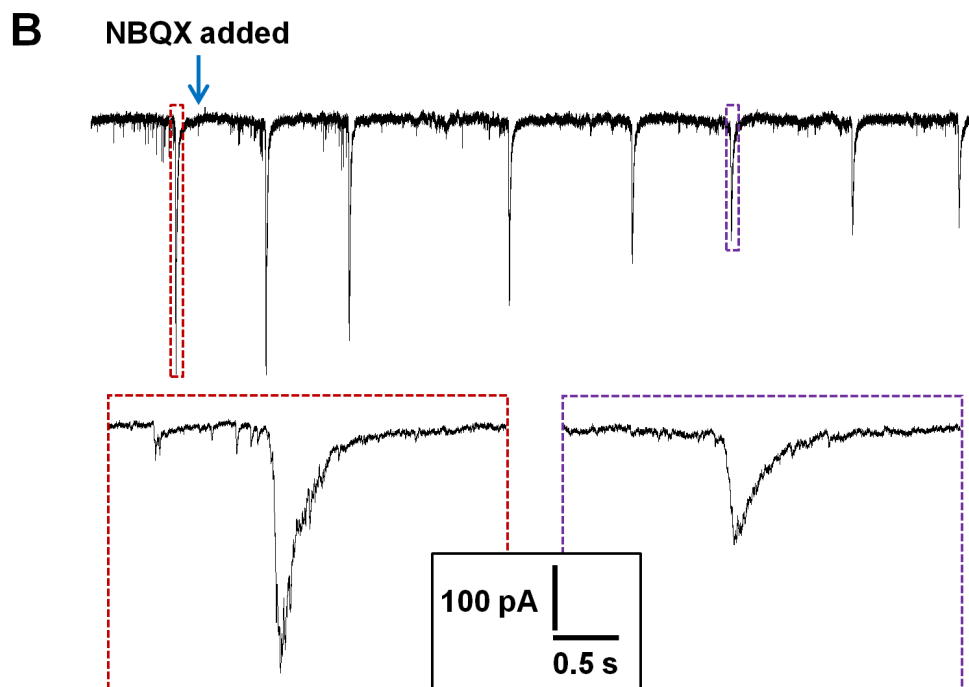
A AP5 added

B NBQX added

100 pA

10 s

100 pA

0.5 s

C

# of events

Time relative to AP5 (30 s bins)

D

# of events
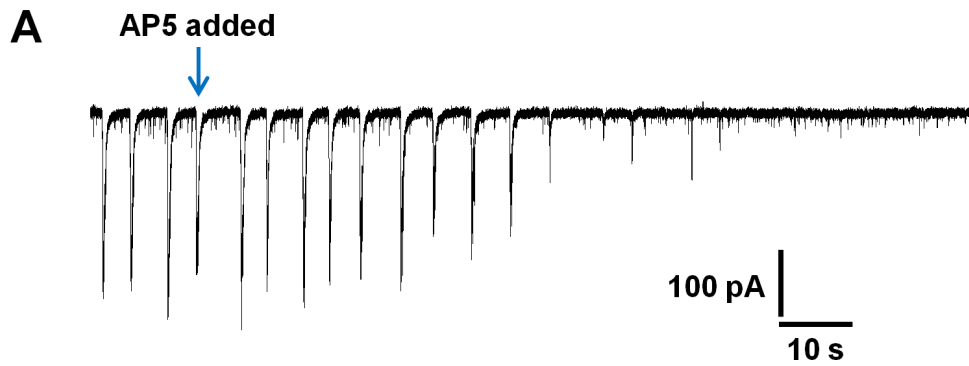
Time relative to NBQX (30 s bins)

Figure 3.2. PDSs are NMDAR-dependent

(A) PDS activity evoked in 8.5 mM K^+ is rapidly abolished following the addition of D,L-AP5, suggesting an NMDA receptor-dependent mechanism. (B) In contrast to (A), PDSs persist after addition of the selective AMPA/kainate receptor antagonist NBQX. Insets (red and purple dashed boxes) provide a zoomed-in view of PDSs before and after NBQX application. Note that while the PDS waveform becomes noticeably "cleaner" due to the absence of AMPA receptor activity, it retains the same basic shape. (C, D) Events before and after AP5 (C) or NBQX (D) application, binned by 30 second intervals starting from 30 s prior to drug application (bin "0", black bars). N=5-7 cells each; $*p < 0.05$, $***p < 0.001$ vs. bin 0.
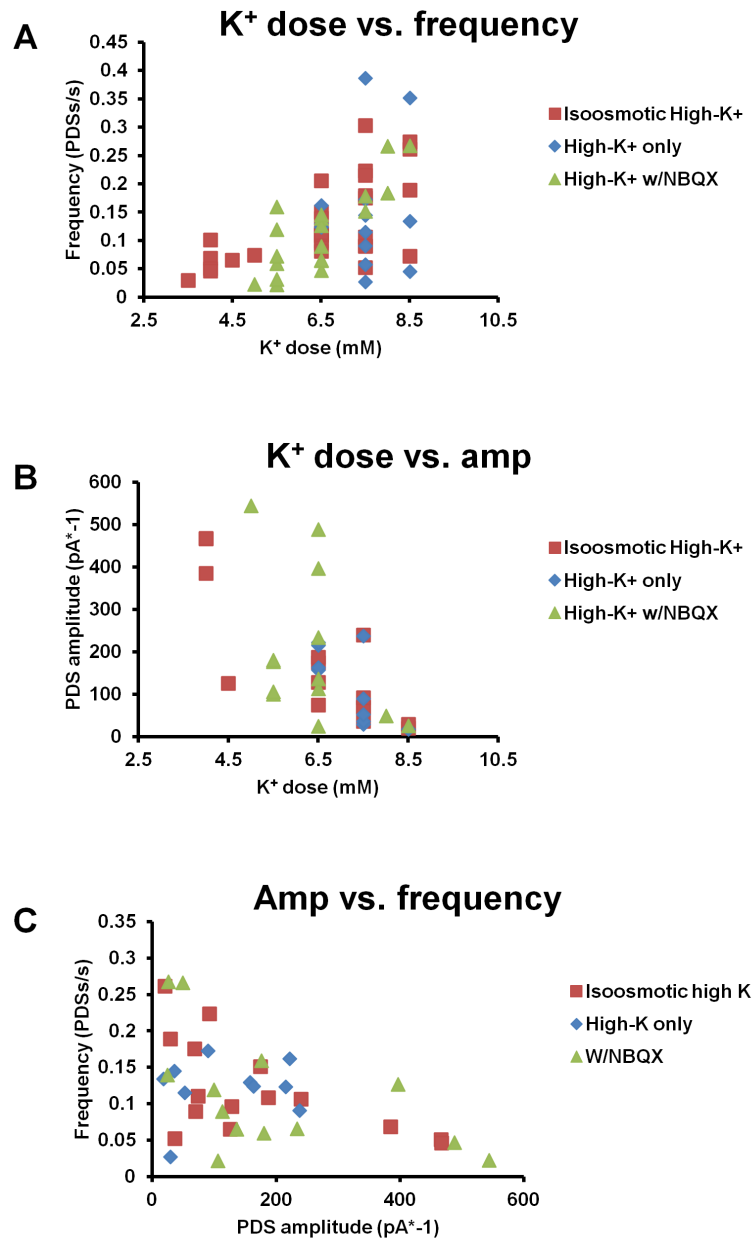
Figure 3.3. Effect of increasing K$^+$ dose on PDS activity
(A) PDSs evoked in high K$^+$ exhibit a gradual increase in average frequency as K$^+$ dose is increased, which is relatively invariant between standard high K$^+$, "isoosmotic" high K$^+$, or high K$^+$ containing NBQX (N=14, 30 and 20 cells respectively). As average frequency increases, average PDS amplitude (B) decreases concomitantly (N=10, 15 and 13 cells respectively). Reduced N from (A) to (B) is a consequence of access resistance changes, as described in Methods. (C) Frequency and amplitude pooled across all K$^+$ doses to highlight the inverse relationship between the two (N is the same as in (B)).

A

Add VRAC antagonist cocktail

100 pA

20 s

B

Event amplitude, % of max

Time (s) relative to antagonist application

C

High-[K$^+$]$_o$ Trial 1 (Control)

High-[K$^+$]$_o$ Trial 2 (Control)

125 pA

2 sec

D

High-[K$^+$]$_o$ Trial 1 (Baseline)

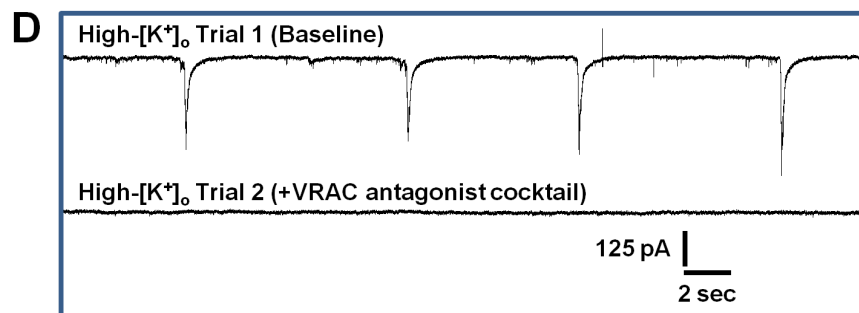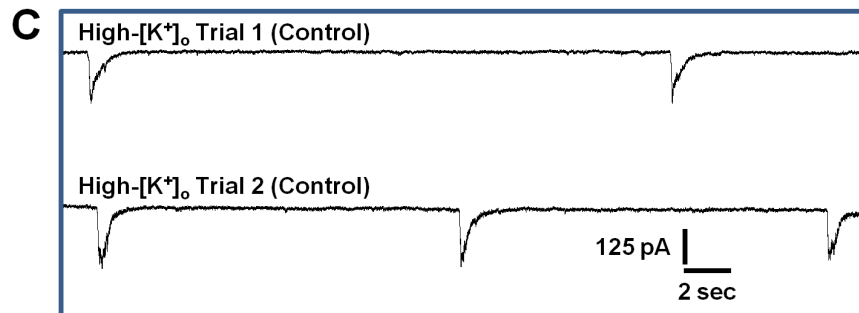High-[K$^+$]$_o$ Trial 2 (+VRAC antagonist cocktail)
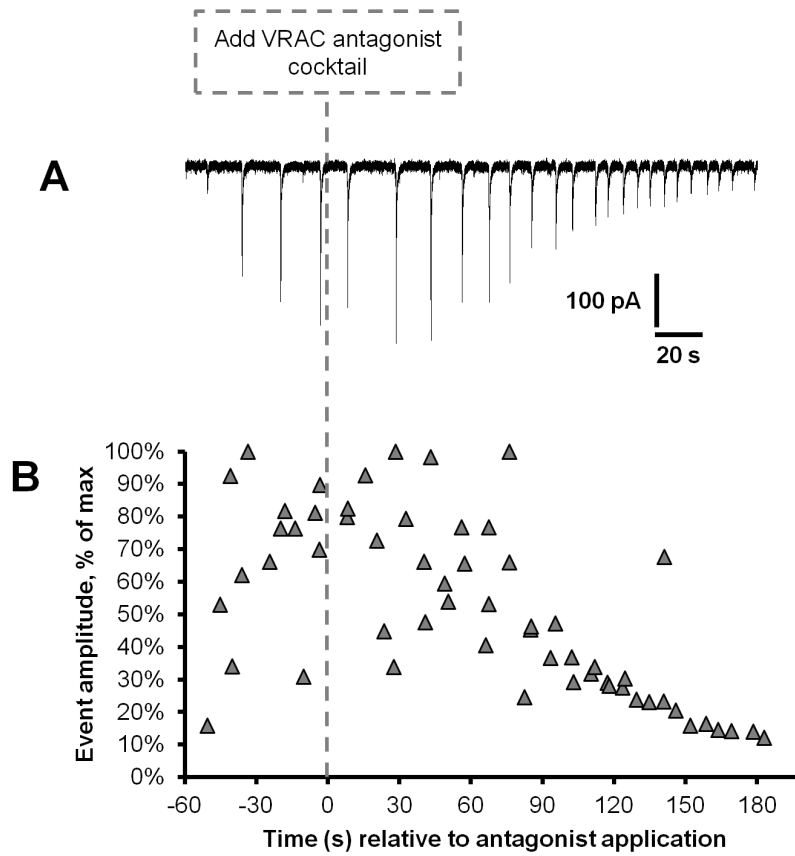
125 pA

2 sec

Figure 3.4. PDSs are rapidly abolished by a VRAC antagonist cocktail
(A) Sample recording of PDS activity evoked in 8.5 mM K^+ before and after application of a VRAC antagonist cocktail containing DCPIB (20 µM), NPPB (? µM) and DIDS (200 µM). PDSs rapidly diminish and eventually disappear in all cells tested. (B) PDS amplitudes are calculated as a percentage of max for each cell (N=58 PDSs from 3 cells) and displayed over the same time scale as in (A). VRAC antagonist cocktail is added at time=0. (C, D) In contrast to their typical nature (C), PDSs cannot be re-evoked by high-$[K^+]_o$ after treatment with the VRAC antagonist cocktail (D).
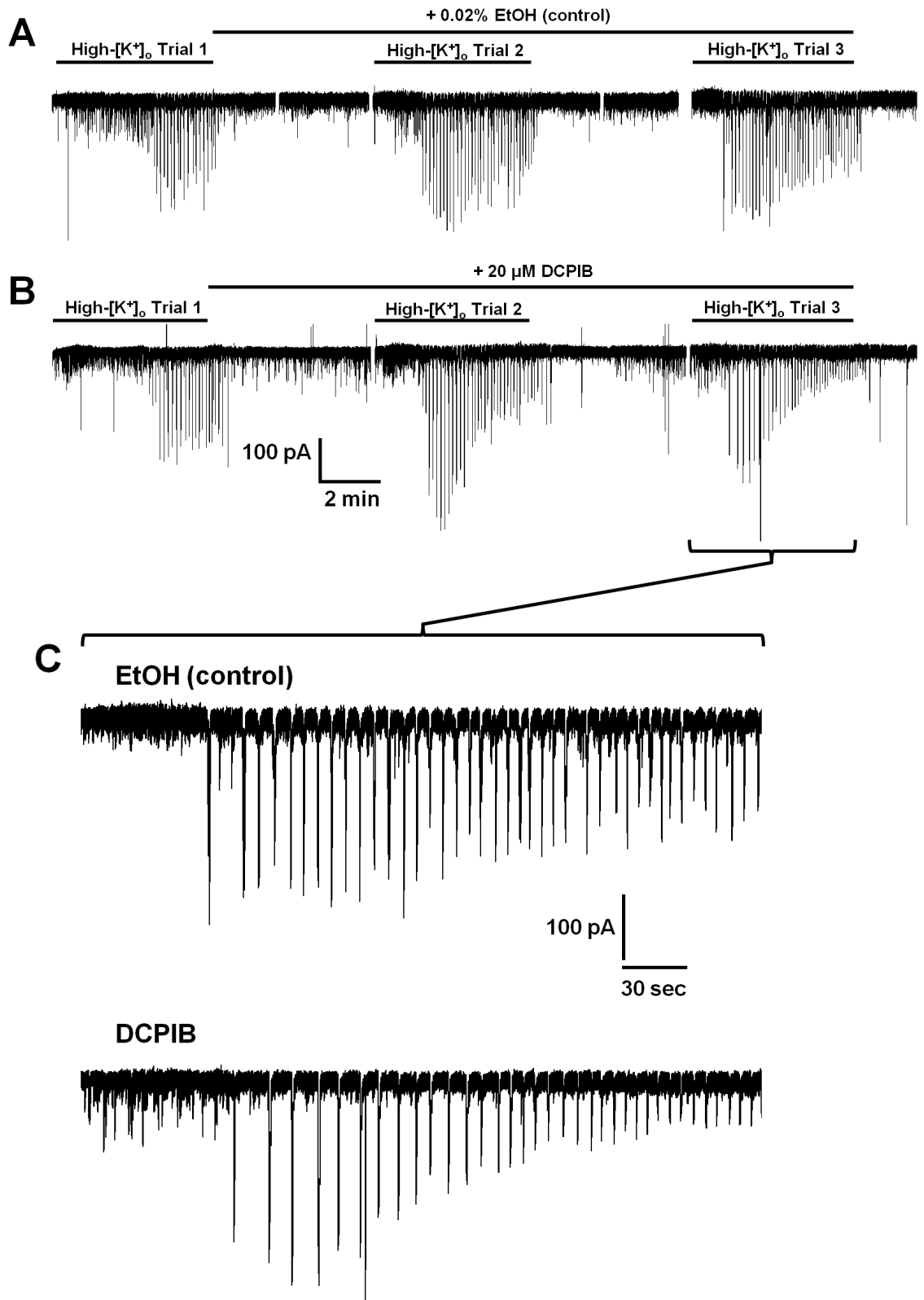
A

+ 0.02% EtOH (control)

High-[K$^+$]$_o$ Trial 1   High-[K$^+$]$_o$ Trial 2   High-[K$^+$]$_o$ Trial 3

B

+ 20 µM DCPIB

High-[K$^+$]$_o$ Trial 1   High-[K$^+$]$_o$ Trial 2   High-[K$^+$]$_o$ Trial 3

100 pA

2 min

C

EtOH (control)

100 pA

30 sec

DCPIB

Figure 3.5. Effect of DCPIB on PDS appearance over multiple applications of high-[K$^+$]$_o$

(A, B) Sample recordings of CA1 pyramidal neurons recorded across 3 applications of high-[K$^+$]$_o$ ACSF, and the resulting appearance of PDSs during each application. Following the end of Trial 1, EtOH vehicle control (A) or DCPIB (B) was added and remained through the end of Trial 3. Effects of DCPIB become most visible in Trial 3 (C), when DCPIB has been in the bath for ~15-20 minutes.
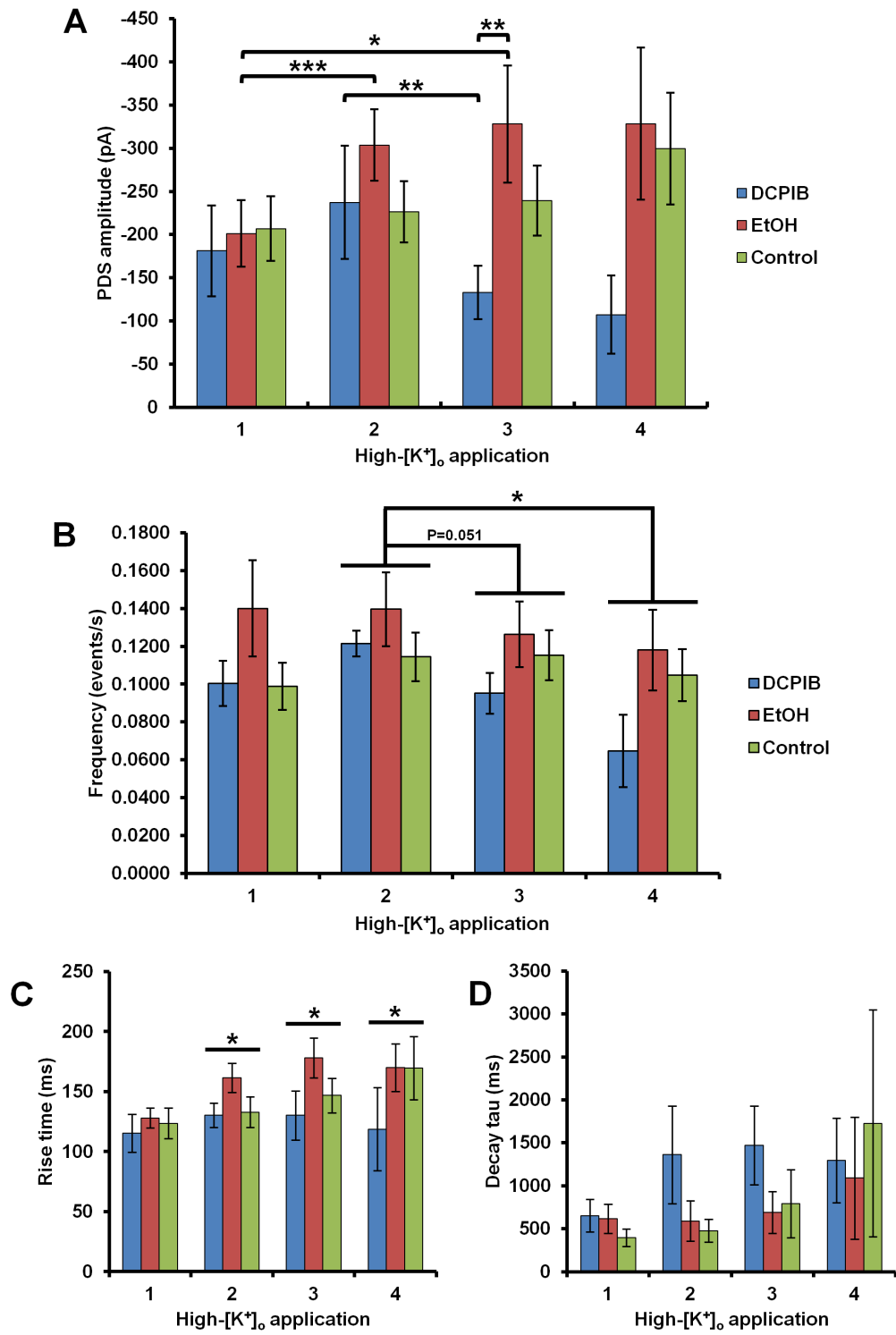
Figure 3.6. Effect of DCPIB on PDS kinetics

(A) Average PDS amplitude (in pA) measured across each high-$[K^+]_o$ application for DCPIB, EtOH or untreated controls. Similar to figure 3.5, high-$[K^+]_o$ application 1 is "Baseline" PDS activity (no drug), applications 2-3 contain EtOH or DCPIB. Application 4 follows a 15 minute wash period (no EtOH or DCPIB). "Control" (untreated) is displayed for comparison with the EtOH vehicle control. Currents are inward (negative) but are displayed in reverse order to better display absolute changes in magnitude. In general, an increase in PDS amplitude is visible over time in EtOH while the reverse is true of DCPIB (note the substantial difference in application 3). (B) PDS frequency generally decreases as a function of time, but is not significantly related to treatment group. (C, D) Rise and decay kinetics of PDSs are also unaffected by treatment group, although rise time generally increases across applications. Decay tau is too variable for accurate conclusions. N = 7-12 cells, first 3 applications; N = 4-5 cells for application 4.
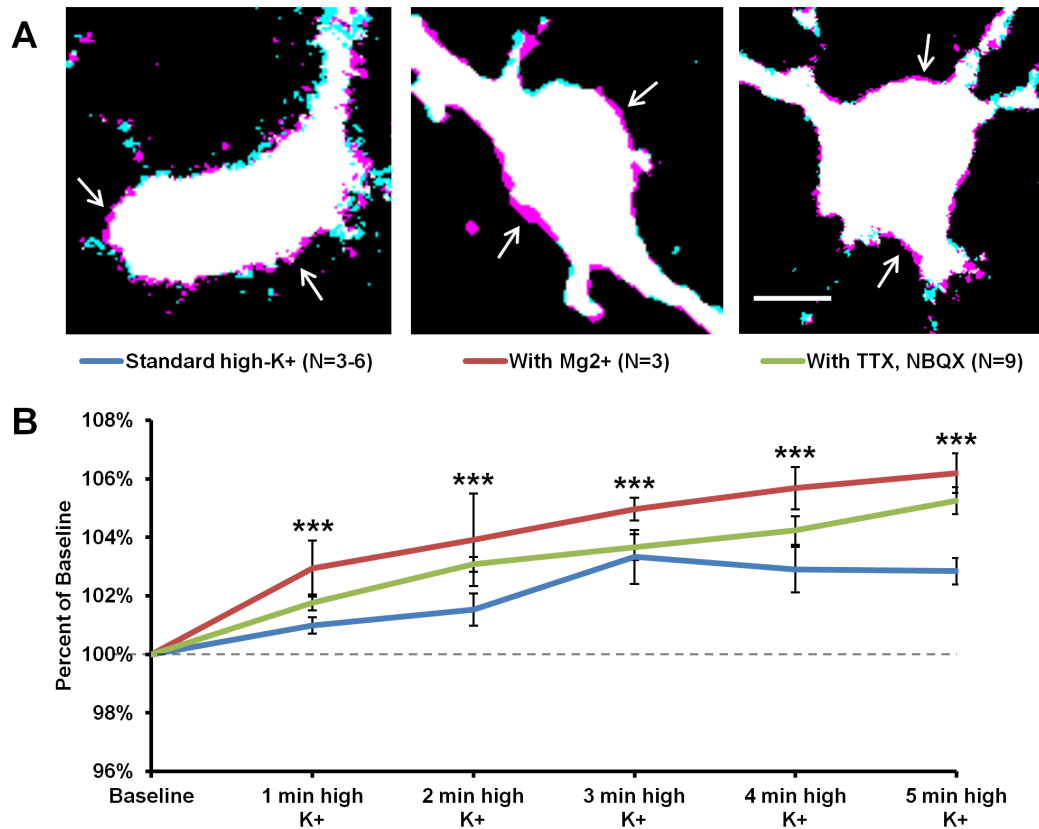
Figure 3.7. Rapid astrocyte swelling in 3 different high-$[K^+]_o$ conditions
(A) Thresholded and pseudocolored overlays of astrocytes imaged in baseline ACSF (cyan) and after 5 minutes in 6.5 mM $[K^+]_o$ ACSF (magenta). Astrocytes were imaged in standard Mg^{2+}-free 6.5 mM $[K^+]_o$ (left) or in 6.5 mM $[K^+]_o$ containing Mg^{2+} (center), and compared to astrocytes in Mg^{2+} high-$[K^+]_o$ ACSF containing TTX and NBQX (right; see also Chapter 2). Increases in cell volume are visible as magenta edges surrounding the cell body and main processes and are indicated by white arrows for clarity. Scale bar = 5 µm. (B) Astrocyte volume in each of the 3 conditions listed, quantified as a percentage of baseline soma area. Reduced volume in standard high-$[K^+]_o$ may be an artifact of patch clamp (see results). ***$P<0.001$ compared to baseline.
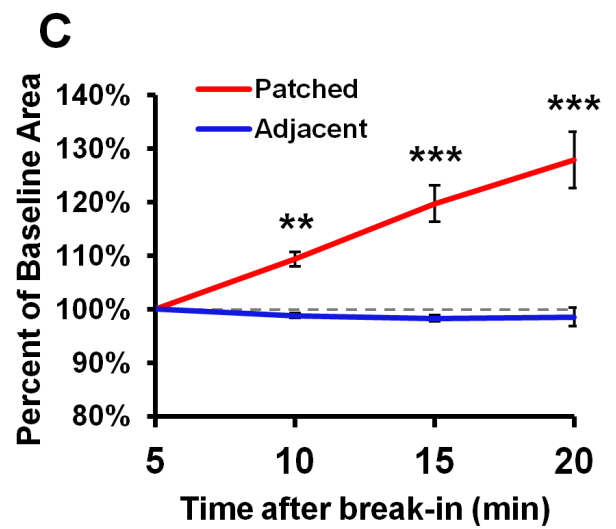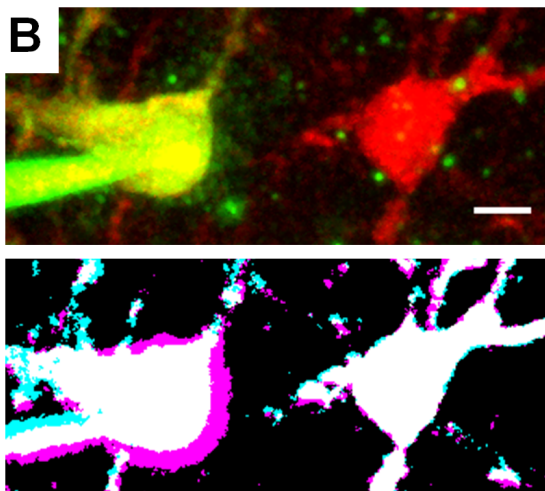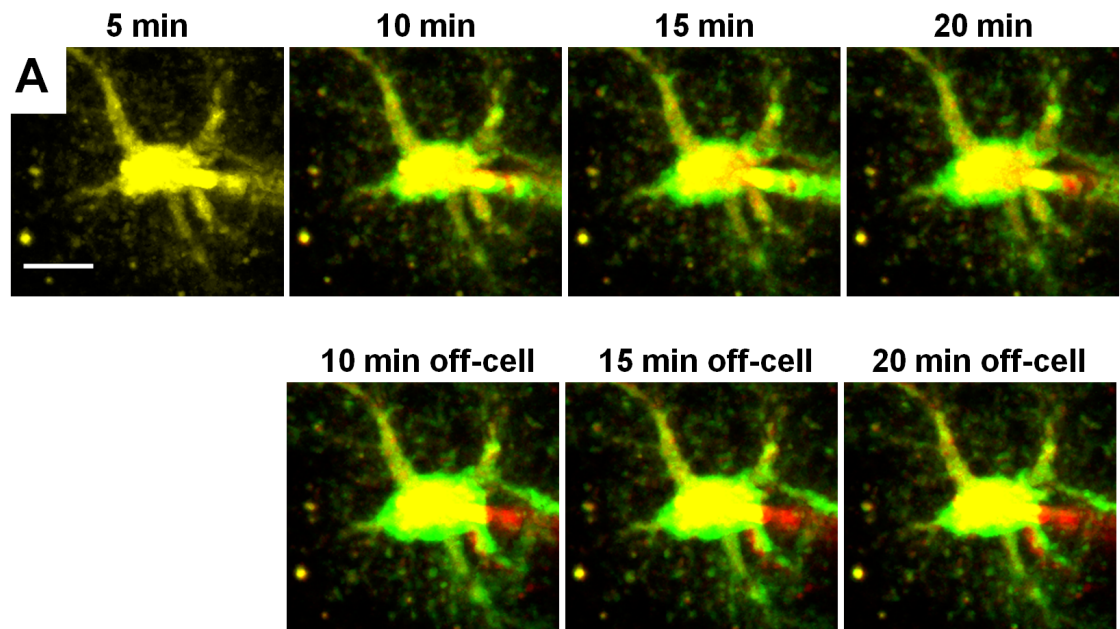
Figure 3.8. Hyperosmotic internal solution selectively swells astrocytes
(A) Time series displaying a typical astrocyte patch-clamped with fluorescein dextran (10,000 m.w.). "Baseline" time point is 5 minutes after break-in, to allow time for dye diffusion into cell. Green regions around the soma are areas where the cell is swelling. Note that the red artifact in the bottom three panels represents the starting location of the pipette, which is removed prior to the last three time points. Scale bar = 10 µm. (B) Adjacent astrocytes cannot be swollen by hyperosmolar solution from a single pipette. Astrocyte loaded with fluorescein dextran by patch clamp (top panel, left) is imaged alongside an adjacent astrocyte loaded with SR-101. After 20 minutes, the patched cell has swollen as expected (lower panel, thick magenta border) but the adjacent cell shows no apparent volume change. Scale bar = 5 µm. (C) Quantification of volume as a percent of baseline (5 minutes) in astrocytes patched with a hyperosmolar internal solution, as compared with adjacent astrocytes. N = 4 patched astrocytes; 2-4 adjacent astrocytes; $**p < 0.01$, $***p < 0.001$.
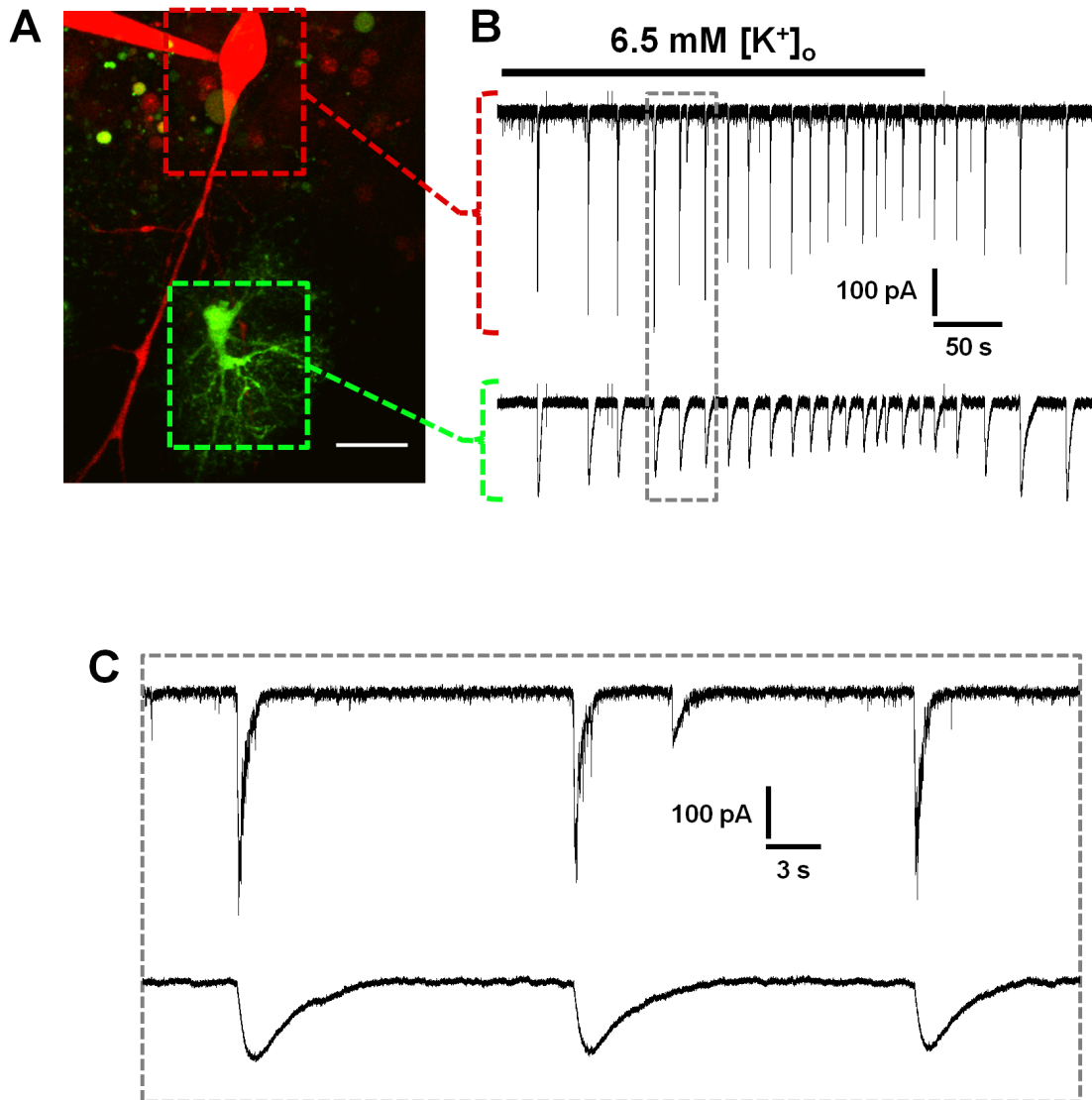
Figure 3.9. Dual-patch clamp for manipulation of astrocyte volume and glutamate release
(A) Merged image depicting a typical patch clamped neuron filled with alexa 568 (red) and nearby astrocyte filled with fluorescein dextran (green), to show general proximity of recorded cells. Image was taken at the end of an experiment, after the astrocyte pipette had been removed. Scale bar, 20 μm. (B) Representative traces showing neuronal PDSs (top) and corresponding inward currents recorded in astrocytes (bottom). (C) Zoomed view of outlined area in B. Note that inward currents on astrocytes are associated with the larger PDS events and appear insensitive to smaller events.

Chapter 4: Conclusions and perspectives

A persisting and challenging question in the study of glial-neuronal interactions, and especially astrocyte-neuron interactions, is: How does one specifically target and manipulate a glial cell? Astrocytes express many of the same or similar receptor types as neurons (Porter and McCarthy, 1997), resulting in complications for pharmacological approaches. For example, the effect of activating metabotropic glutamate receptors (mGluRs) on astrocytes cannot be specifically extricated from the effects on neuronal mGluRs by bath applying an mGluR-specific drug (D'Antoni et al., 2008; Fiacco et al., 2009). Genetic approaches are sometimes used, as in the case of the widely-used AQP4 or α-syntrophin knockouts. Both approaches are, however, prone to nonspecific effects – especially in disease models when cells may substantially alter their expression profiles (Hubbard et al., 2013). Both of these potential problems can be illustrated with microglia, the resident macrophage of the brain whose important functions and interactions are too numerous to list here. Reactive microglia (responding to a pathological insult such as a bacterial protein) begin expressing AQP4, increasing their water permeability (Tomas-Camardiel et al., 2004), and reactive or hACSF-exposed microglia may release glutamate through DCPIB-sensitive VRAC (Harrigan et al., 2008; Schlichter et al., 2014). The problem of specificity was further illustrated in the preceding two chapters. Hypoosmolar conditions, reported (and widely cited) to swell only astrocytes in intact brain tissue, were found to be just as effective at swelling neurons in our

preparation. In further contrast to the published literature, we found that AQP4 was not responsible for hACSF-induced swelling. Perhaps the simplest explanation for these phenomena is that water simply diffuses down its osmotic gradient, across cell membranes, whether or not AQP4 is present (Papahadjopoulos and Kimelberg, 1974). Certainly, this would help explain rapid excitotoxic neuronal swelling, a result of the osmotic pressure exerted by excessive Na^+ and Cl^- influx (Lee et al., 1999; Liang et al., 2007). The ease with which water can apparently enter neurons may have important implications for our second model. While it was not assumed that high-$[K^+]_o$ would have effects only on one cell type, a central hypothesis of this study was that astrocyte swelling in high-$[K^+]_o$ would lead to VRAC opening and glutamate release, which we attempted to test pharmacologically. The results, however, were not easily interpretable. DCPIB, the most specific VRAC antagonist for astrocytes, had at best a limited effect on neuronal epileptiform activity and required an extremely long time to act. Whether this reflects a nonspecific effect is unclear (discussed further in Chapter 3), but it contrasted strongly with the effects of DIDS and NPPB, two antagonists with known (albeit considerably more nonspecific) blocking effects on both neuronal and astrocytic VRAC. The possibility therefore exists that neuronal VRAC were participating in PDS generation. However, we also found in both studies that astrocytes readily swell in high-$[K^+]_o$, whereas neurons (at least in the presence of TTX) do not. Therefore, the question of what

role astrocyte swelling, astrocytic VRAC, and glutamate release plays in epileptiform activity remains largely unresolved.

To answer this question, a primary first step would be measuring neuronal volume during high-$[K^+]_o$ application. This has not yet been systematically examined in our hands. Preliminary observations suggest that neuronal volume remains constant (unpublished), and at least one study (Zhou et al., 2010) indicates that neuronal volume in high-$[K^+]_o$ is only elevated during spreading depression, a phenomenon not present in our conditions. However, it is known that excessive neuronal depolarization and firing leads to Na^+ influx, followed by Cl^- and finally water (Choi, 1992). This obviously is not a concern at our levels of high-$[K^+]_o$ + TTX, as the blockade of neuronal firing would also block excitotoxic swelling (Rungta et al., 2015). It seems highly likely, however, that the population-wide burst firing which characterizes the PDS would be capable of producing excitotoxic swelling, especially as our PDSs are NMDA-receptor driven. If neuronal swelling is indeed observed, it would suggest a role for excitotoxic neuronal swelling in PDS generation. As Rungta and colleagues showed (2015), excitotoxic swelling in neurons depends upon a voltage-activated chloride channel which can be blocked by DIDS, but not NPPB. Testing the effects of these compounds on neuronal volume in high-$[K^+]_o$ may provide further clarification and help explain the effects of our VRAC antagonist cocktail on PDSs. It should be noted, though, that DIDS is a particularly promiscuous drug and would likely have many unintended but experimentally-relevant effects. For

143

example, astrocyte swelling in physiological elevations of $[K^+]_o$ has been reported to be driven (at least partially) by the Na^+/HCO_3^- cotransporter (NBC), which is also blocked by DIDS (Florence et al., 2012).

If neurons are found to swell in high-$[K^+]_o$, it would be prudent to investigate further the role of neuronal VRAC in PDS activity. Neurons appear to express VRAC with very similar properties to astrocytes (Inoue et al., 2005) and which are reported to contribute to excitotoxic death in oxygen-glucose deprivation, another condition in which neurons swell (Risher et al., 2009; Zhang et al., 2011). In this case, applying the VRAC antagonist NPPB should strongly inhibit or eliminate PDSs, although it should once again be noted that NPPB, like DIDS, has many nonspecific targets (Evanko et al., 2004).

Recent work has shown that VRAC are heteromeric hexamers, composed of LRRC8A and at least one of the other four members in the LRRC8 family. Thus, there are potentially many different variants of VRAC, which may explain differences in kinetics and drug sensitivities of VRAC between different tissues (Voss et al., 2014). The identification of this channel will no doubt enable more specific research tools for elucidating the role of VRAC in seizures and other disorders, such as cell type-specific knockouts of LRRC8A or RNAi knockdowns for certain subunits. This carries the somewhat optimistic assumption, of course, that different cell types do express different subtypes of receptor.

It is important to reiterate that there are two components to epilepsy: the interictal burst (which we studied, by proxy, through the PDS); and the ictal burst

(which comprises the seizure discharge itself). Our data suggest that cell volume change and volume-dependent glutamate release may play a role in the maintenance, if not initiation, of interictal bursts. In regard to our original model (Figure 1.1), it is clear that astrocytes swell under high-$[K^+]_o$ conditions within a physiological range, regardless of synaptic transmission, but the role of astrocytic VRAC (as assessed by DCPIB) appears to be minor. One possibility is that astrocytic swelling does play a role in shrinking the extracellular space (promoting excitability), but is not rapid or sufficient enough to trigger RVD and open VRAC (Mola et al., 2016). Astrocytic VRAC may therefore play a much more prominent role in interictal-ictal transitions, as the initiation of an ictal phase is preceded by gradual astrocytic depolarization (Traynelis and Dingledine, 1988) and accelerated tissue swelling (Binder et al., 2004b; Olsson et al., 2006), presumably driven by astrocytes. This enhanced tissue swelling might be sufficient to induce astrocytic RVD through VRAC opening (Mola et al., 2016) which would also release glutamate. Future work will address the role of astrocyte swelling in interictal-ictal transitions.

An alternative mechanism for astrocyte swelling aside from AQP4 might be explained by the therapeutic effect of furosemide, an NKCC1 cotransporter antagonist, on both interictal and ictal discharges (Hochman et al., 1999; Haglund and Hochman, 2005). NKCC1 is water-permeable, and has been reported to swell astrocytes through K^+ and water influx (Walz, 1987; MacVicar et al., 2002; Macaulay and Zeuthen, 2012). Accordingly, blocking NKCC1 also

blocks activity-dependent swelling (Holthoff and Witte, 1996), increasing extracellular space and ameliorating epileptiform activity (Hochman, 2012). As with VRAC, however, NKCC1 is also expressed by neurons and thus it is difficult to make conclusions from these data as to the specific role of astrocytes in tissue swelling and generation of epileptiform activity. Ultimately, determining the role of astrocytic swelling and VRAC in epilepsy will require development of more specific approaches.

In closing, we have demonstrated, consistent with our overall hypothesis, that rapid astrocyte swelling occurs in two different models of neuronal hyperexcitability. VRAC appear to be major players in the development of high-$[K^+]_o$-induced epileptiform activity. Our data also reveal, however, that such models are not simple to interpret. Neurons swell in hypoosmolar conditions and contain VRAC which are blocked by many similar antagonists as those on astrocytes. These data highlight the necessity of techniques and tools specifically targeting astrocyte swelling or astrocytic VRAC, which we have begun to develop.

4.1. References

Binder DK, Papadopoulos MC, Haggie PM, Verkman AS (2004b) In vivo measurement of brain extracellular space diffusion by cortical surface photobleaching. J Neurosci 24:8049-8056.

Choi DW (1992) Excitotoxic cell death. Journal of neurobiology 23:1261-1276.

D'Antoni S, Berretta A, Bonaccorso CM, Bruno V, Aronica E, Nicoletti F, Catania MV (2008) Metabotropic glutamate receptors in glial cells. Neurochem Res 33:2436-2443.

Evanko DS, Zhang Q, Zorec R, Haydon PG (2004) Defining pathways of loss and secretion of chemical messengers from astrocytes. GLIA 47:233-240.

Fiacco TA, Agulhon C, McCarthy KD (2009) Sorting out astrocyte physiology from pharmacology. Annu Rev Pharmacol Toxicol 49:151-174.

Florence CM, Baillie LD, Mulligan SJ (2012) Dynamic volume changes in astrocytes are an intrinsic phenomenon mediated by bicarbonate ion flux. PLoS ONE 7:e51124.

Haglund MM, Hochman DW (2005) Furosemide and mannitol suppression of epileptic activity in the human brain. J Neurophysiol 94:907-918.

Harrigan TJ, Abdullaev IF, Jourd'heuil D, Mongin AA (2008) Activation of microglia with zymosan promotes excitatory amino acid release via volume-regulated anion channels: the role of NADPH oxidases. J Neurochem 106:2449-2462.

Hochman DW, D'Ambrosio R, Janigro D, Schwartzkroin PA (1999) Extracellular chloride and the maintenance of spontaneous epileptiform activity in rat hippocampal slices. J Neurophysiol 81:49-59.

Hochman DW (2012) The extracellular space and epileptic activity in the adult brain: explaining the antiepileptic effects of furosemide and bumetanide. Epilepsia 53 Suppl 1:18-25.

Holthoff K, Witte OW (1996) Intrinsic optical signals in rat neocortical slices measured with near-infrared dark-field microscopy reveal changes in extracellular space. J Neurosci 16:2740-2749.

Hubbard JA, Hsu MS, Fiacco TA, Binder DK (2013) Glial cell changes in epilepsy: overview of the clinical problem and therapeutic opportunities. Neurochem Int 63:638-651.

Inoue H, Mori S, Morishima S, Okada Y (2005) Volume-sensitive chloride channels in mouse cortical neurons: characterization and role in volume regulation. Eur J Neurosci 21:1648-1658.

Lee JM, Zipfel GJ, Choi DW (1999) The changing landscape of ischaemic brain injury mechanisms. Nature 399:A7-14.

Liang D, Bhatta S, Gerzanich V, Simard JM (2007) Cytotoxic edema: mechanisms of pathological cell swelling. Neurosurg Focus 22:E2.

Macaulay N, Zeuthen T (2012) Glial K(+) clearance and cell swelling: key roles for cotransporters and pumps. Neurochem Res 37:2299-2309.

MacVicar BA, Feighan D, Brown A, Ransom B (2002) Intrinsic optical signals in the rat optic nerve: role for K(+) uptake via NKCC1 and swelling of astrocytes. GLIA 37:114-123.

Mola MG, Sparaneo A, Gargano CD, Spray DC, Svelto M, Frigeri A, Scemes E, Nicchia GP (2016) The speed of swelling kinetics modulates cell volume regulation and calcium signaling in astrocytes: A different point of view on the role of aquaporins. GLIA 64:139-154.

Olsson T, Broberg M, Pope KJ, Wallace A, Mackenzie L, Blomstrand F, Nilsson M, Willoughby JO (2006) Cell swelling, seizures and spreading depression: an impedance study. Neuroscience 140:505-515.

Papahadjopoulos D, Kimelberg HK (1974) Phospholipid vesicles (liposomes) as models for biological membranes: Their properties and interactions with cholesterol and proteins. Progress in Surface Science 4:141-232.

Porter JT, McCarthy KD (1997) Astrocytic neurotransmitter receptors in situ and in vivo. Prog Neurobiol 51:439-455.

Risher WC, Andrew RD, Kirov SA (2009) Real-time passive volume responses of astrocytes to acute osmotic and ischemic stress in cortical slices and in vivo revealed by two-photon microscopy. GLIA 57:207-221.

Rungta RL, Choi HB, Tyson JR, Malik A, Dissing-Olesen L, Lin PJ, Cain SM, Cullis PR, Snutch TP, MacVicar BA (2015) The cellular mechanisms of neuronal swelling underlying cytotoxic edema. Cell 161:610-621.

Schlichter LC, Mertens T, Liu B (2014) Swelling activated Cl- channels in microglia. Channels 5:128-137.

Tomas-Camardiel M, Venero JL, de Pablos RM, Rite I, Machado A, Cano J (2004) In vivo expression of aquaporin-4 by reactive microglia. J Neurochem 91:891-899.

Traynelis SF, Dingledine R (1988) Potassium-induced spontaneous electrographic seizures in the rat hippocampal slice. J Neurophysiol 59:259-276.

Voss FK, Ullrich F, Munch J, Lazarow K, Lutter D, Mah N, Andrade-Navarro MA, von Kries JP, Stauber T, Jentsch TJ (2014) Identification of LRRC8 heteromers as an essential component of the volume-regulated anion channel VRAC. Science 344:634-638.

Walz W (1987) Swelling and potassium uptake in cultured astrocytes. Can J Physiol Pharmacol 65:1051-1057.

Zhang H, Cao HJ, Kimelberg HK, Zhou M (2011) Volume regulated anion channel currents of rat hippocampal neurons and their contribution to oxygen-and-glucose deprivation induced neuronal death. PLoS ONE 6:e16803.

Zhou N, Gordon GR, Feighan D, MacVicar BA (2010) Transient swelling, acidification, and mitochondrial depolarization occurs in neurons but not astrocytes during spreading depression. Cereb Cortex 20:2614-2624.